AD NUMBER

AD912061

LIMITATION CHANGES

TO:

Approved for public release; distribution is unlimited.

FROM:

Distribution authorized to U.S. Gov't. agencies only; Test and Evaluation; DEC 1971. Other requests shall be referred to Air Force Aeronautical Systems Division, SDXT, Wright-Patterson AFB, OH 45433.

AUTHORITY

asd, usaf ltr, 8 apr 1974

Cy 2

AEDC-TR-71-271

[redacted]

1972

AERODYNAMIC CHARACTERISTICS OF A 0.12-SCALE MODEL OF THE A-9A AIRCRAFT AT MACH NUMBERS FROM 0.30 TO 0.80

Warren E. White

ARO, Inc.

December 1971

This document has been approved for public release its distribution is unlimited. per TAB 74-10 dtd. 10 May '74

PROPULSION WIND TUNNEL FACILITY

ARNOLD ENGINEERING DEVELOPMENT CENTER

AIR FORCE SYSTEMS COMMAND

ARNOLD AIR FORCE STATION, TENNESSEE

NOTICES

When U. S. Government drawings specifications, or other data are used for any purpose other than a definitely related Government procurement operation, the Government thereby incurs no responsibility nor any obligation whatsoever, and the fact that the Government may have formulated, furnished, or in any way supplied the said drawings, specifications, or other data, is not to be regarded by implication or otherwise, or in any manner licensing the holder or any other person or corporation, or conveying any rights or permission to manufacture, use, or sell any patented invention that may in any way be related thereto.

Qualified users may obtain copies of this report from the Defense Documentation Center.

References to named commercial products in this report are not to be considered in any sense as an endorsement of the product by the United States Air Force or the Government.

AERODYNAMIC CHARACTERISTICS OF A 0.12-SCALE MODEL OF THE A-9A AIRCRAFT AT MACH NUMBERS FROM 0.30 TO 0.80

Warren E. White
ARO, Inc.

FOREWORD

The work reported herein was done at the request of the Aeronautical Systems Division (ASD), Air Force Systems Command (AFSC), for the Northrop Corporation, Hawthorne, California, under Program Element 64211F, System 329A.

The results of the test presented were obtained by ARO, Inc. (a subsidiary of Sverdrup & Parcel and Associates, Inc.), contract operator of the Arnold Engineering Development Center (AEDC), AFSC, Arnold Air Force Station, Tennessee, under Contract F40600-72-C-0003. The tests were conducted from August 17 through 24, 1971, under ARO Project No. PB0190. The manuscript was submitted for publication on November 1, 1971.

This technical report has been reviewed and is approved.

George F. Garey
Lt Colonel, USAF
AF Representative, PWT
Directorate of Test

Duncan W. Rabey, Jr.
Colonel, USAF
Director of Test

ABSTRACT

Wind tunnel tests were conducted at Mach numbers from 0.30 to 0.80 and Reynolds numbers from 2.3 to 7.0 million on a 0.12-scale model of the A-9A aircraft to determine the effects of control surface deflections on the aerodynamic characteristics of the airplane. The results showed that the horizontal stabilizer was 20 to 50 percent more effective in pitching moment per degree of deflection than the elevator, the rudder remained effective at all Mach numbers, and the aileron deflections produced significant effects on lift, drag, and pitching and rolling moment. Minimum drag was increased by approximately 100 and 600 percent for speed brake deflections of 20 and 60 deg, respectively, at Mach numbers from 0.70 to 0.80.

CONTENTS

APPENDIXES

NOMENCLATURE

b	Reference wing span, 82.08 in.
BETA	Sideslip angle, deg
BL	Buttock line, in.
C_D	Drag coefficient, drag/$q_\infty S$
C_L	Lift coefficient, lift/$q_\infty S$
C_ℓ	Rolling-moment coefficient, rolling moment/$q_\infty Sb$
C_m	Pitching-moment coefficient, pitching moment/$q_\infty S\bar{c}$
C_n	Yawing-moment coefficient, yawing moment/$q_\infty Sb$
C_Y	Side-force coefficient, side force/$q_\infty S$
$\bar{c}$	Reference chord, 14.46 in.
F.S.	Fuselage station, in.
H_L	Control surface hinge line
M_∞	Free-stream Mach number
q_∞	Free-stream dynamic pressure, psf
Re	Reynolds number based on model $\bar{c}$
S	Reference wing area, 8.064 sq ft
WL	Waterline, in.
α	Angle of attack, deg
δ_{AL}	Left aileron only, positive, trailing edge down, deg
δ_B	Speedbrake deflection, measured from the centerline of the aileron trailing edge, deg
δ_E	Elevator deflection, positive, trailing edge down, deg
δ_H	Horizontal stabilizer incidence angle, positive, leading edge up, deg
δ_R	Rudder deflection, positive, trailing edge left, deg

SECTION I
INTRODUCTION

Wind tunnel investigations of a 0.12-scale model of the A-9A aircraft were conducted in the Propulsion Wind Tunnel (16T) for the Northrop Corporation at Mach numbers of 0.30, 0.60, 0.70, 0.75, and 0.80 at angles of attack and sideslip from -10 to 20 deg and 0 to 5 deg, respectively. Configuration variables included elevator, rudder, aileron, and speed brake deflections, horizontal tail dihedral angles, horizontal stabilizer incidence angles, external stores, and exit-nozzle core cowls. In addition, internal-duct drag was determined from the pressure data obtained from the exit nozzle and core cowl rakes. The primary purpose of the test was to obtain data at high subsonic Mach numbers at high Reynolds numbers.

SECTION II
APPARATUS

2.1 TEST FACILITY

Tunnel 16T is a continuous flow, closed-circuit, variable density wind tunnel capable of operating at Mach numbers from 0.15 to 1.60. The test section is 16 by 16 ft in cross section and 40 ft long. Perforated walls in the test section allow continuous operation through the Mach number range with a minimum of wall interference. A more extensive description of the test facility is given in the Test Facilities Handbook.[1] The sting support system was composed of a vertical support strut, sting support boom, and the high-angle-of-attack sting support system with an auxiliary roll mechanism.

The high-angle-of-attack sting support system was utilized to obtain angles of attack from -12 to 20 deg and also enable variations in sideslip by rolling the sting. Location of the model in the test section and details of the perforated walls are shown in Fig. 1 (Appendix I). Photographs of the model are presented in Fig. 2.

2.2 TEST ARTICLE

2.2.1 Aircraft Model

The test article was a 0.12-scale model of the A-9A aircraft which represented the prototype configuration. Details of the model are presented in Figs. 3 and 4 where the complete configuration is shown and the individual components are identified. The aileron (left wing only), elevators, and rudder were remotely controlled, whereas the speed brakes, horizontal tail dihedral, and horizontal stabilizer incidence angles were set manually during configuration changes. The model had flow-through inlets with ducts to simulate exit nozzles. The wing incidence angle was 0 deg with respect to the fuselage waterline. A 0.10-in.-wide boundary-layer trip was composed of number 80 grit and was located 0.80 in. from the leading edge of both surfaces of the wings and vertical and horizontal

[1]Test Facilities Handbook (Ninth Edition). "Propulsion Wind Tunnel Facility, Vol. 4." Arnold Engineering Development Center, July 1971.

stabilizers. In addition, a 0.10-in.-wide boundary-layer trip was affixed 0.80 in. aft of the nose. The index to model components and the configurations tested are listed in Table I (Appendix II).

2.2.2 Pylons and Store Models

The stores tested during this investigation were the MK-82 500-lb Bomb and the BLU-1/B Napalm Bomb. Sketches of these stores, associated pylons, and dispenser racks are presented in Figs. 4e, f, g, and h. All stores and pylons were nonmetric and were installed symmetrically on the parent model about its plane of symmetry.

2.3 INSTRUMENTATION

The overall aerodynamic forces and moments on the model were measured with a six-component, internal, strain-gage balance. The sensing components of the balance consisted of forward and aft normal-force elements (for determination of normal force and pitching moment), forward and aft side-force elements (for determination of side force and yawing moment), an axial-force element, and a rolling-moment element. Static pressures were measured at the sting entrance to the model and within the model cavity. A rake was attached to the model and positioned to measure pressures at the exit plane of the engine duct. The sting pitch angle was determined from the output of a strain-gaged angular position indicator. Sting roll angle was determined from the output of a potentiometer. The aileron, elevator, and rudder were instrumented with strain-gage hinge moment beams. The rotational angle of these surfaces was determined from the outputs of potentiometers. Electrical signals from the balances, pressure transducers, model attitude systems, and hinge-moment beams were digitized and recorded on magnetic tape, as well as fed directly to a computer for on-line data reduction. The balance and hinge-moment outputs were also recorded on an oscillograph for monitoring model dynamics.

SECTION III
TEST CONDITIONS AND PROCEDURE

3.1 TEST DESCRIPTION

The test was conducted at Mach numbers from 0.30 to 0.80 and Reynolds numbers of 2.3, 4.5, and 7.0 million based on the wing mean aerodynamic chord. The total pressure ranged from approximately 3660 psfa at M_∞ = 0.60 and Re = 7.0 x 10^6 to 1071 psfa at M_∞ = 0.8 and Re = 2.3 x 10^6. Total temperature was maintained at approximately 105°F for all Mach numbers.

Tunnel conditions were held constant at each Mach number, while the angle of attack was varied from -10 to 20 deg. For related configurations, combinations of a constant beta of 5 deg and angles of attack were obtained by pitching and rolling the model. The maximum angle of attack was limited to lower values in certain cases because of reaching dynamic load limits. Model variables included remotely controlled aileron, elevator, and rudder angles of 0, ±5, ±10, ±20, and ±30 deg; 0, ±5, and ±10 deg; and 0, 10, 20, and 30 deg, respectively. Additional configurations consisted of manually controlled

speedbrake, horizontal tail dihedral, and horizontal stabilizer incidence angles of 0, -20, and -60 deg; 0 and 10 deg; and 0 and ±2 deg, respectively.

3.2 ACCURACY OF MEASUREMENTS

The precision of setting and maintaining Mach number is estimated to be within ±0.004 for Mach numbers of 0.3 and ±0.003 and for Mach numbers from 0.60 to 0.80. Flow angularity corrections in the vertical plane of the tunnel, deduced from the upright and inverted runs, have been applied. Measured force and moment data on the balance were corrected for weight tares. No corrections have been made for cavity pressure base drag; however, internal duct drag-force data were measured and subtracted from the total drag force of the model. In addition to the measured drag values, interpolated values were used where measured data were not available.

The estimated uncertainties in the static-force data are given in the following table and are based on 95-percent probability.

	M_∞				
Parameter	0.30	0.60	0.70	0.75	0.80
α	±0.1	±0.1	±0.1	±0.1	±0.1
β	±0.1	±0.1	±0.1	±0.1	±0.1
C_L	±0.0158	±0.0083	±0.0060	±0.0047	±0.0037
C_m	±0.0031	±0.0082	±0.0010	±0.0011	±0.0011
C_Y	±0.0104	±0.0028	±0.0025	±0.0023	±0.0022
C_n	±0.0006	±0.0002	±0.0002	±0.0008	±0.0002
C_ℓ	±0.0004	±0.0001	±0.0001	±0.0005	±0.0001
C_D	±0.0031	±0.0019	±0.0020	±0.0012	±0.0011

SECTION IV
RESULTS AND DISCUSSION

4.1 GENERAL

The primary purpose of this investigation was to determine the effects of deflecting the aileron, elevator, rudder, and speed brakes on the aerodynamic forces and moments. These forces and moments were reduced to aerodynamic coefficients in the stability axes system about a moment reference center that was located at the quarter chord of the mean aerodynamic chord. The large volume of data obtained during this test precludes making detailed analysis of all the test data. Consequently, this report includes only the analysis of data from aileron, elevator, rudder, and speed brake deflections of the basic model with and without the empennage for nominal Reynolds numbers of 2.3 and 4.5 million at Mach numbers 0.3 and from 0.60 to 0.80, respectively. The complete test is documented in Table II where the part numbers are presented for each model configuration and test conditions for which data were obtained.

4.2 LONGITUDINAL STABILITY AND CONTROL

Presented in Fig. 5 are the curves of C_N, C_m, and C_D obtained during the tail component buildup tests. The ailerons, elevator, and rudder remained at zero, whereas the horizontal tail was installed at -2-deg incidence angle. As expected, Configurations XD_6 and $XD_6S_{1\text{-}5}$ V_2 d_2 r_3 (see Table I) were statically unstable, since these configurations were without a horizontal tail. The complete model was longitudinally statically stable for the Mach numbers and Reynolds numbers shown. The increase in drag at a lift coefficient of zero for the addition of the vertical tail and the horizontal tail were approximately 11 and 40 percent, 11 and 31 percent, 11 and 33 percent, 4 and 20 percent, and 0 and 10 percent for Mach numbers of 0.30, 0.60, 0.70, 0.75, and 0.80, respectively.

Presented in Fig. 6 are data showing the effectiveness of the horizontal stabilizer for providing longitudinal control as well as the increase in drag because of the change in incidence angle of the horizontal stabilizer. The data showed that linear changes in C_m were produced by deflecting the horizontal stabilizer at Mach numbers of 0.30, 0.60, and 0.70 until buffet onset or stall occurred. The stabilizer effectiveness remained unchanged as free-stream Mach number was increased from 0.30 to 0.70 but decreased with further increases in Mach number. The deflection of the horizontal tail to ±2 deg showed an incremental shift in the lift curve.

The effects of deflecting the elevator on the aerodynamic characteristics of the A-9A model are presented in Fig. 7. Deflections of the horizontal stabilizer and the elevator showed similar effects in pitching moments but with different orders of magnitude which were attributable to the difference in surface areas. The stabilizer was 20 to 50 percent more effective in pitching moment per degree of deflection than the elevator.

4.3 LATERAL STABILITY AND CONTROL

Figure 8 shows a noticeable effect on the lift, drag, pitching moment, and rolling-moment coefficients attributable to aileron deflections. The data showed that as the aileron on the left wing was deflected ±10 deg a proportional increase occurred in C_ℓ at M_∞ = 0.30, 0.60, and 0.70. However, at M_∞ = 0.75 and 0.80, the negative 10-deg (trailing edge up) deflection did not produce an equivalent ΔC_ℓ to the values obtained for the positive aileron deflection. At M_∞ = 0.80, a reversal in the sign of the rolling moment occurred for model angles of attack between 1 and 9 deg for δ_{AL} = -10 deg. This anomaly in the data was eliminated when the speed brakes were deflected 20 and 60 deg at M_∞ = 0.75 and 0.80 for δ_{AL} = -10 deg as shown in Figs. 8f and g. Therefore, the reversal in rolling moment at M_∞ = 0.80 for the negative 10-deg aileron deflection is attributed to some type of local flow separation which reduced the aileron's effectiveness.

4.4 DIRECTIONAL STABILITY AND CONTROL

The changes in aerodynamic coefficients resulting from rudder deflections at β = 0 deg are presented in Fig. 9. These data show that the rudder effectiveness was essentially

constant for C_Y, C_n, and C_ℓ up to 20 deg. At rudder deflection angles greater than 20 deg, there was less rudder effectiveness. The rudder remained effective for all Mach numbers.

4.5 SPEED BRAKE EFFECTIVENESS

For data presented in Fig. 10 with the speed brakes deflected, the elevator and the rudder were at 0 deg, whereas the horizontal stabilizer incidence angle was at -2 deg. Deflecting the speed brake 60 deg reduced the value of the lift curve slope and significantly delayed the onset of buffet at Mach numbers of 0.70, 0.75, and 0.80. The speed brake deflection angle of 20 and 60 deg increased the minimum drag by 100 and 600 percent, respectively. The deflection of the speed brake from 20 to 60 deg produced a large destabilizing moment.

SECTION V
CONCLUSIONS

The results of a test conducted at Mach numbers from 0.3 to 0.8 to determine the aerodynamic characteristics of the A-9A aircraft led to the following remarks:

1. The stabilizer effectiveness remained unchanged as free-stream Mach number was increased from 0.30 to 0.70 but decreased with a further increase in free-stream Mach number.

2. The effectiveness of the aileron to produce a corresponding rolling moment for a negative aileron deflection was reduced to zero for angles of attack from approximately 1 to 9 deg at Mach number 0.80.

3. The rudder remained effective for all Mach numbers from 0.30 to 0.80.

4. Increasing the deflection angle of the speed brakes produced a destabilizing pitching moment and delayed the onset of wing buffet.

5. Minimum drag was increased by factors of approximately 100 and 600 percent for speed brake deflection angles of 20 and 60 deg, respectively, at Mach numbers from 0.70 to 0.80.

6. The horizontal stabilizer was 20 to 50 percent more effective in pitching moment per deg of deflection than the elevator.

APPENDIXES

I. ILLUSTRATIONS

II. TABLES

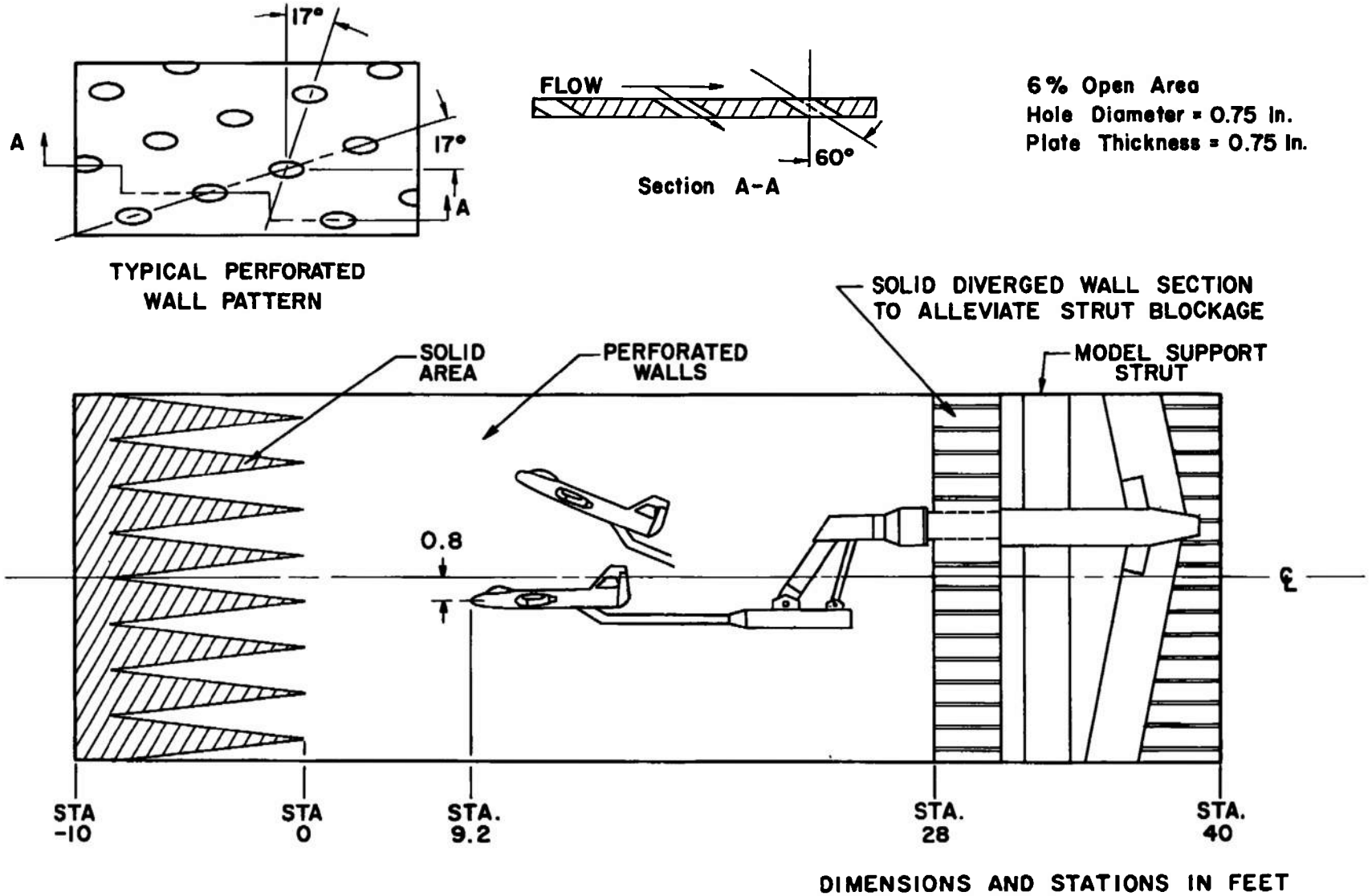

Fig. 1 Schematic of Model Installation

AEDC-TR-71-271

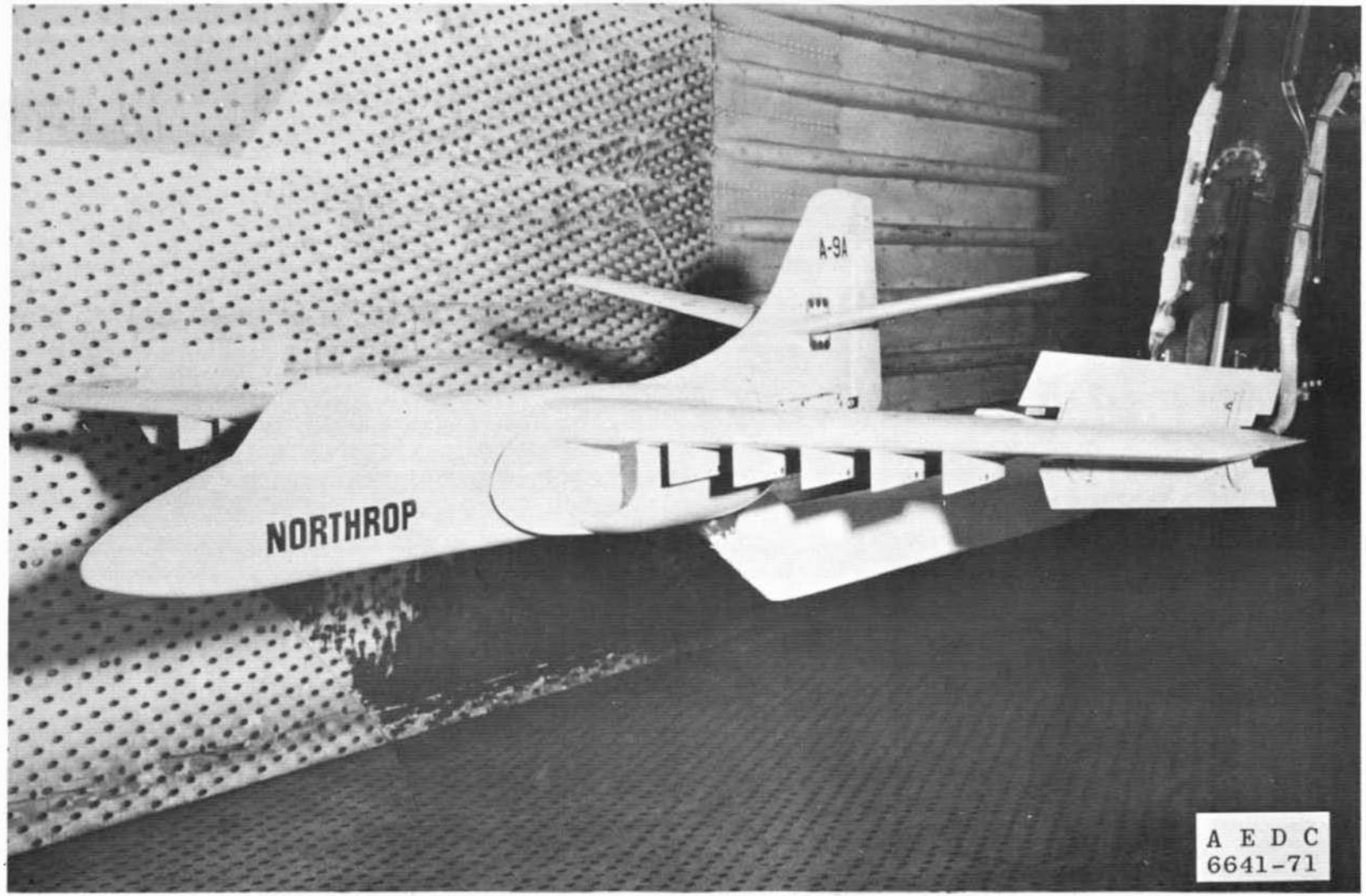

a. Speed Brake Extended

Fig. 2 Photograph of Model Installation

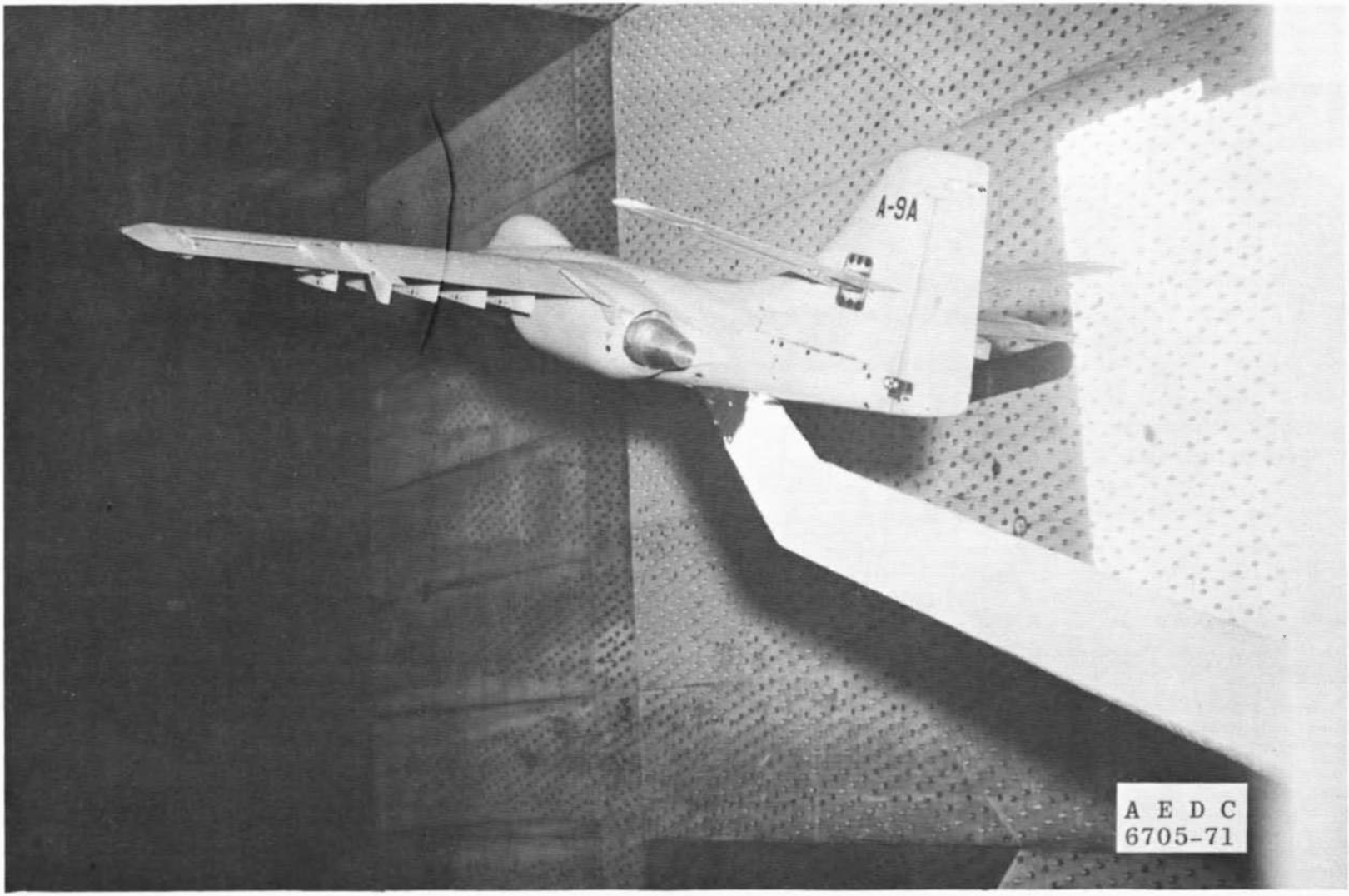

b. Speed Brake Retracted
Fig. 2 Concluded

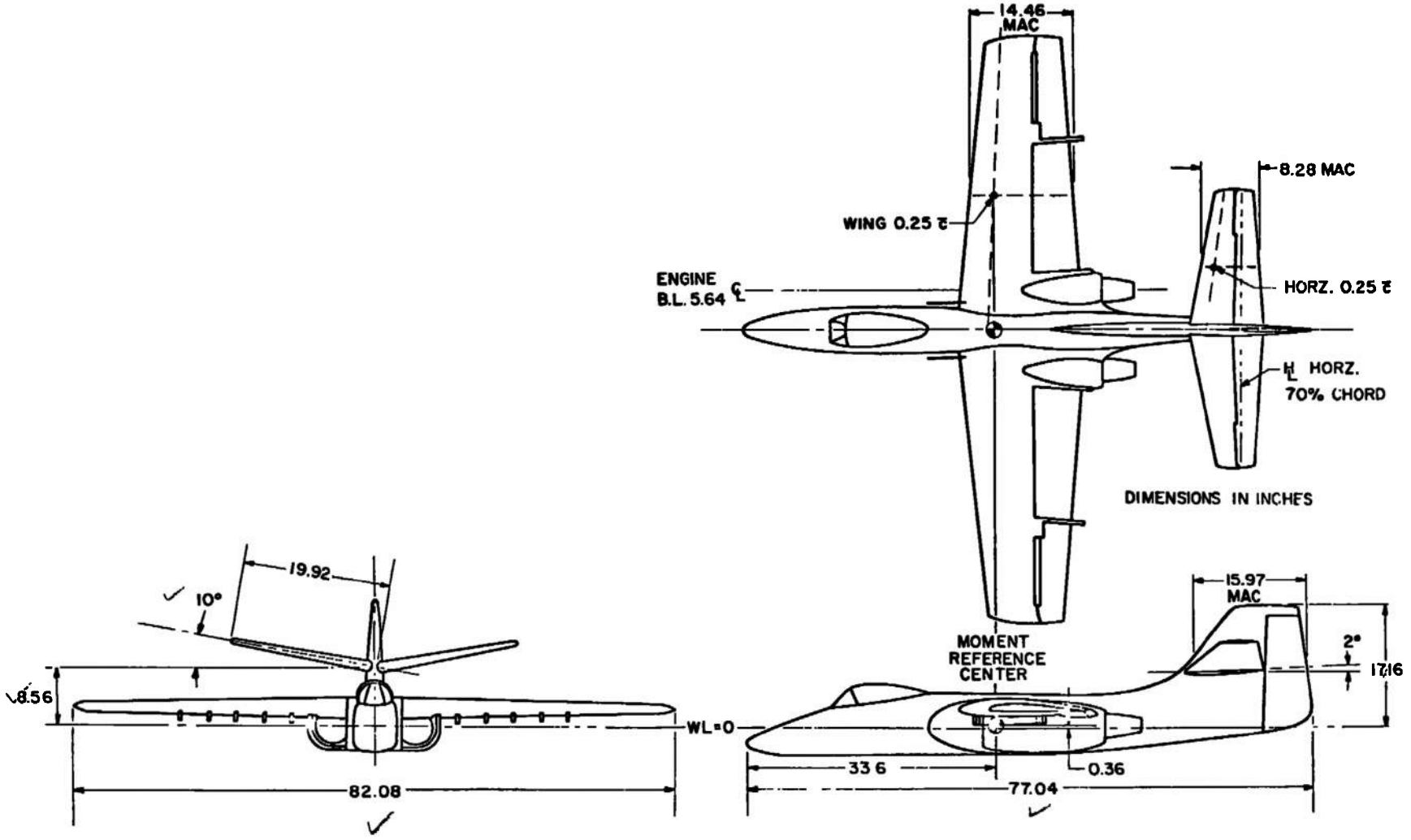

Fig. 3 Model Sketch

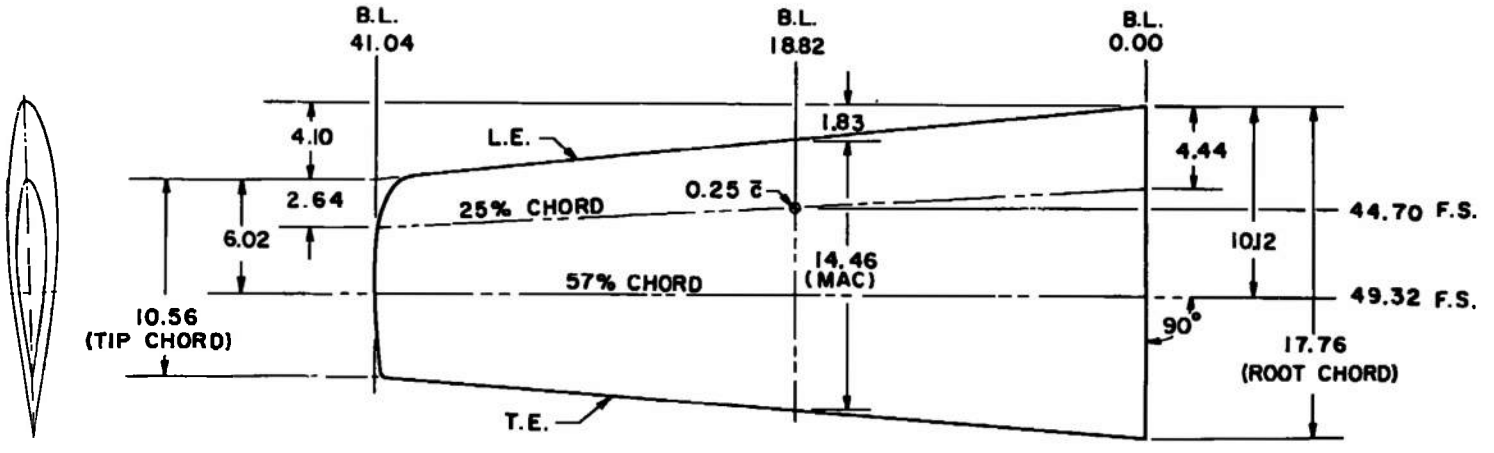

DIMENSIONS IN INCHES

a. Wing

Fig. 4 Dimensional Sketches of Model Components

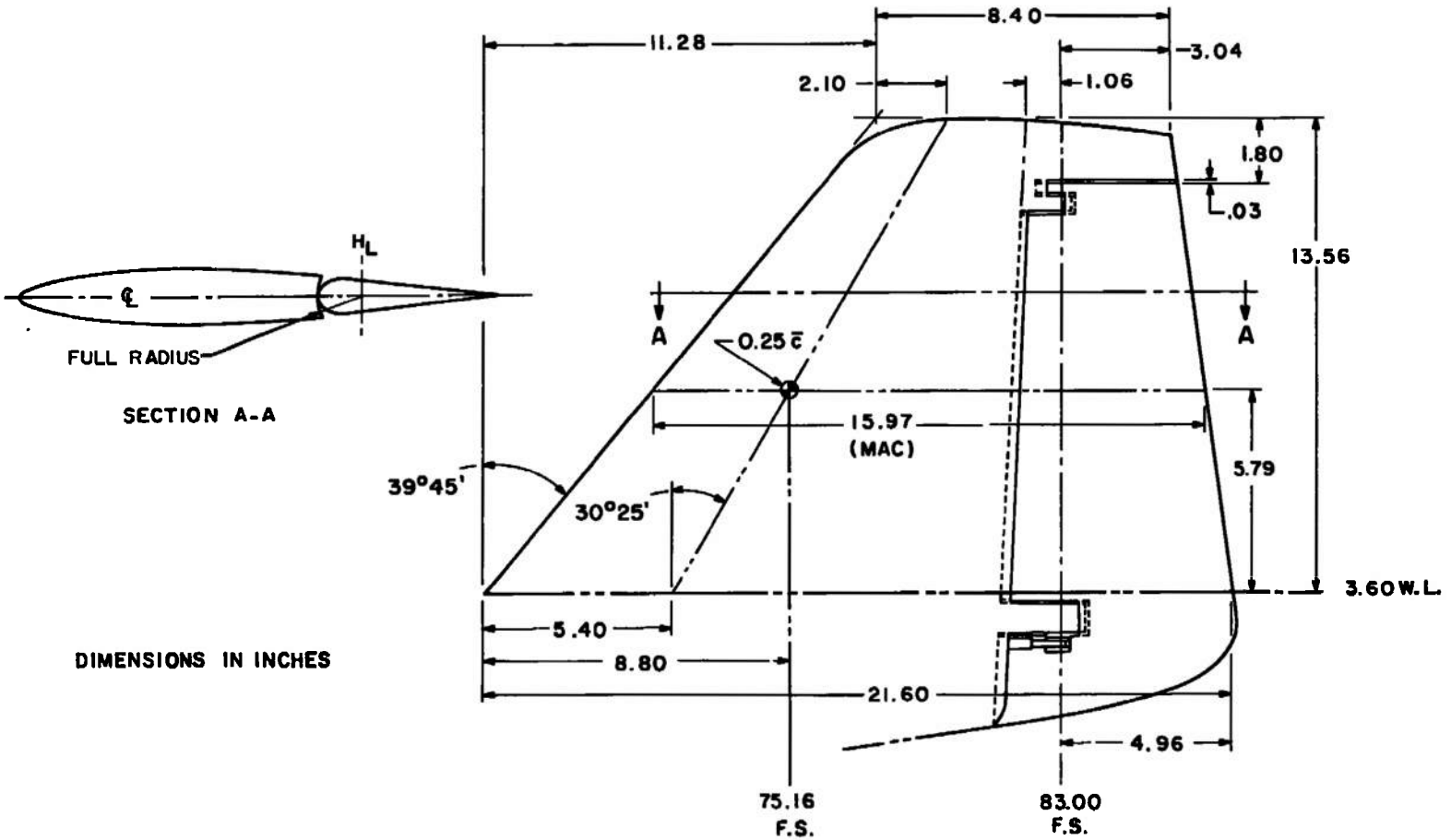

b. Vertical Tail
Fig. 4 Continued

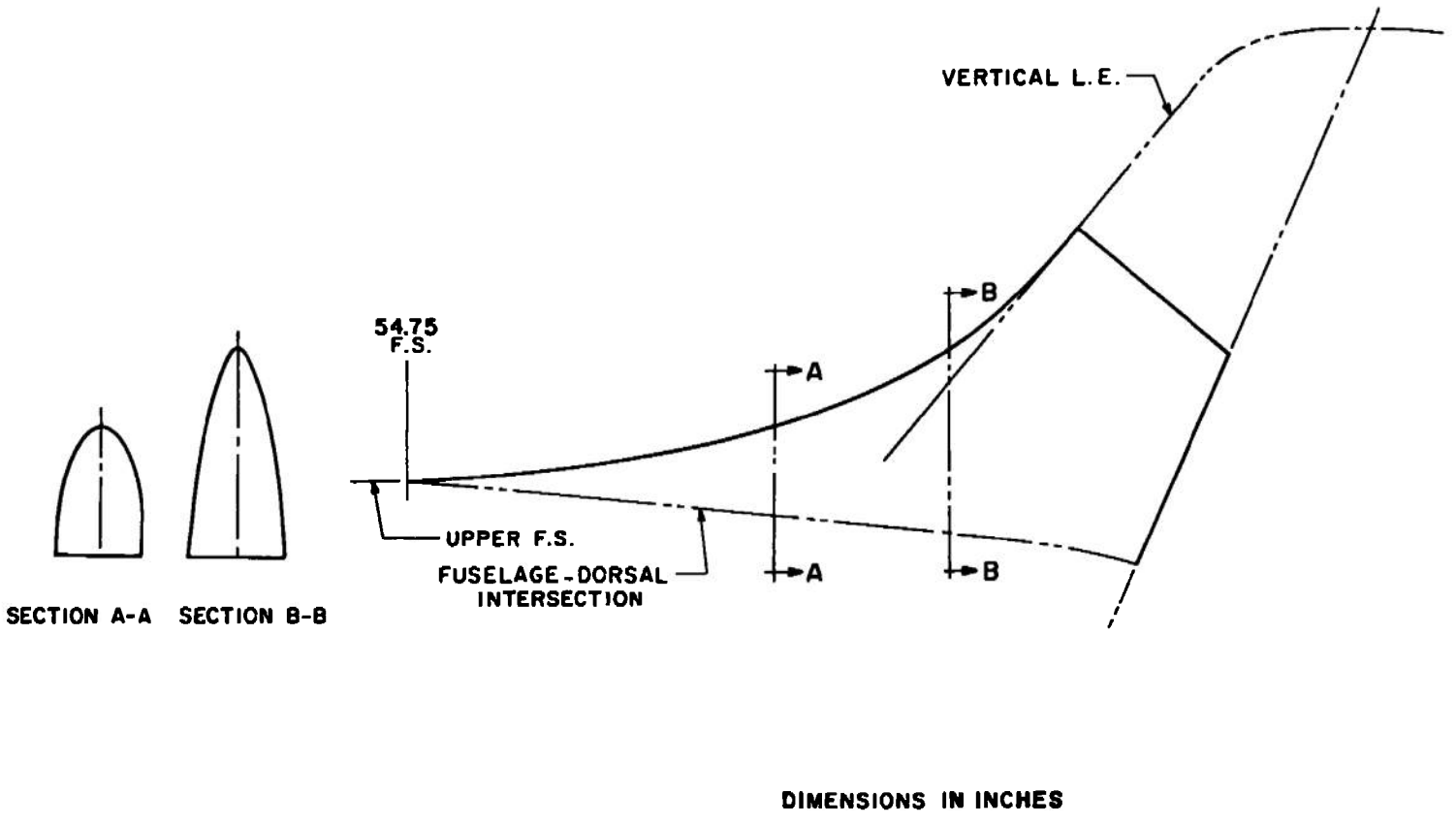

c. Dorsal Fin
Fig. 4 Continued

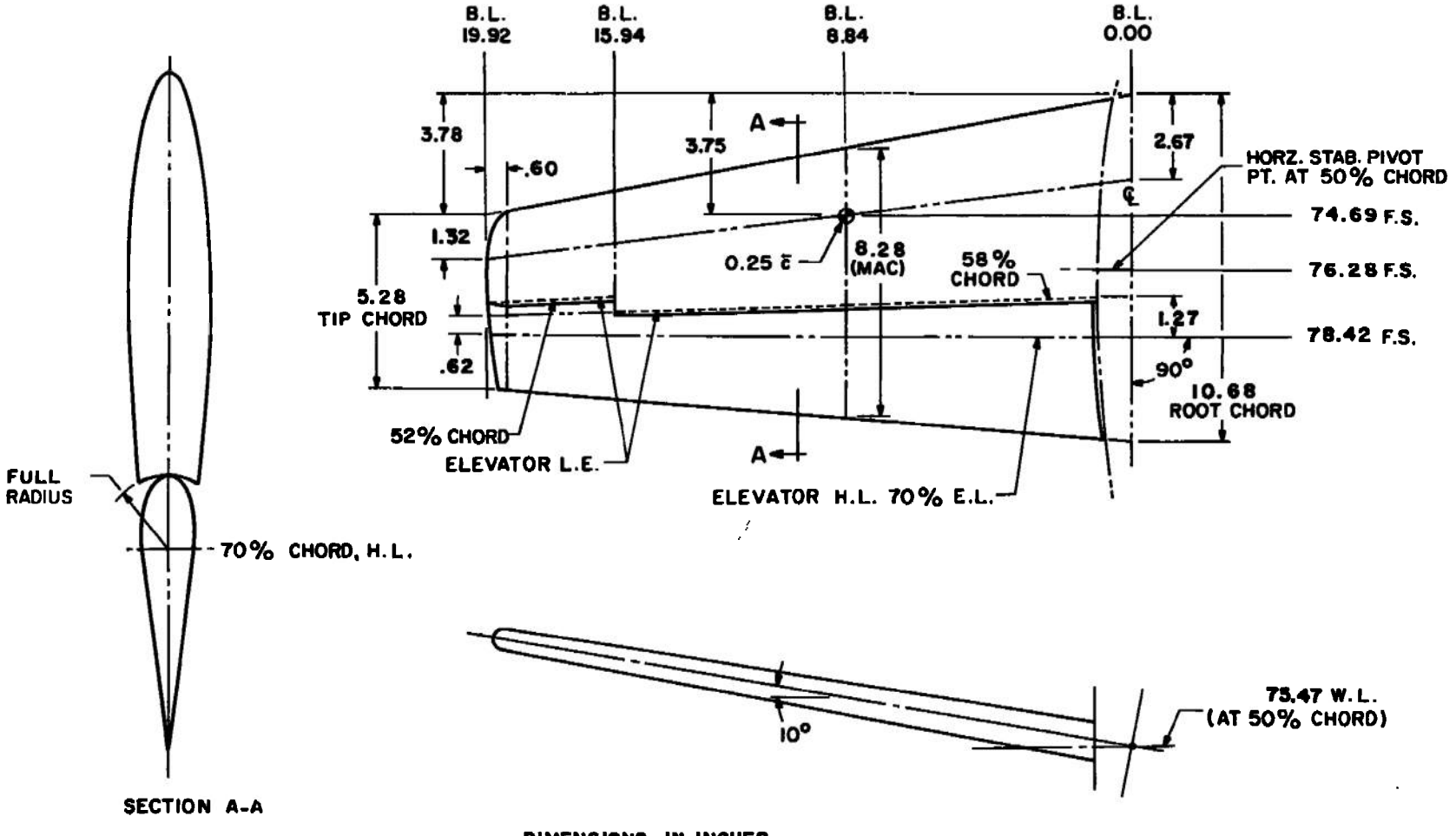

DIMENSIONS IN INCHES

d. Horizontal Tail
Fig. 4 Continued

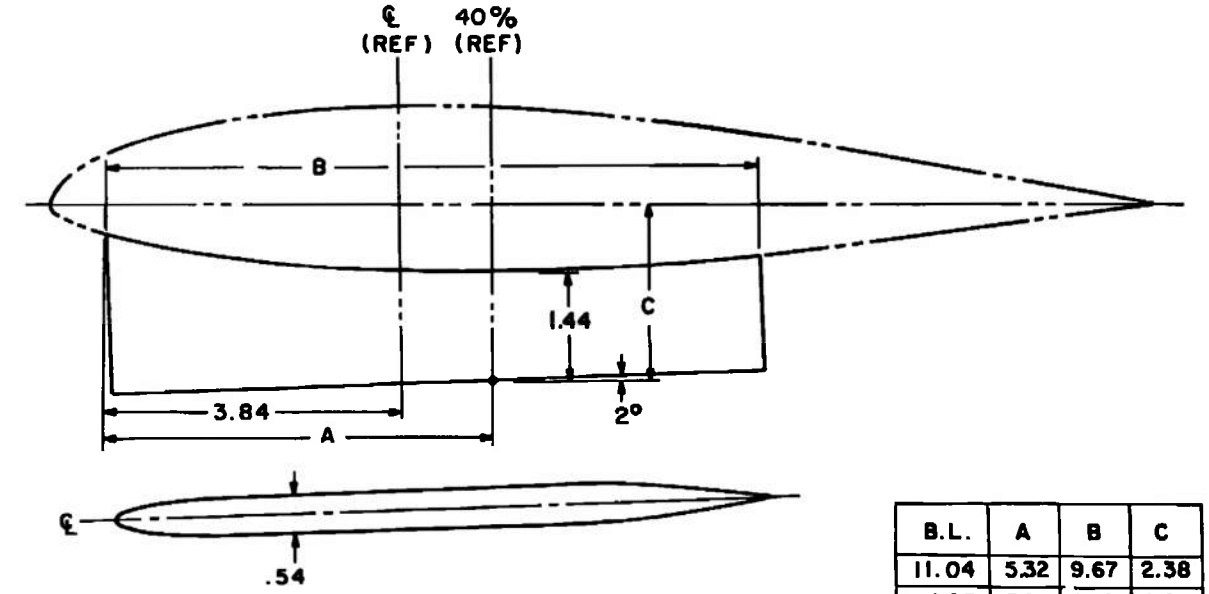

B.L.	A	B	C
11.04	5.32	9.67	2.38
14.88	5.31	9.13	2.34
18.72	5.06	8.60	2.30
22.56	4.92	8.09	2.26
26.40	4.79	7.52	2.22

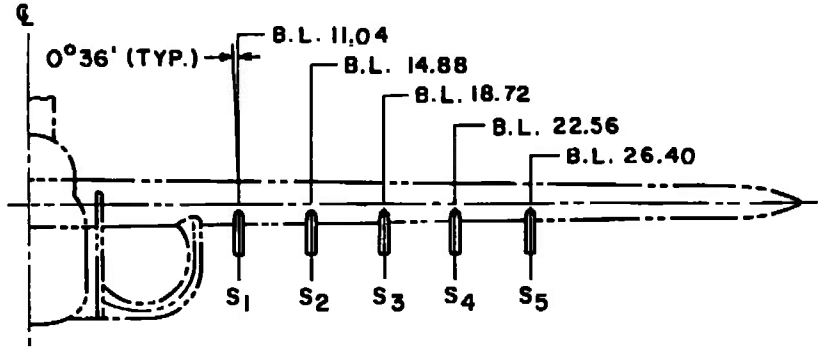

DIMENSIONS IN INCHES

e. Wing Pylon Locations
Fig. 4 Continued

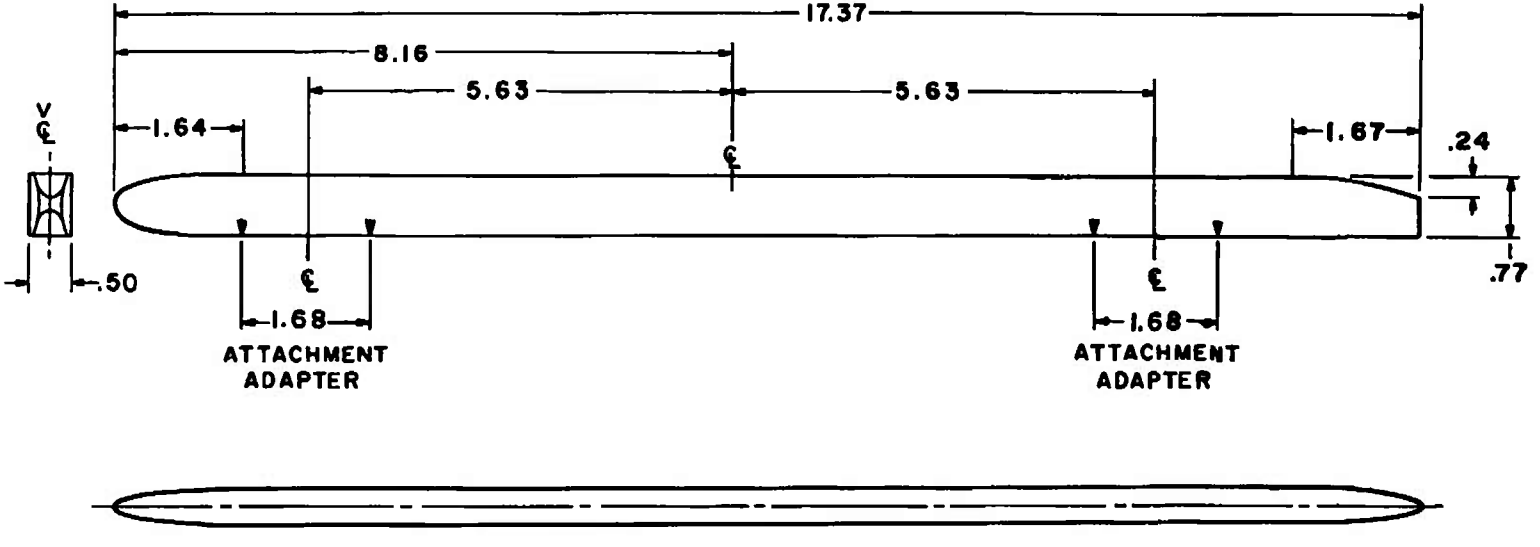

DIMENSIONS IN INCHES

f. Pylon Extension Rack
Fig. 4 Continued

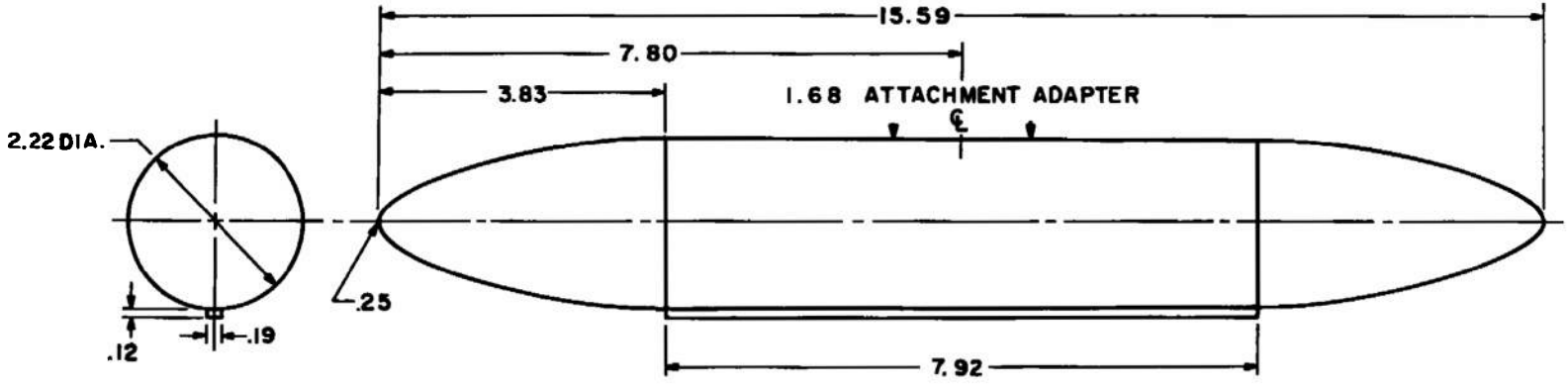

DIMENSIONS IN INCHES

g. BLU-1/B
Fig. 4 Continued

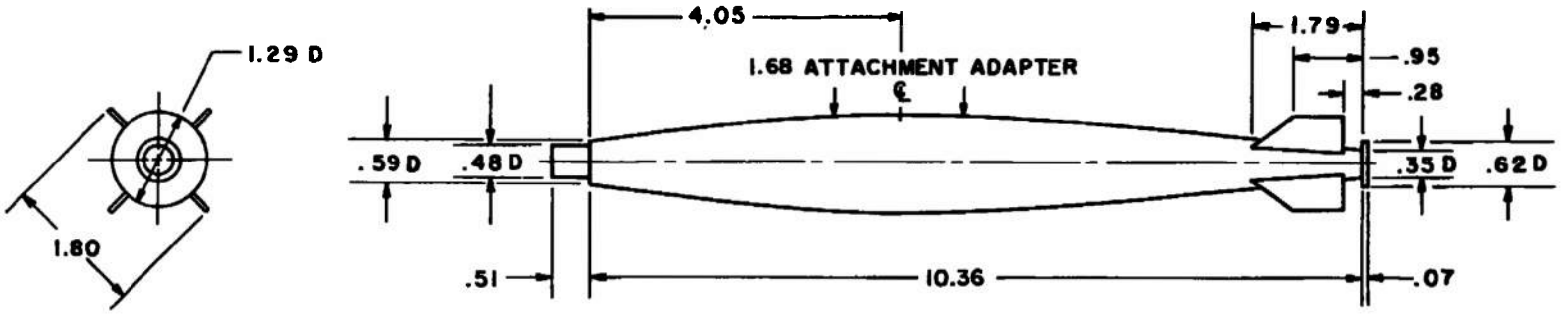

DIMENSIONS IN INCHES

h. MK-82

Fig. 4 Concluded

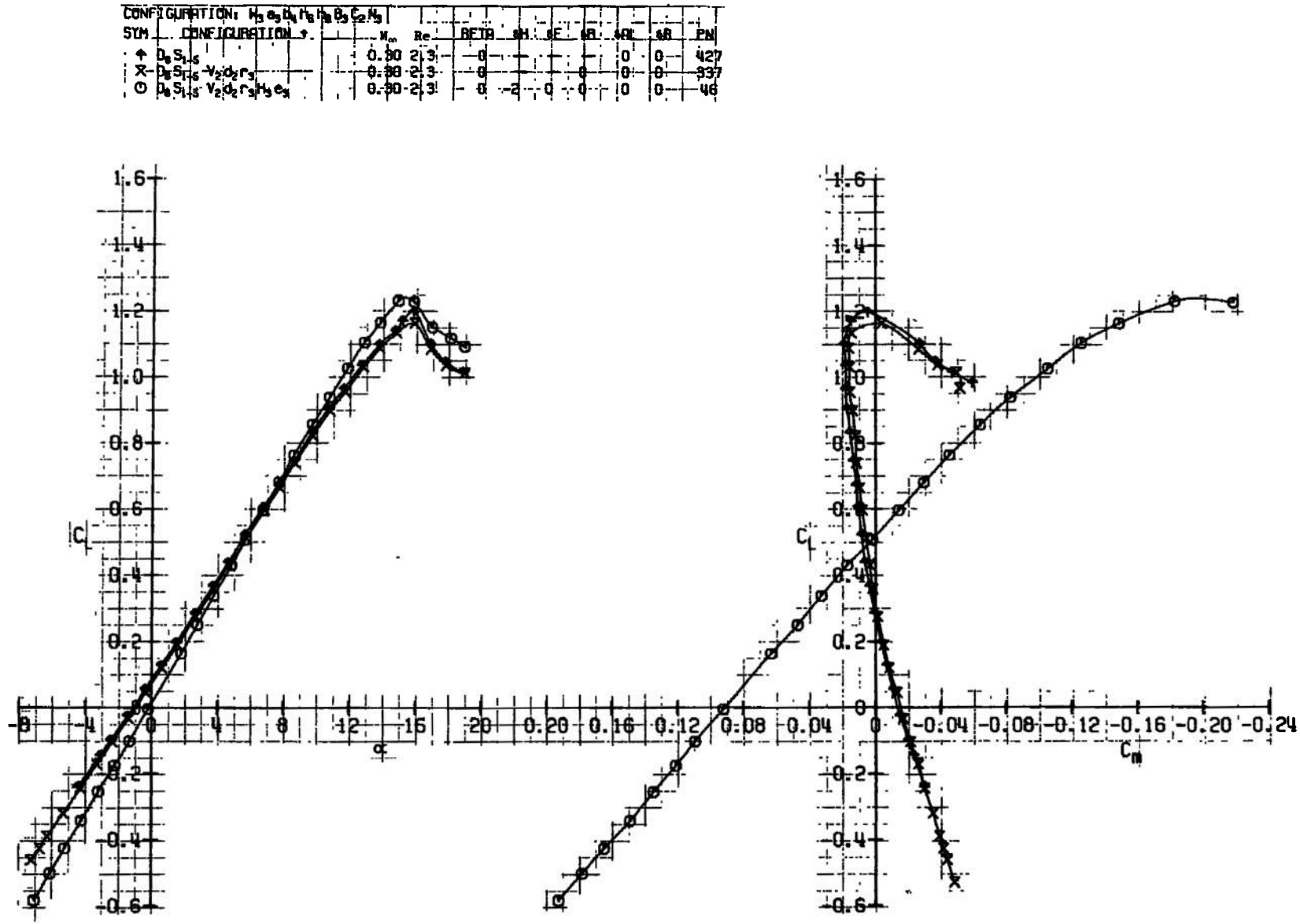

a. $M_\infty = 0.30$

Fig. 5 Effect of Tail Components

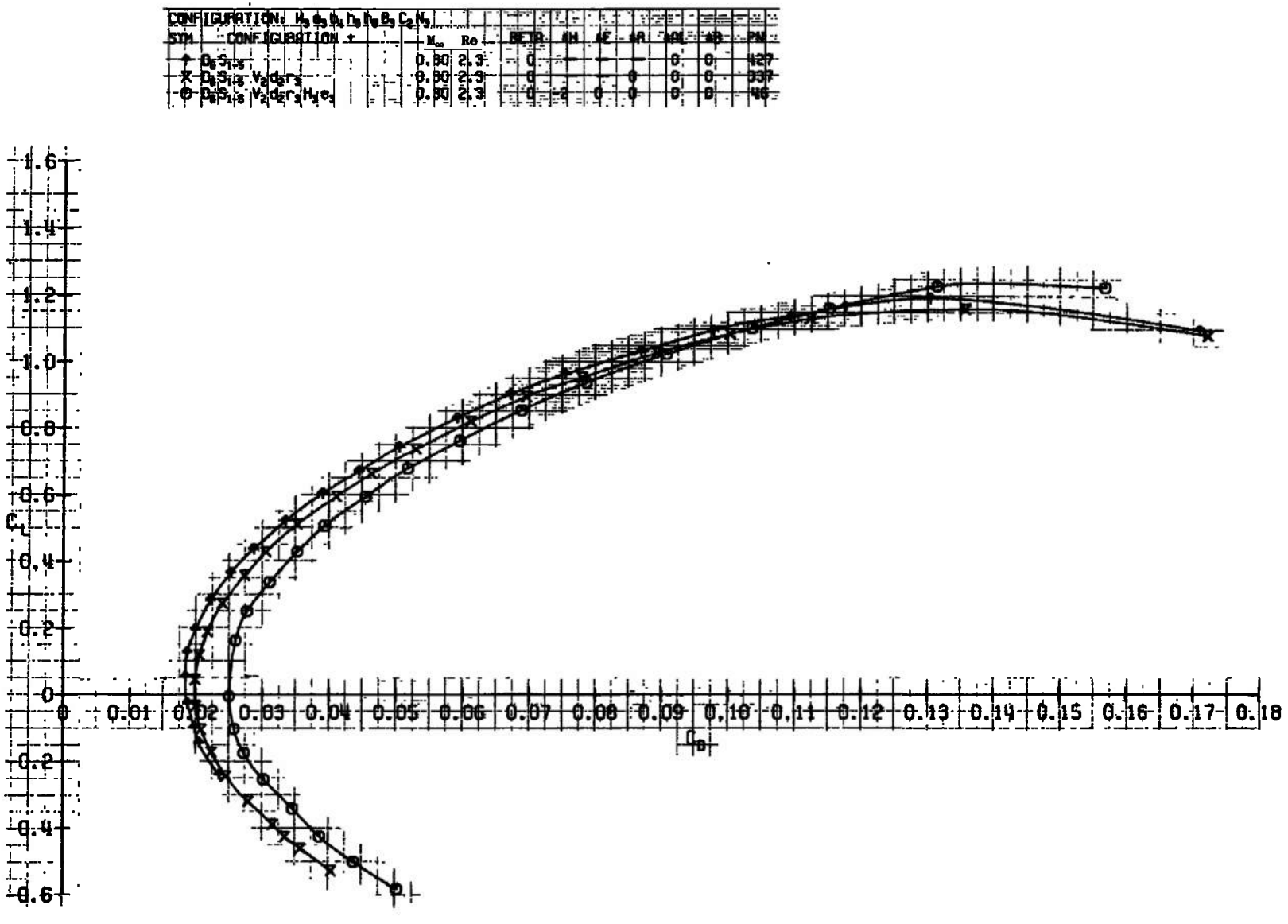

a. Concluded

Fig. 5 Continued

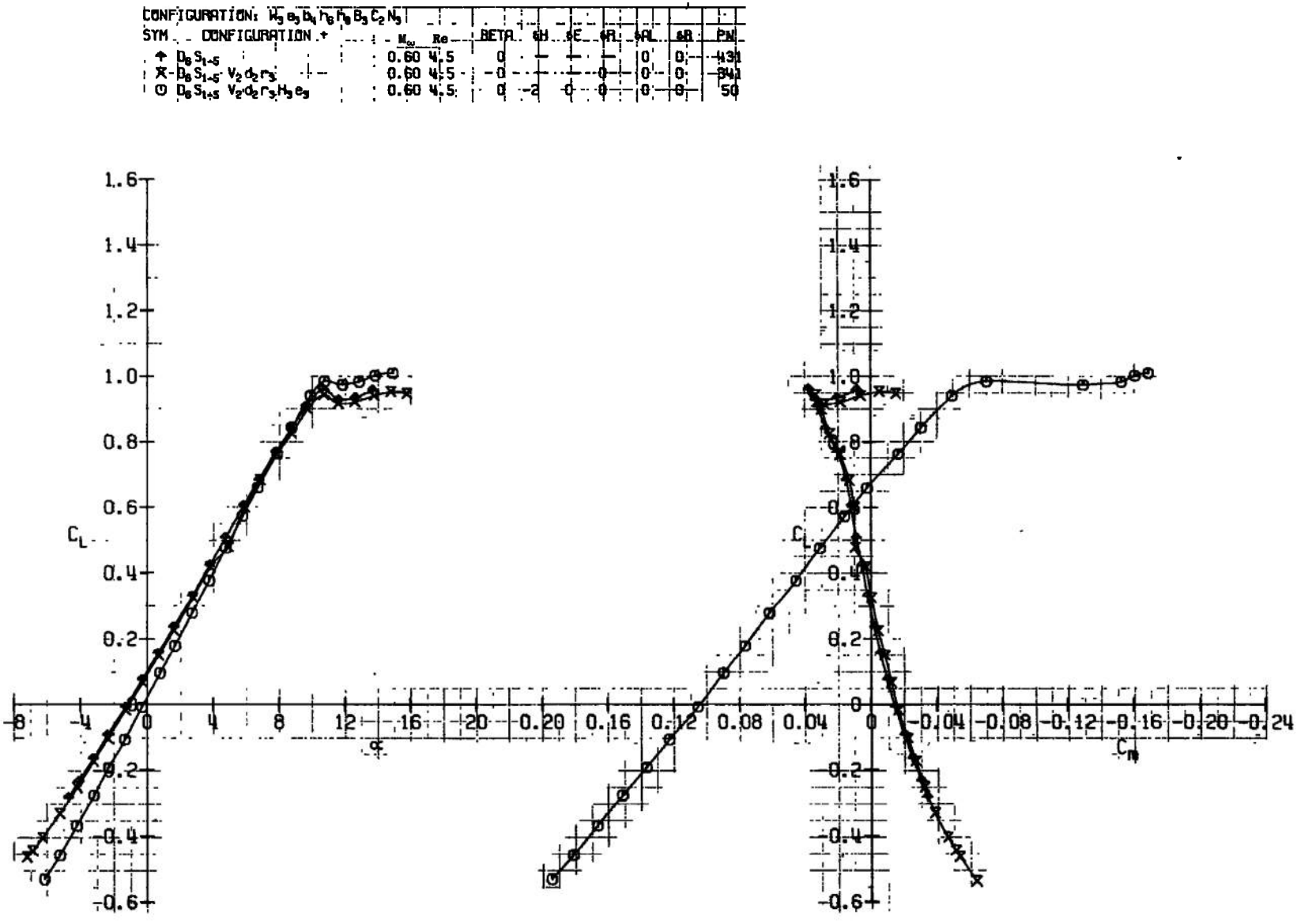

b. $M_\infty = 0.60$

Fig. 5 Continued

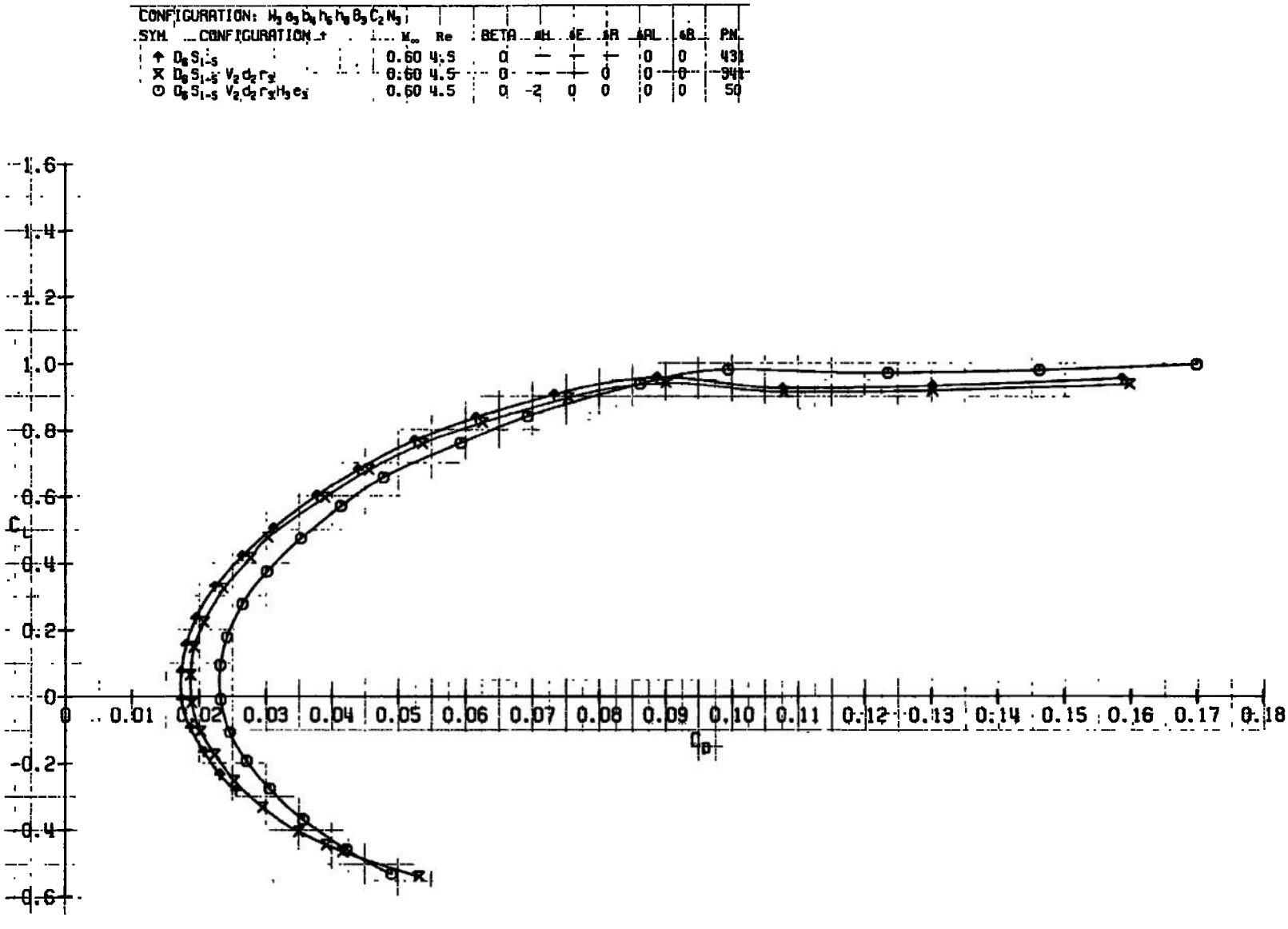

b. Concluded
Fig. 5 Continued

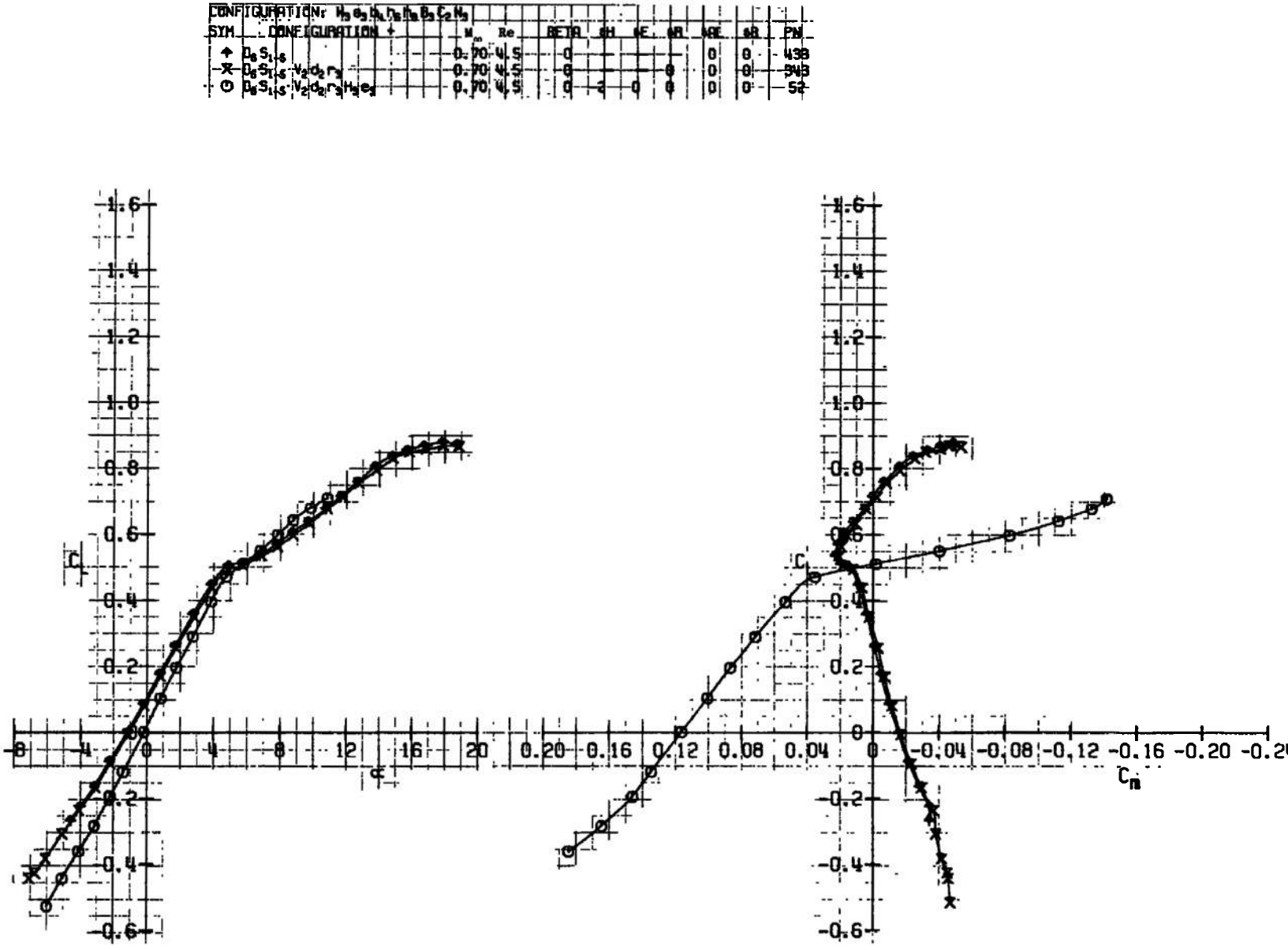

c. $M_\infty = 0.70$

Fig. 5 Continued

CONFIGURATION: $W_2 e_3 b_4 h_8 H_8 B_3 C_2 N_3$

SYM	CONFIGURATION →	M_∞	Re	BETA	δH	δE	δR	δRL	δR	PN
↑	$D_6 S_{1+5}$	0.70	4.5	0	+	—	—	0	0	439
✕	$D_6 S_{1+5} V_2 d_2 r_3$	0.70	4.5	0	—	—	0	0	0	345
⊙	$D_6 S_{1+5} V_2 d_2 r_3 H_3 e_3$	0.70	4.5	0	-2	0	0	0	0	52

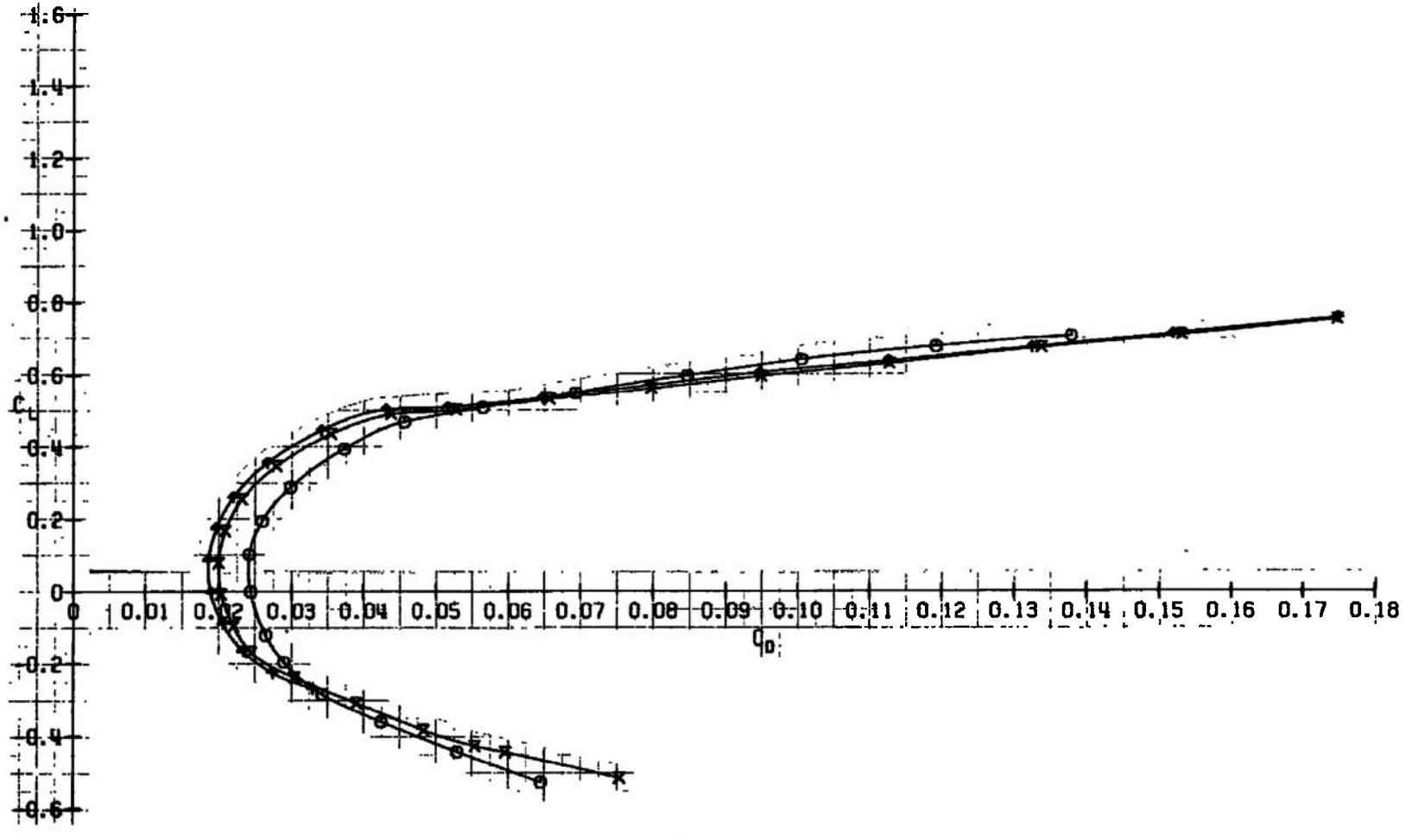

c. Concluded

Fig. 5 Continued

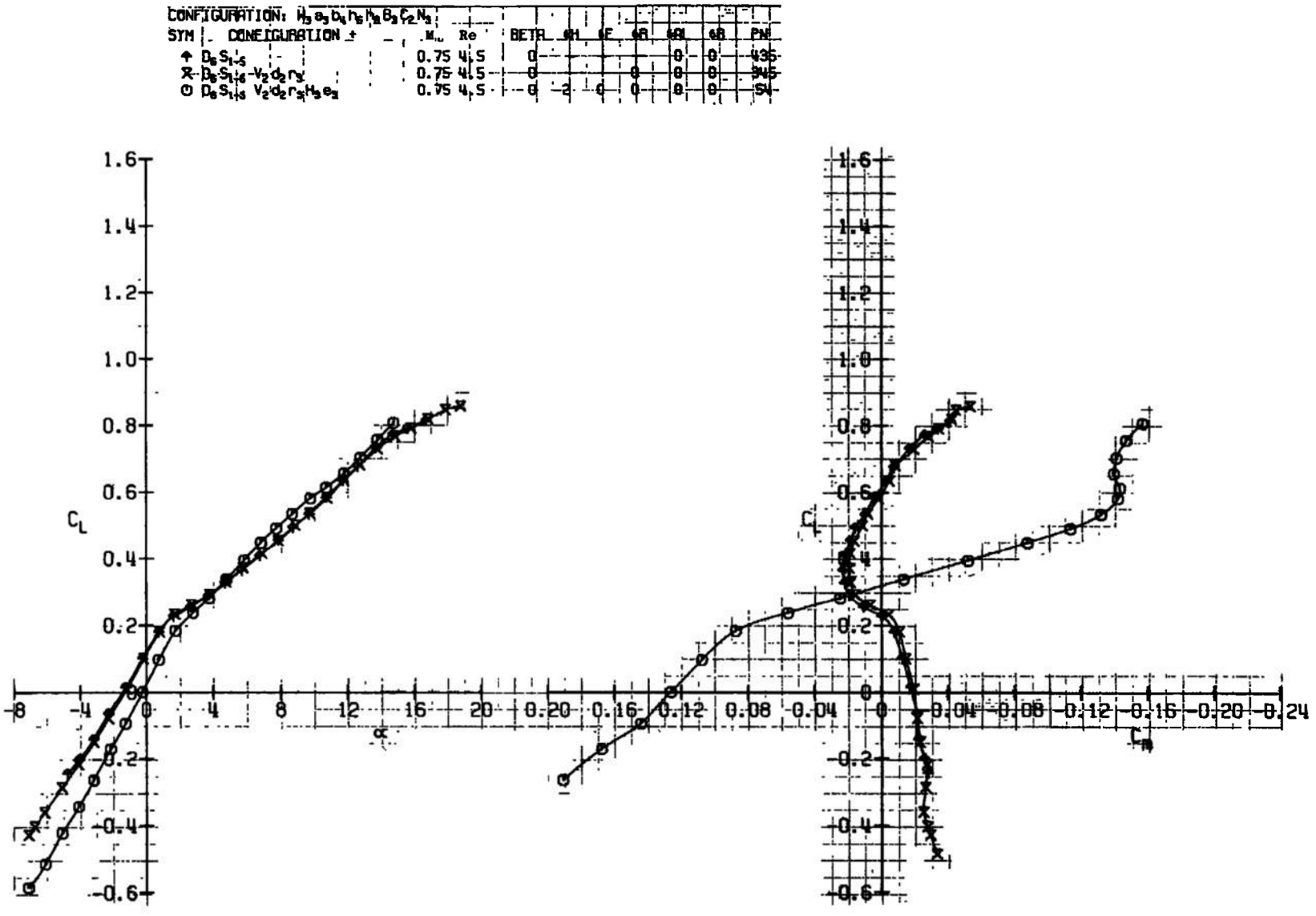

d. $M_\infty = 0.75$

Fig. 5 Continued

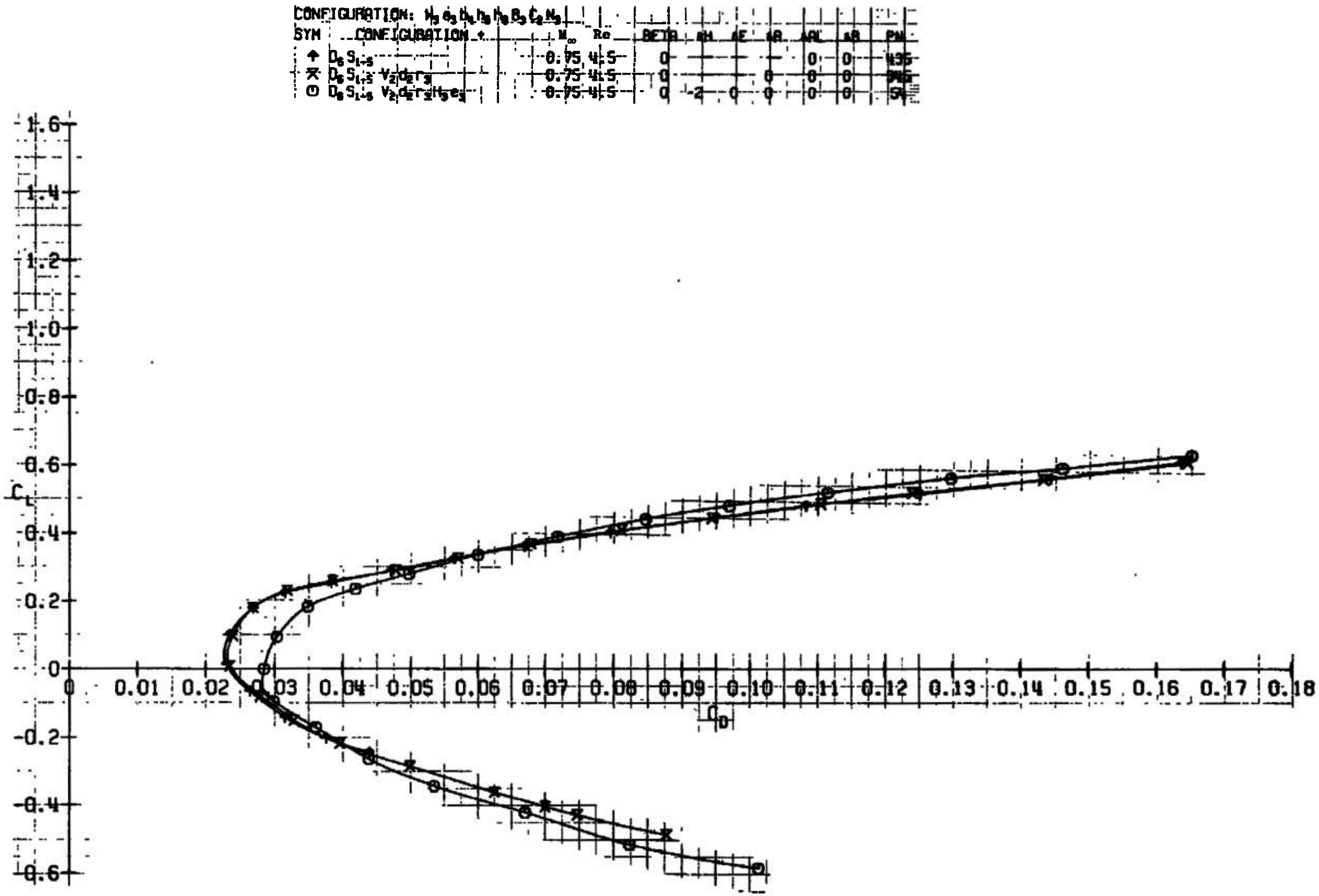

d. Concluded

Fig. 5 Continued

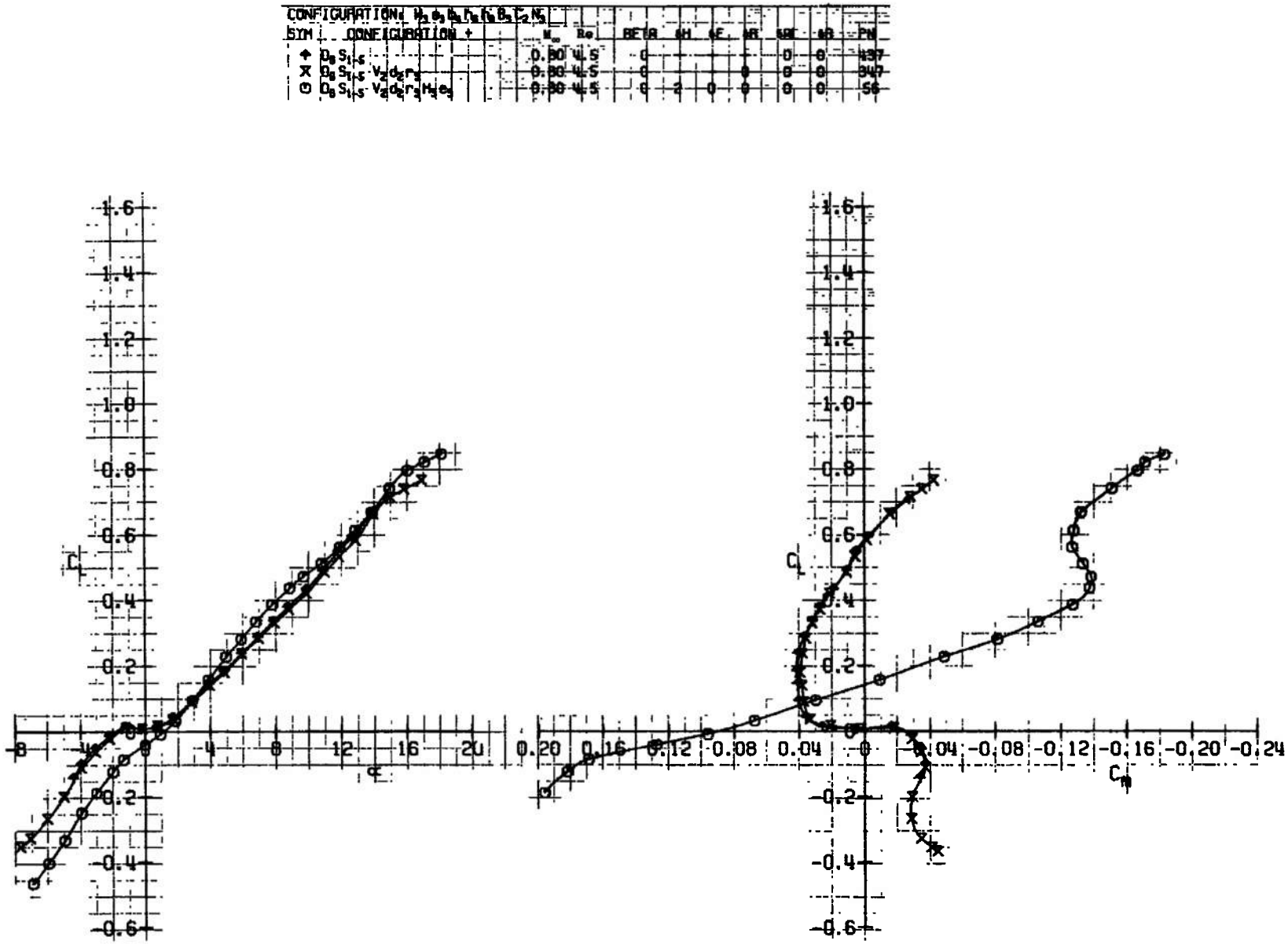

e. $M_\infty = 0.80$

Fig. 5 Continued

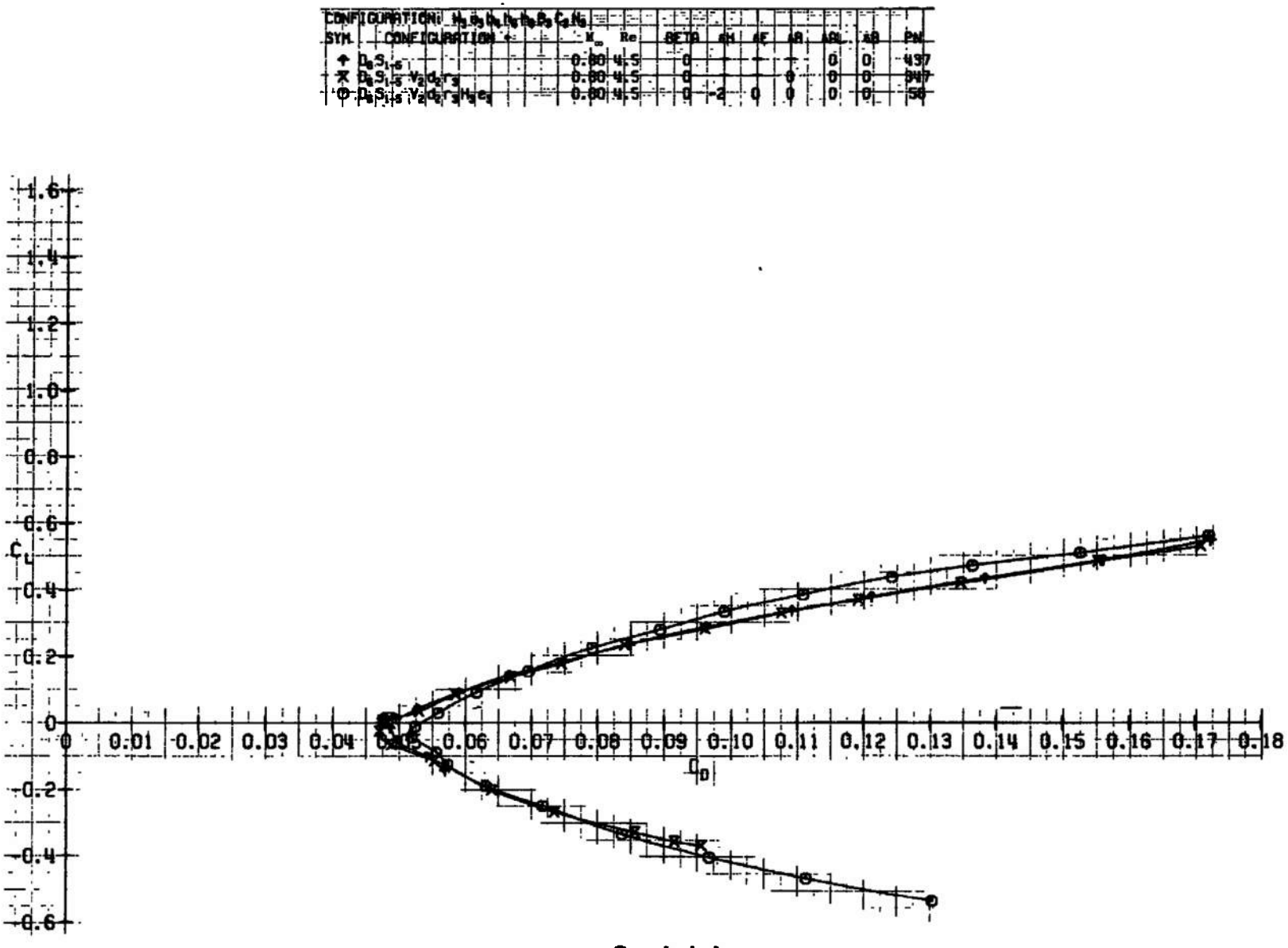

e. Concluded

Fig. 5 Concluded

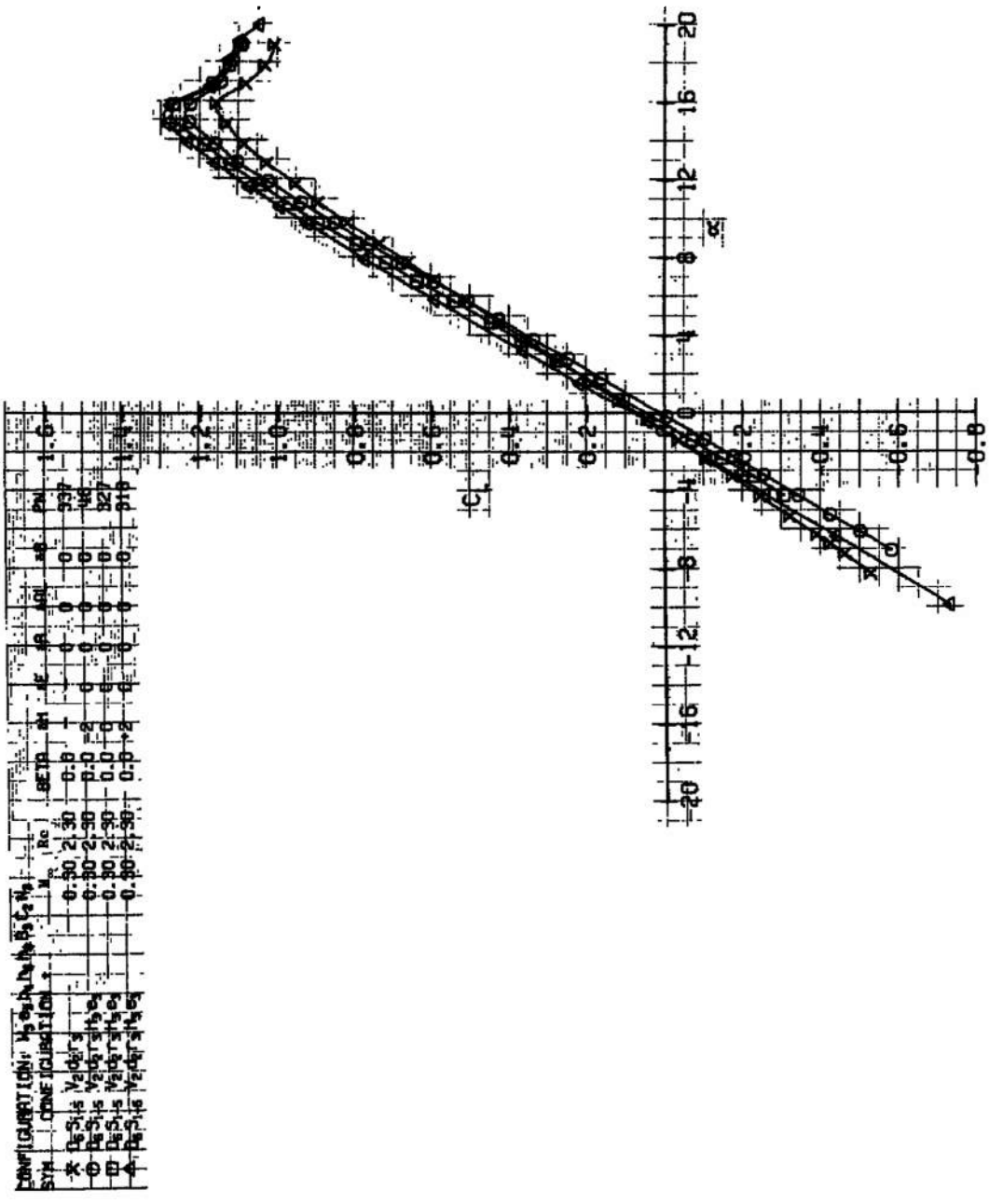

a. $M_\infty = 0.30$

Fig. 6 Stabilizer Effectiveness

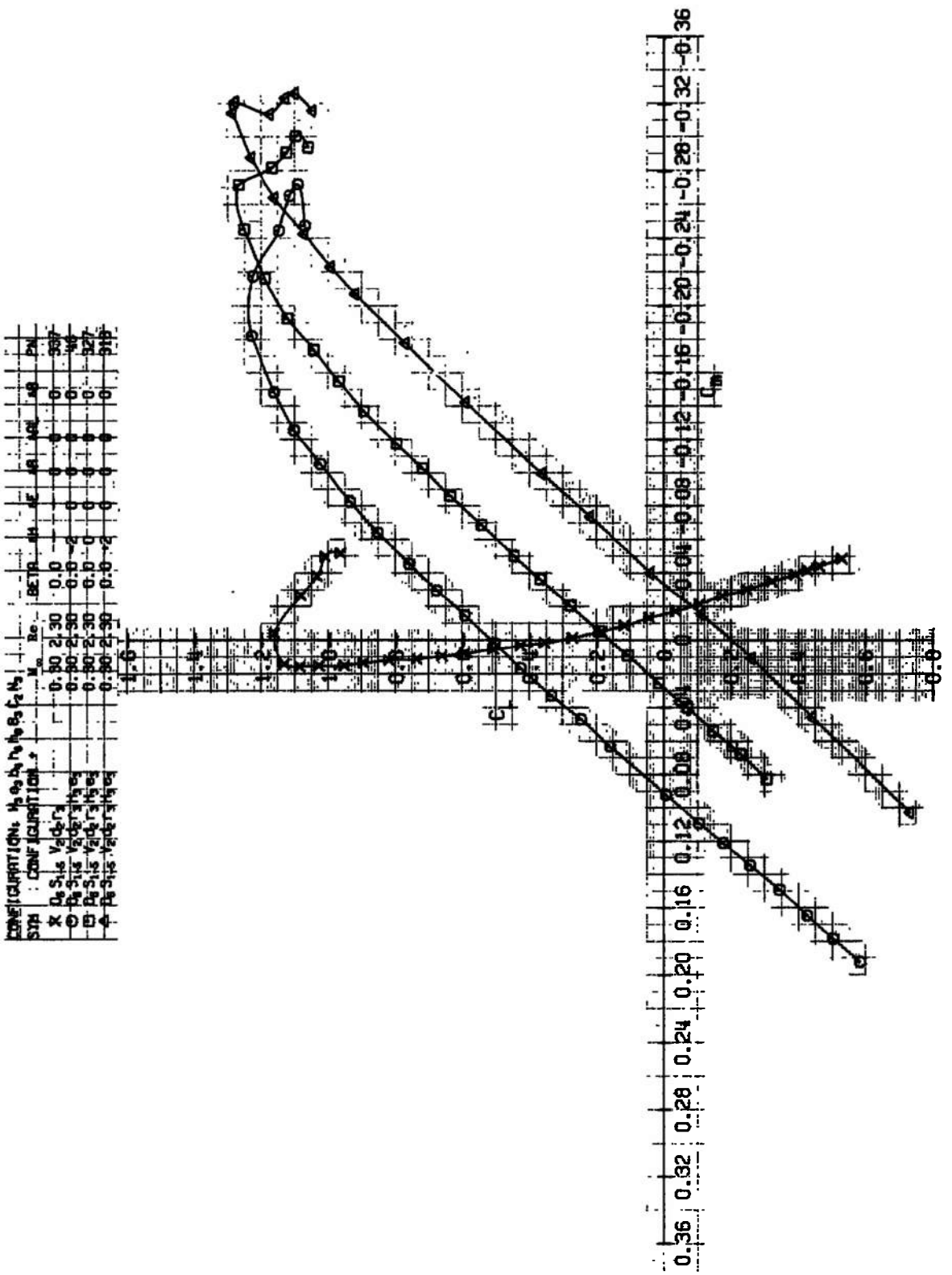

a. Continued
Fig. 6 Continued

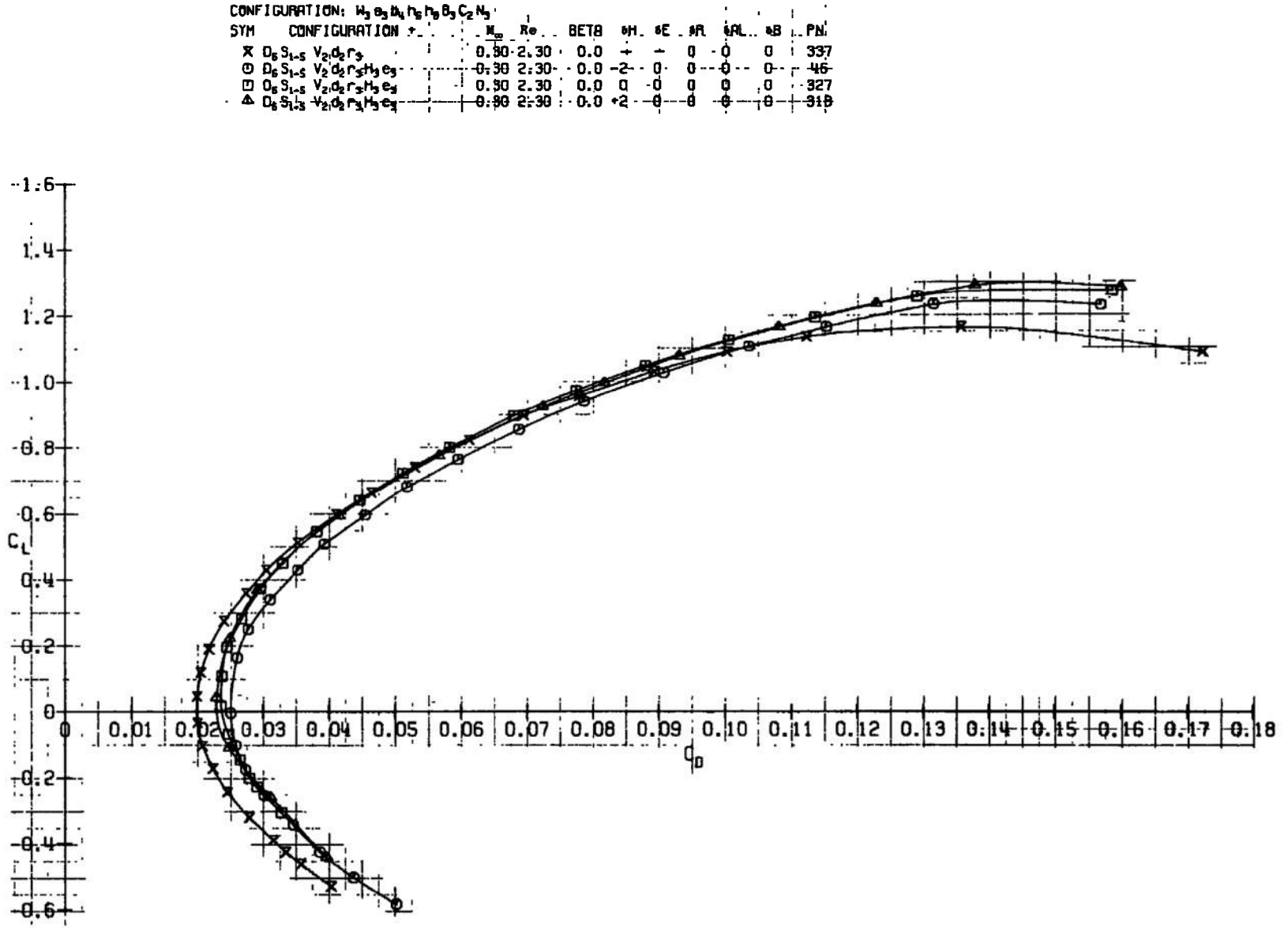

a. Concluded

Fig. 6 Continued

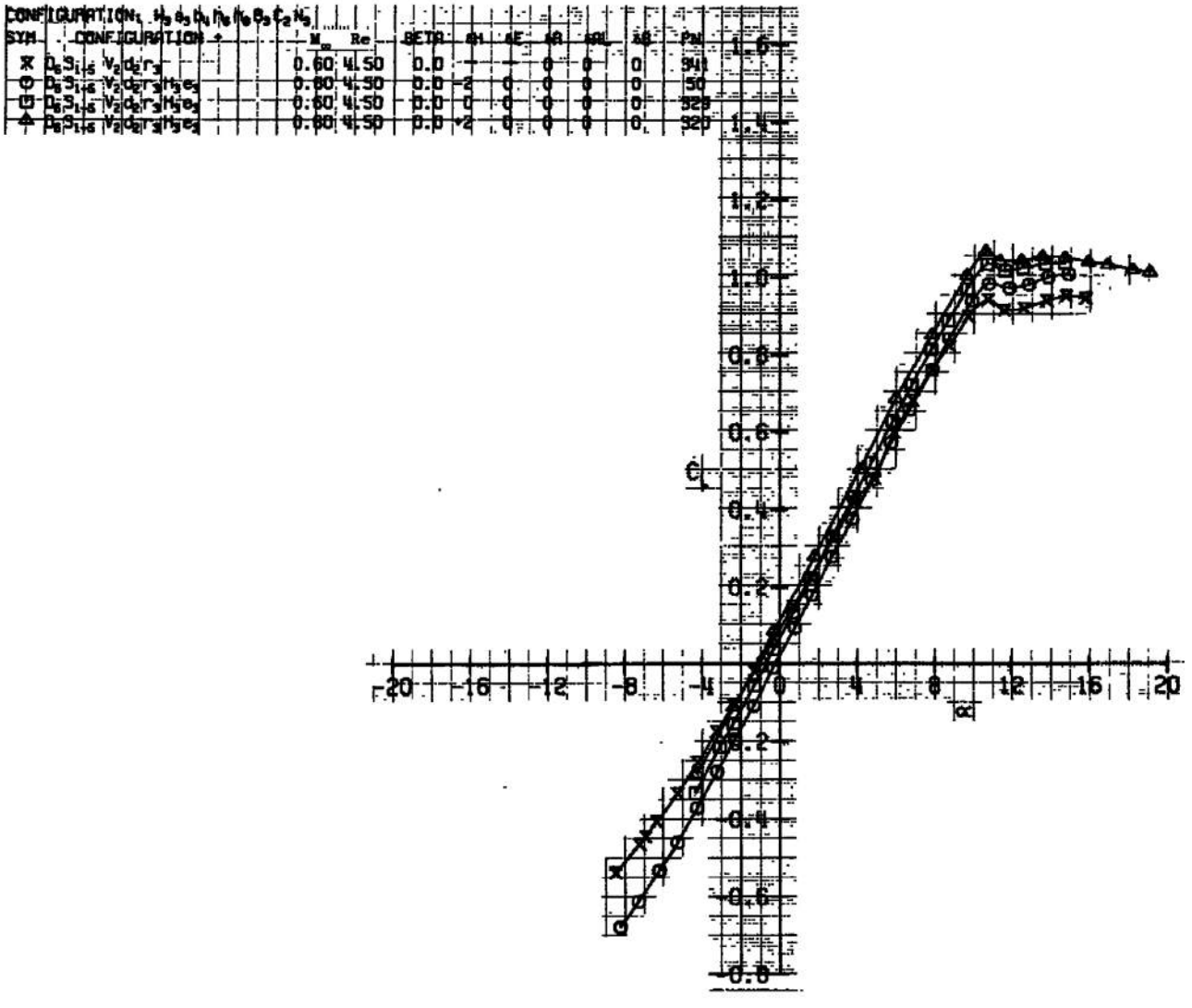

b. $M_\infty = 0.60$

Fig. 6 Continued

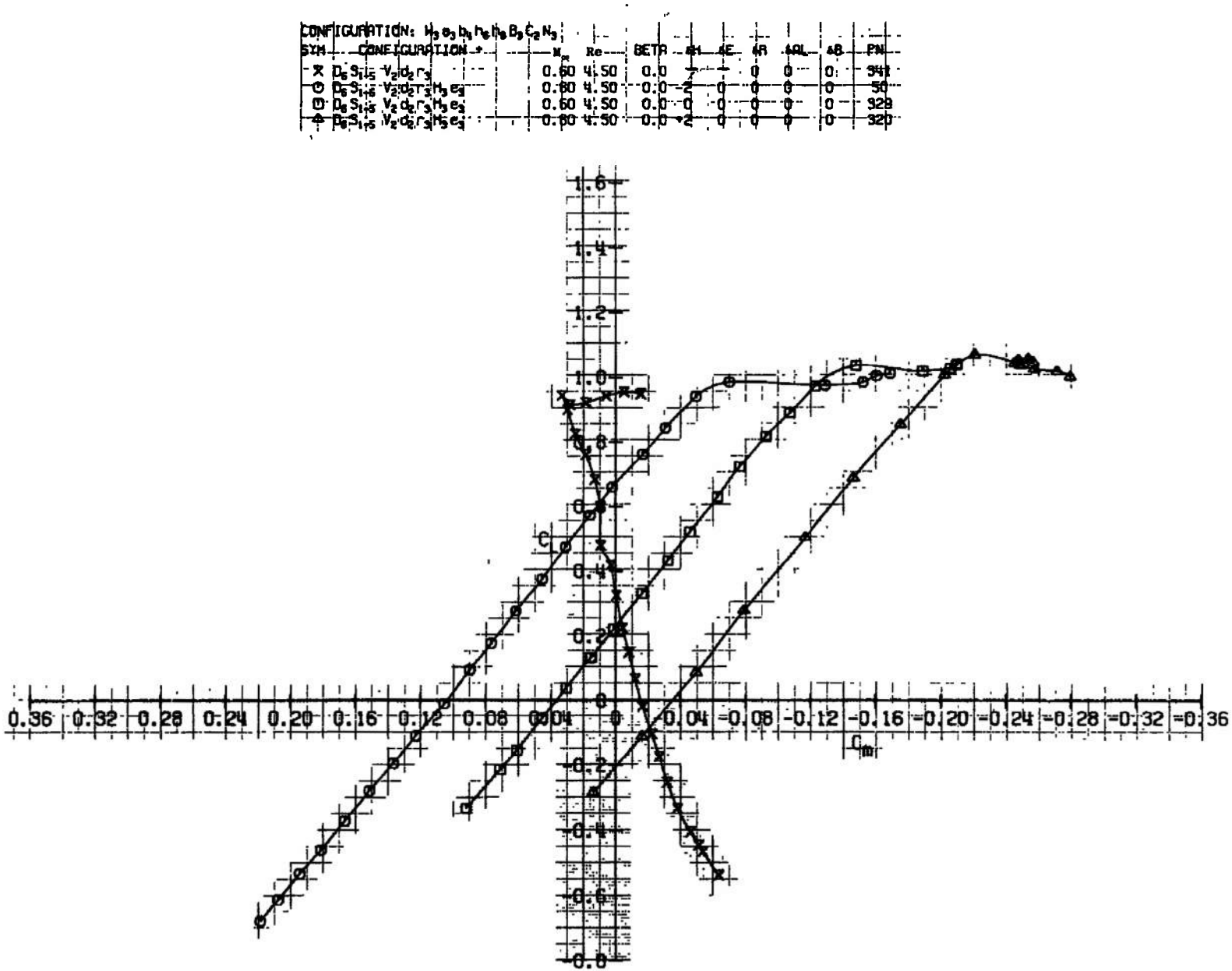

b. Continued

Fig. 6 Continued

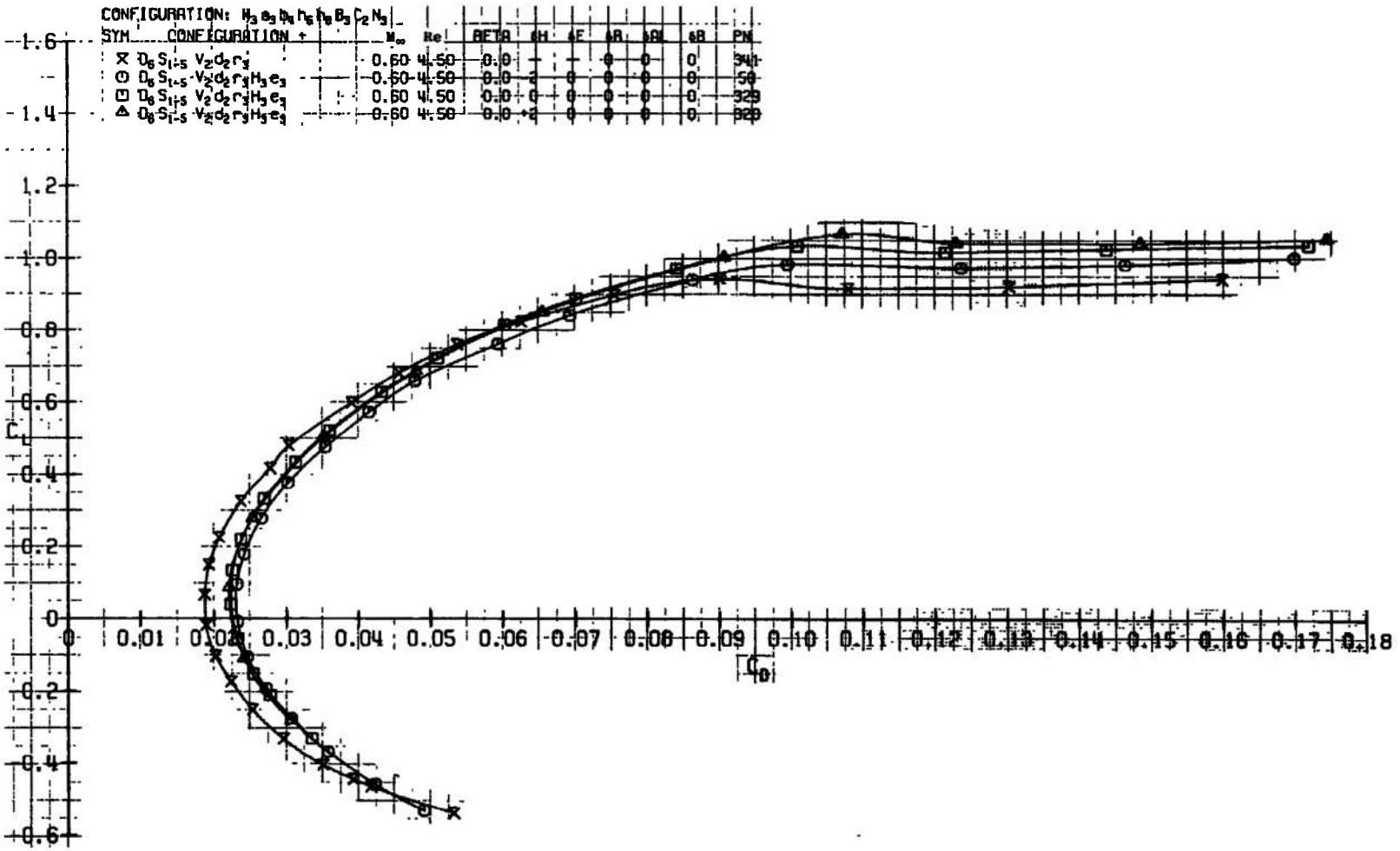

b. Concluded
Fig. 6 Continued

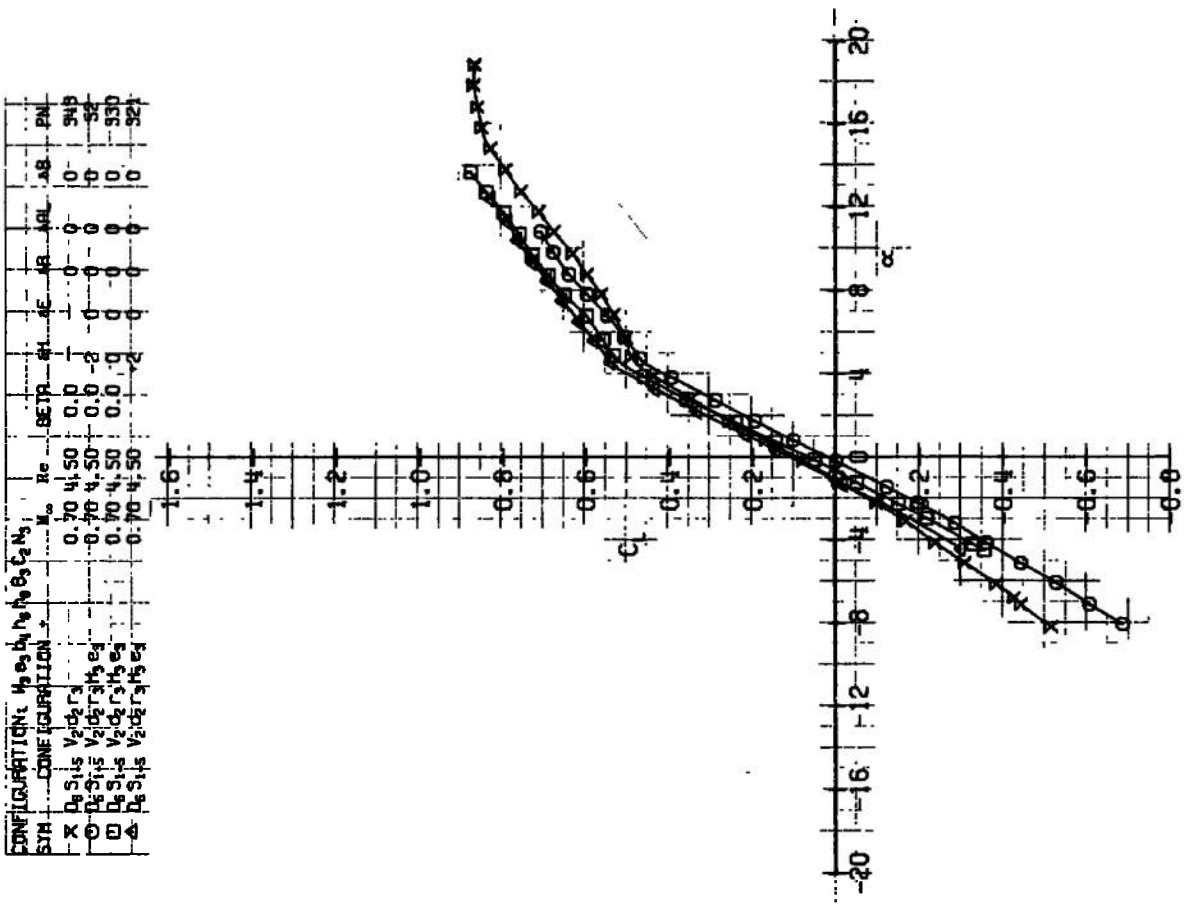

c. $M_\infty = 0.70$

Fig. 6 Continued

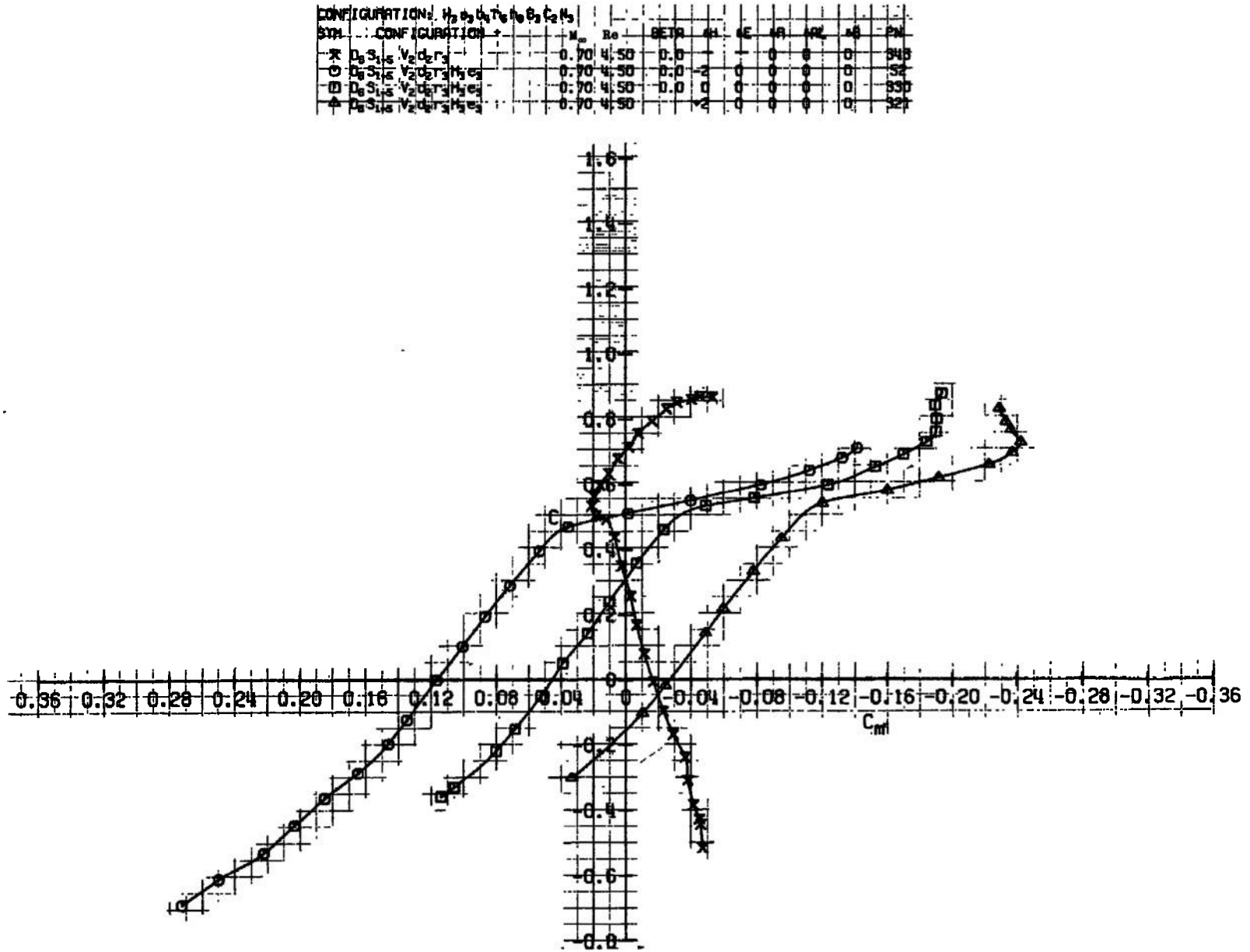

c. Continued

Fig. 6 Continued

SYM	CONFIGURATION	M_∞	Re	BETA	δH	δF	δR	δRL	δB	P.N.
✕	$D_8 S_{1.5} V_2 d_2 r_3$	0.70	4.50	0.0	—	—	0	0	0	343
⊙	$D_8 S_{1.5} V_2 d_2 r_3 H_3 e_3$	0.70	4.50	0.0	2	0	0	0	0	52
⊡	$D_8 S_{1.5} V_2 d_2 r_3 H_3 e_3$	0.70	4.50	0.0	0	0	0	0	0	330
▲	$D_8 S_{1.5} V_2 d_2 r_3 H_3 e_3$	0.70	4.50	0.0	-2	0	0	0	0	321

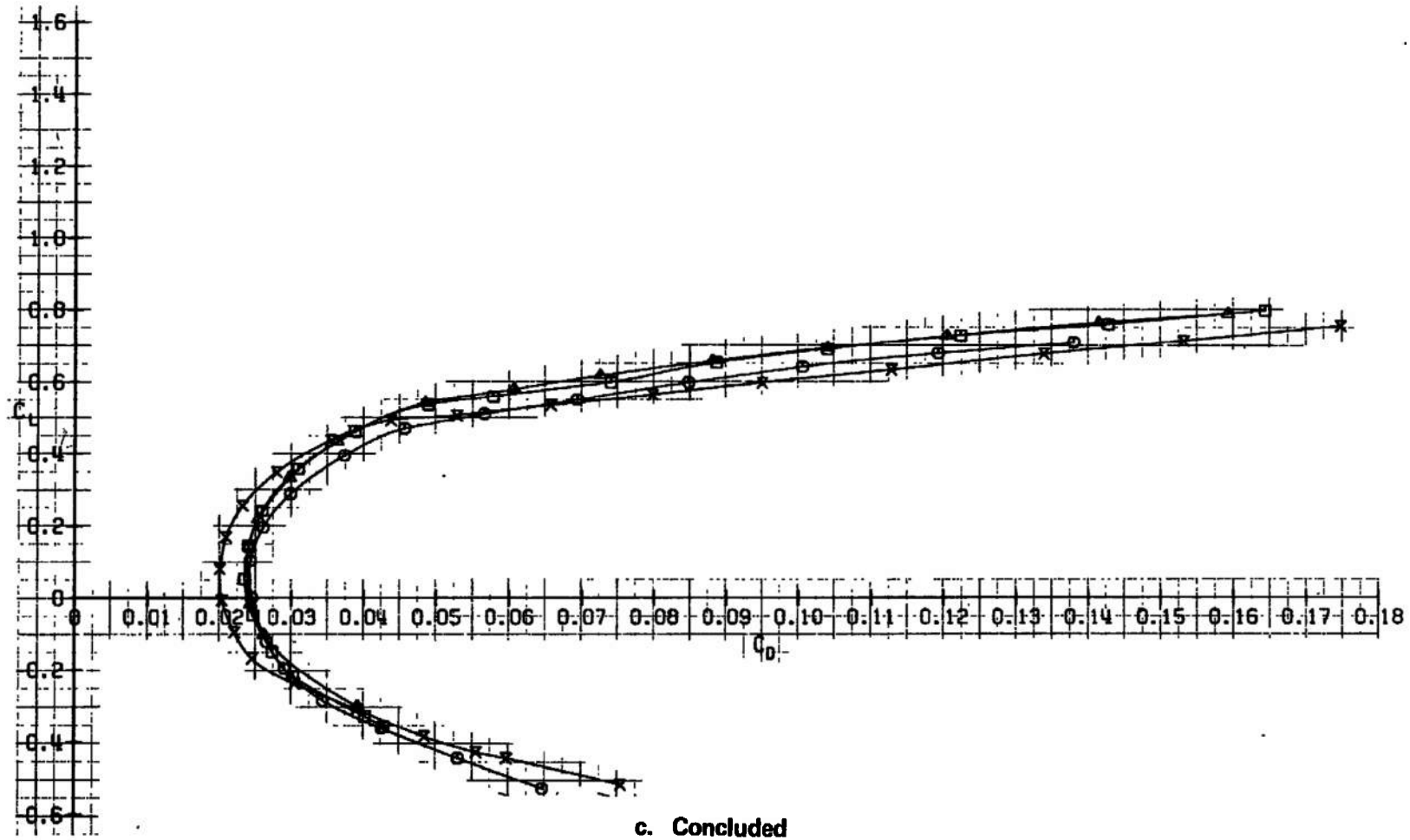

c. Concluded

Fig. 6 Continued

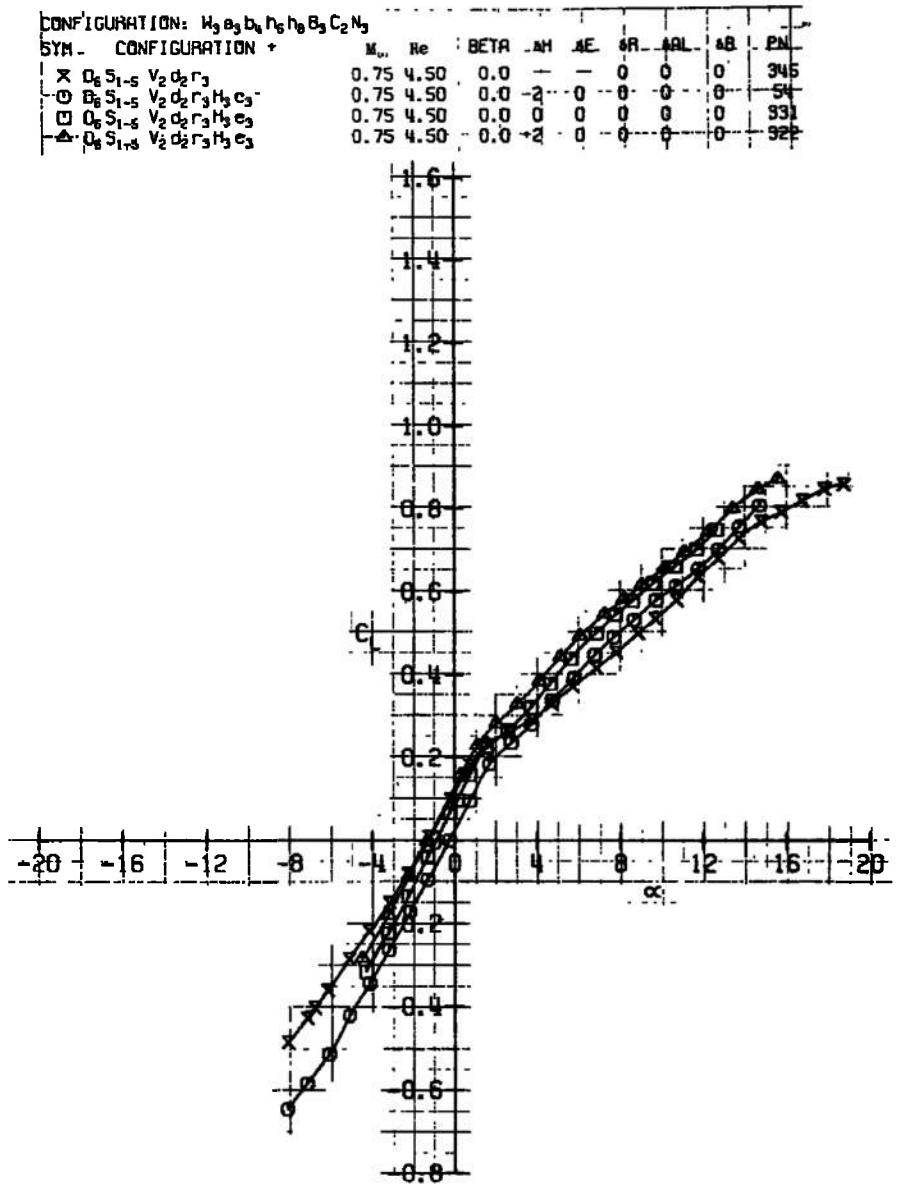

d. $M_\infty = 0.75$

Fig. 6 Continued

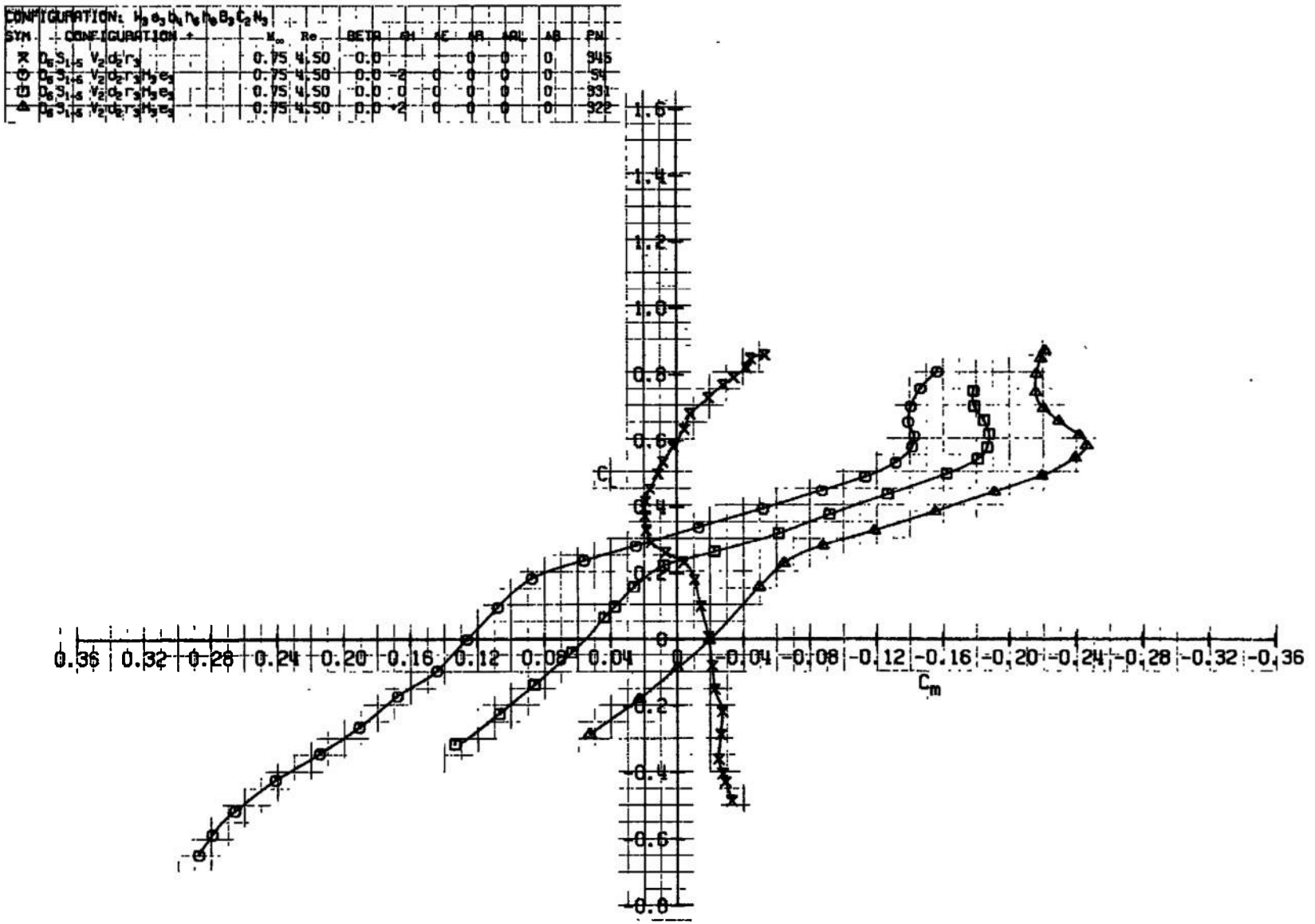

d. Continued

Fig. 6 Continued

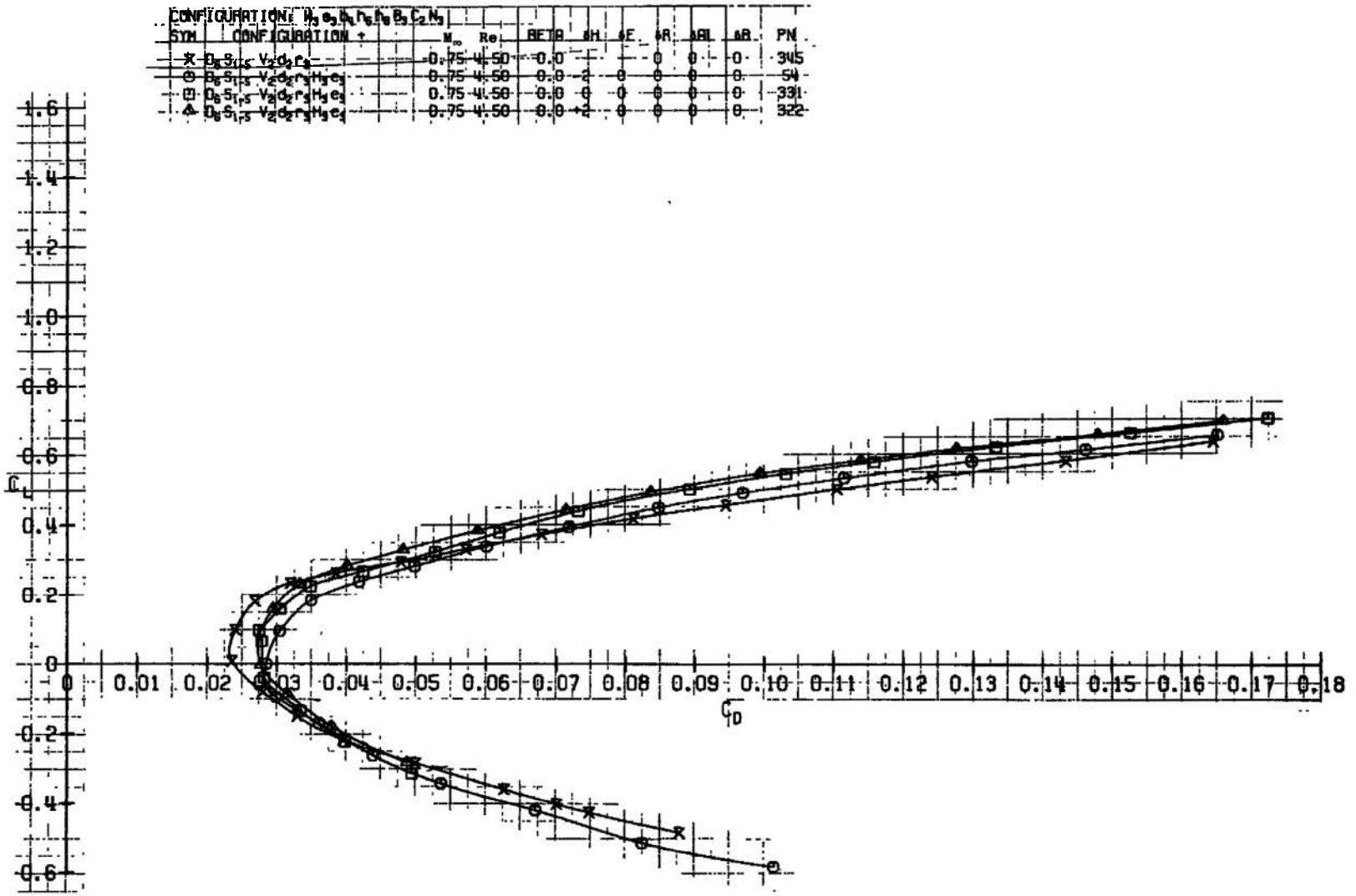

d. Concluded
Fig. 6 Continued

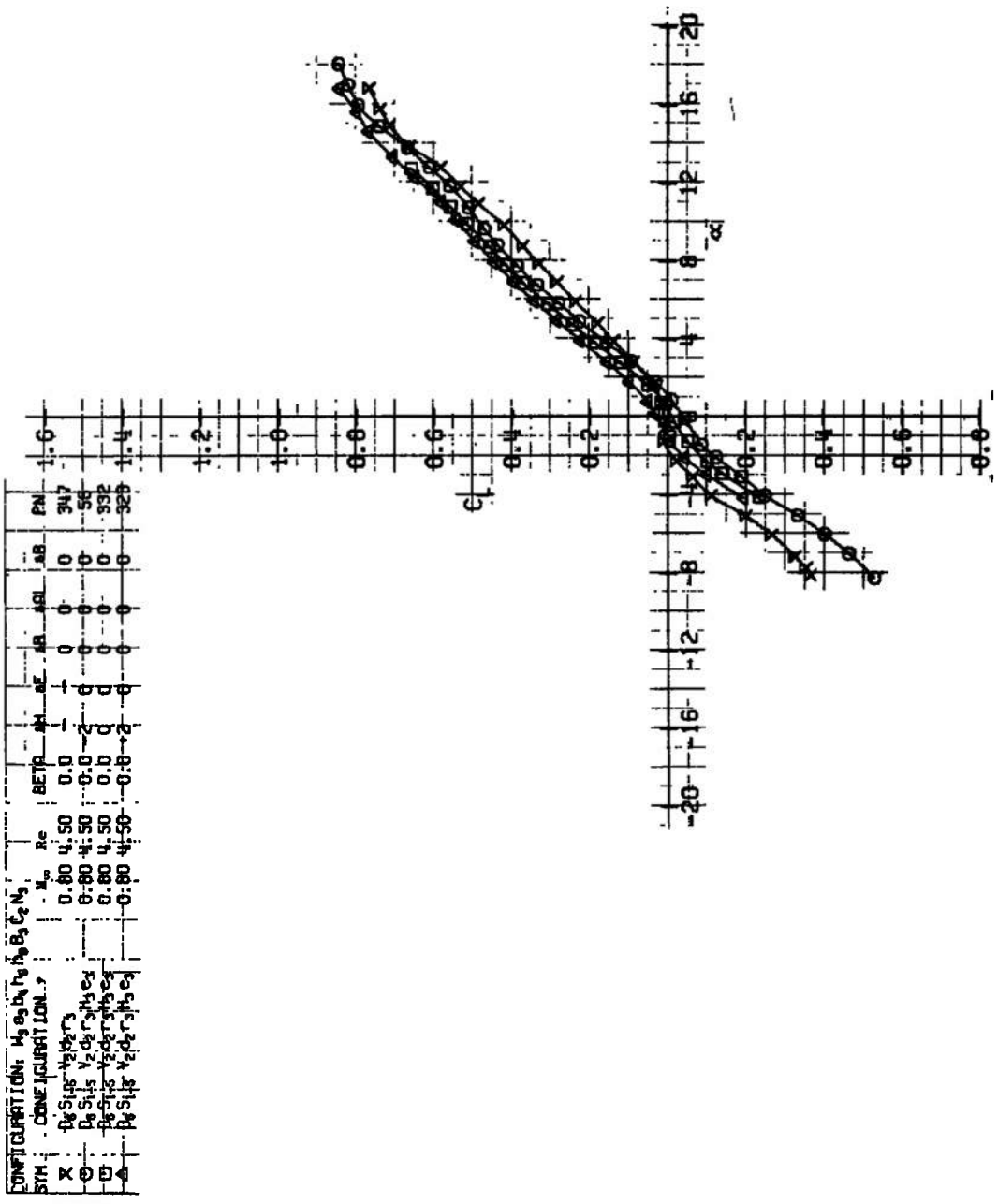

e. $M_\infty = 0.80$

Fig. 6 Continued

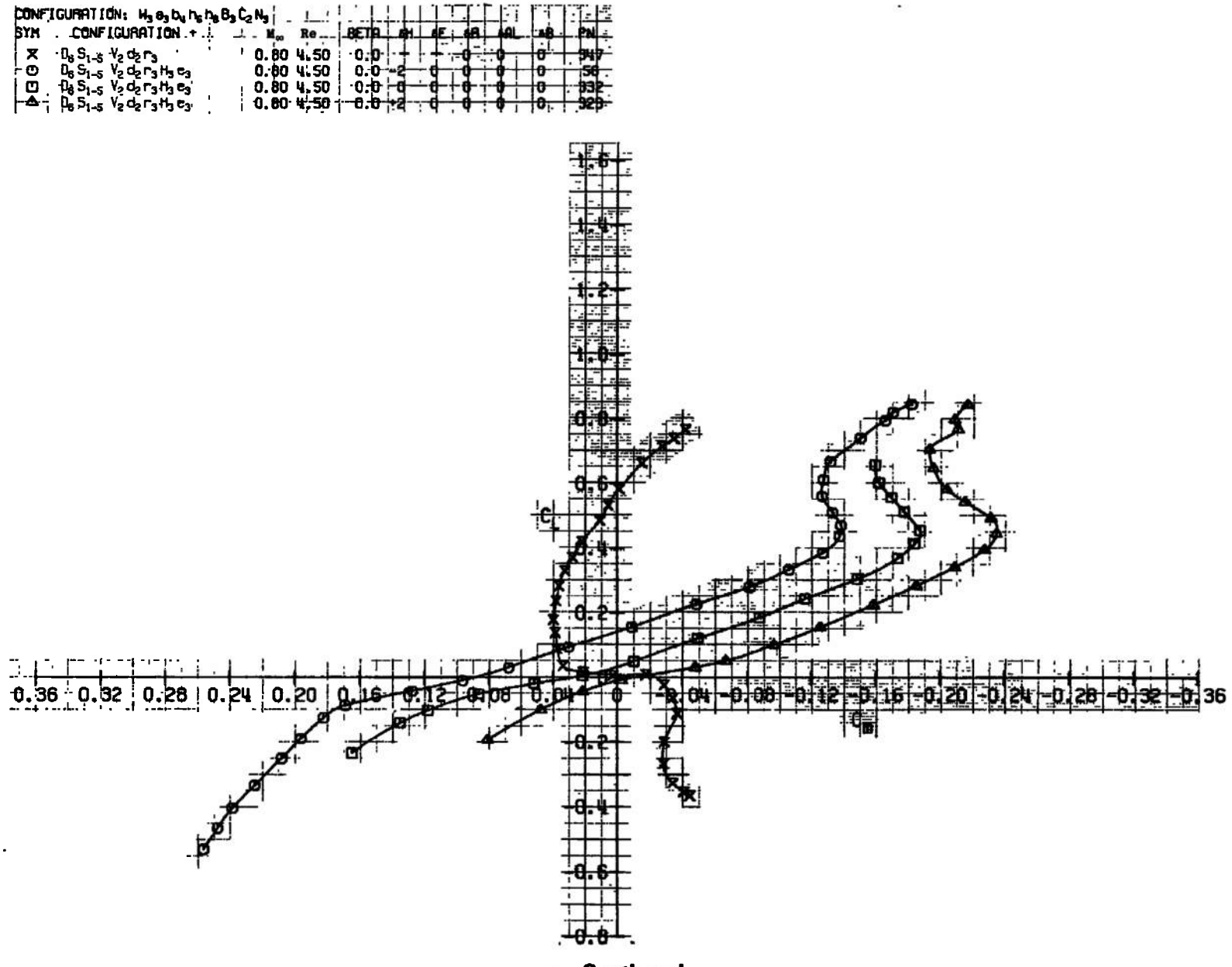

e. Continued

Fig. 6 Continued

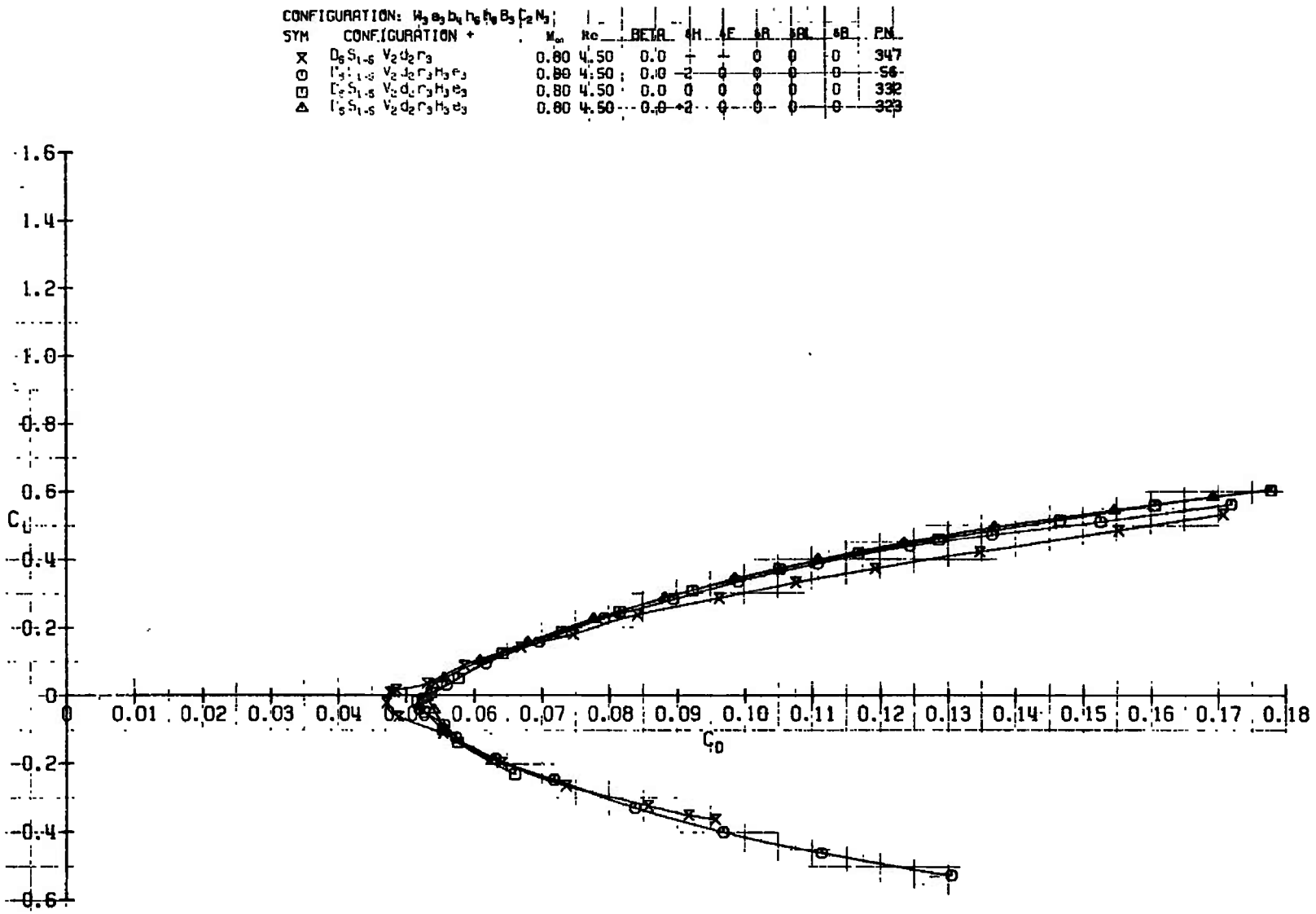

e. Concluded

Fig. 6 Concluded

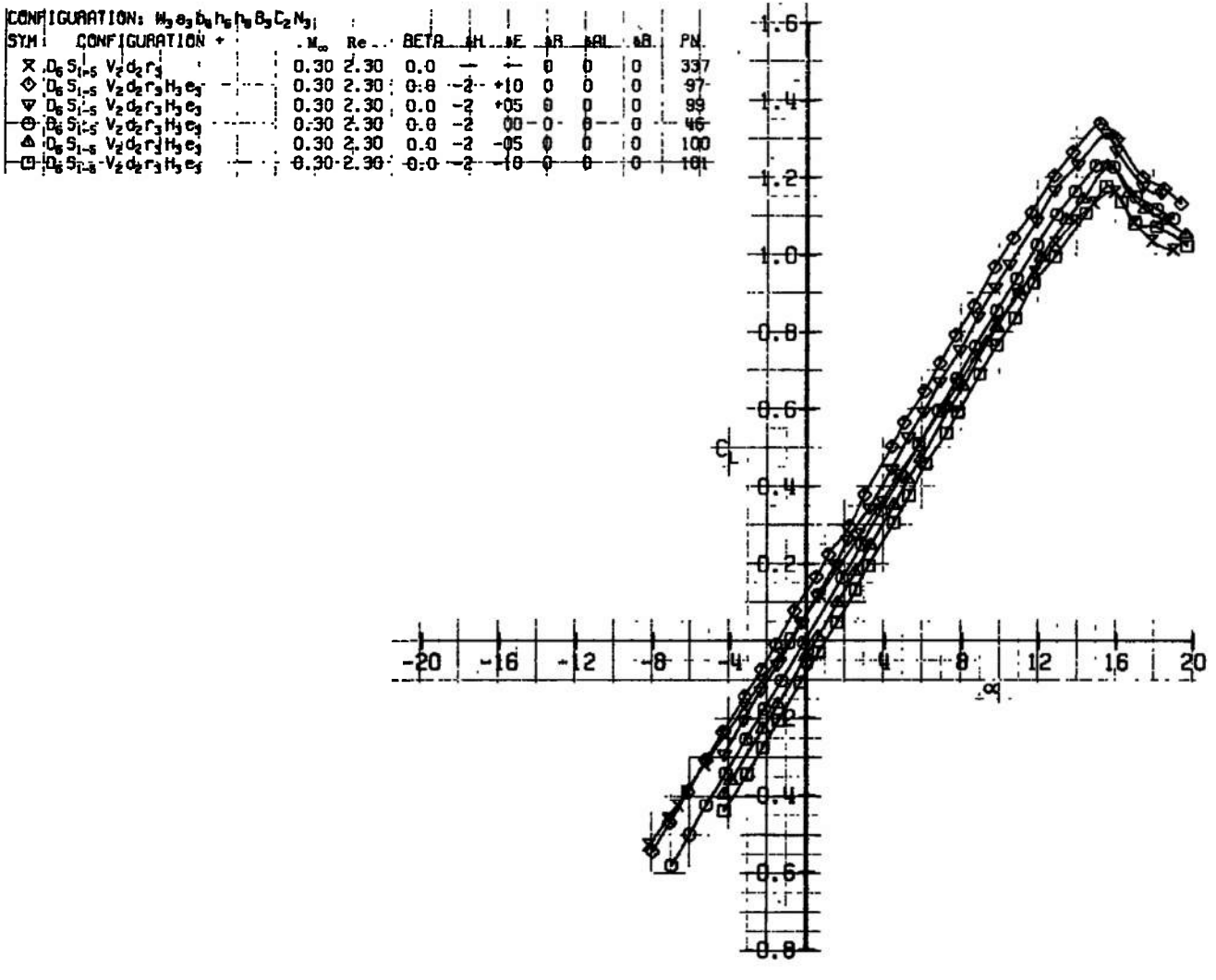

a. $M_\infty = 0.30$

Fig. 7 Elevator Effectiveness

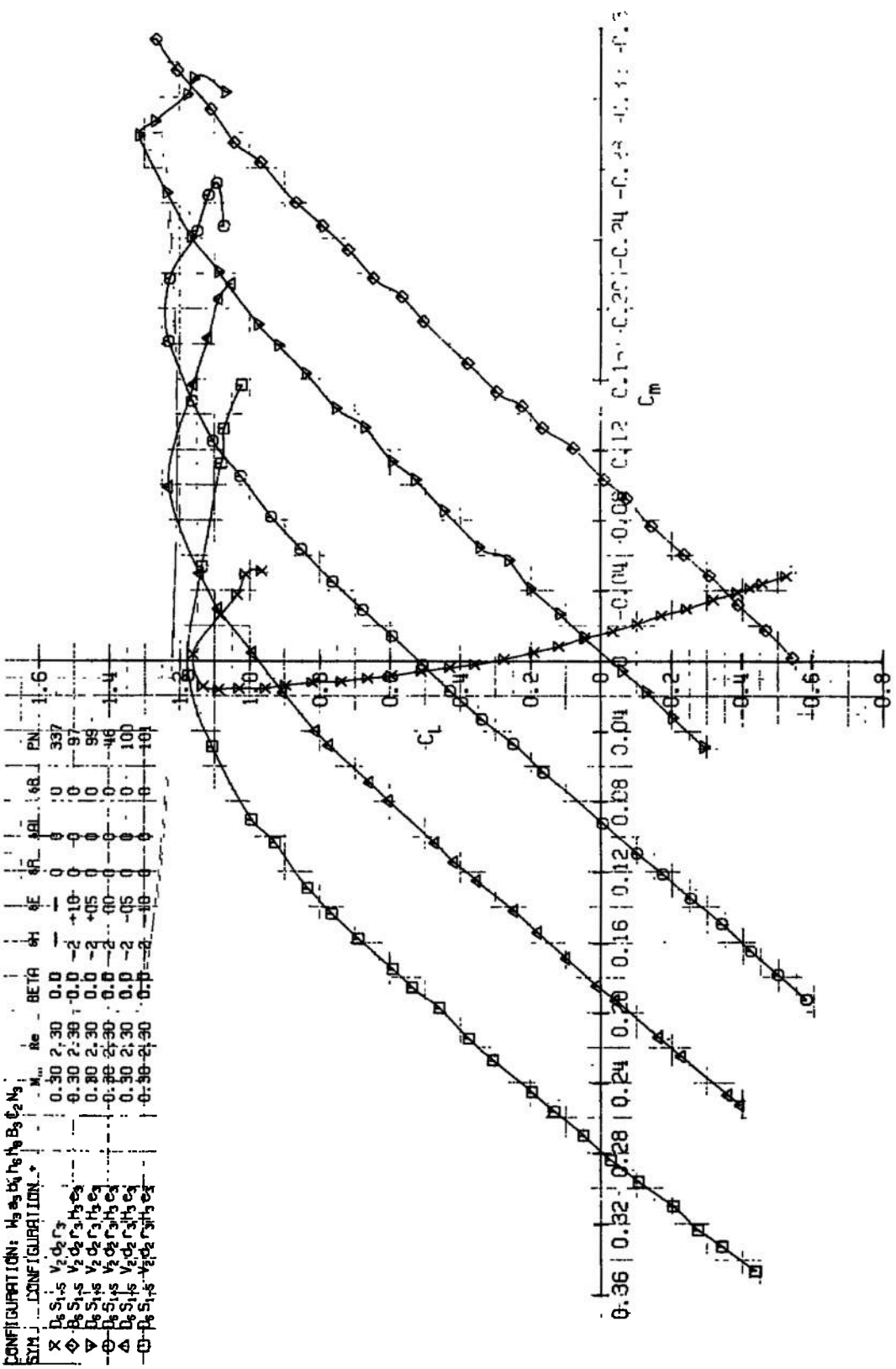

a. Continued

Fig. 7 Continued

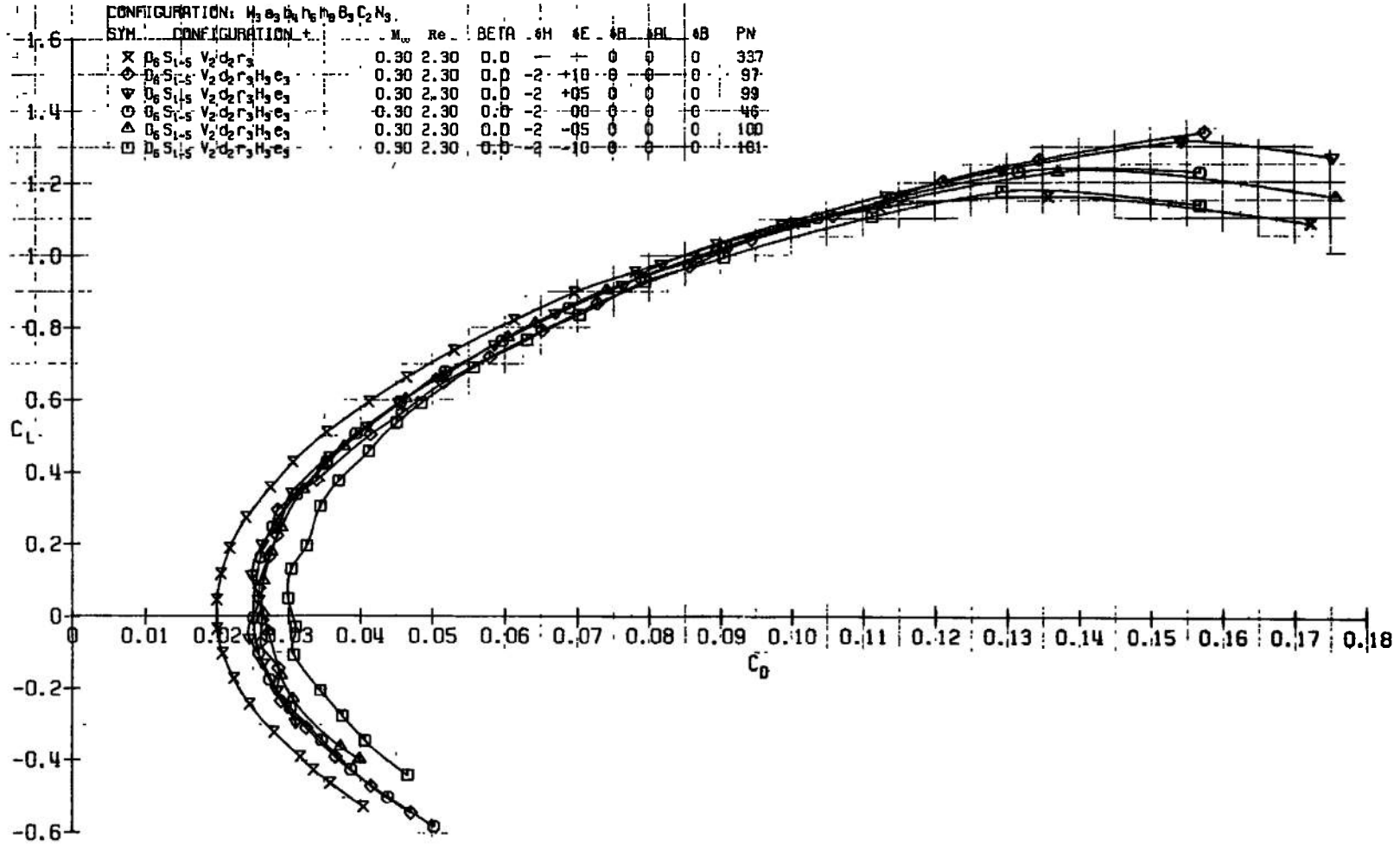

a. Concluded
Fig. 7 Continued

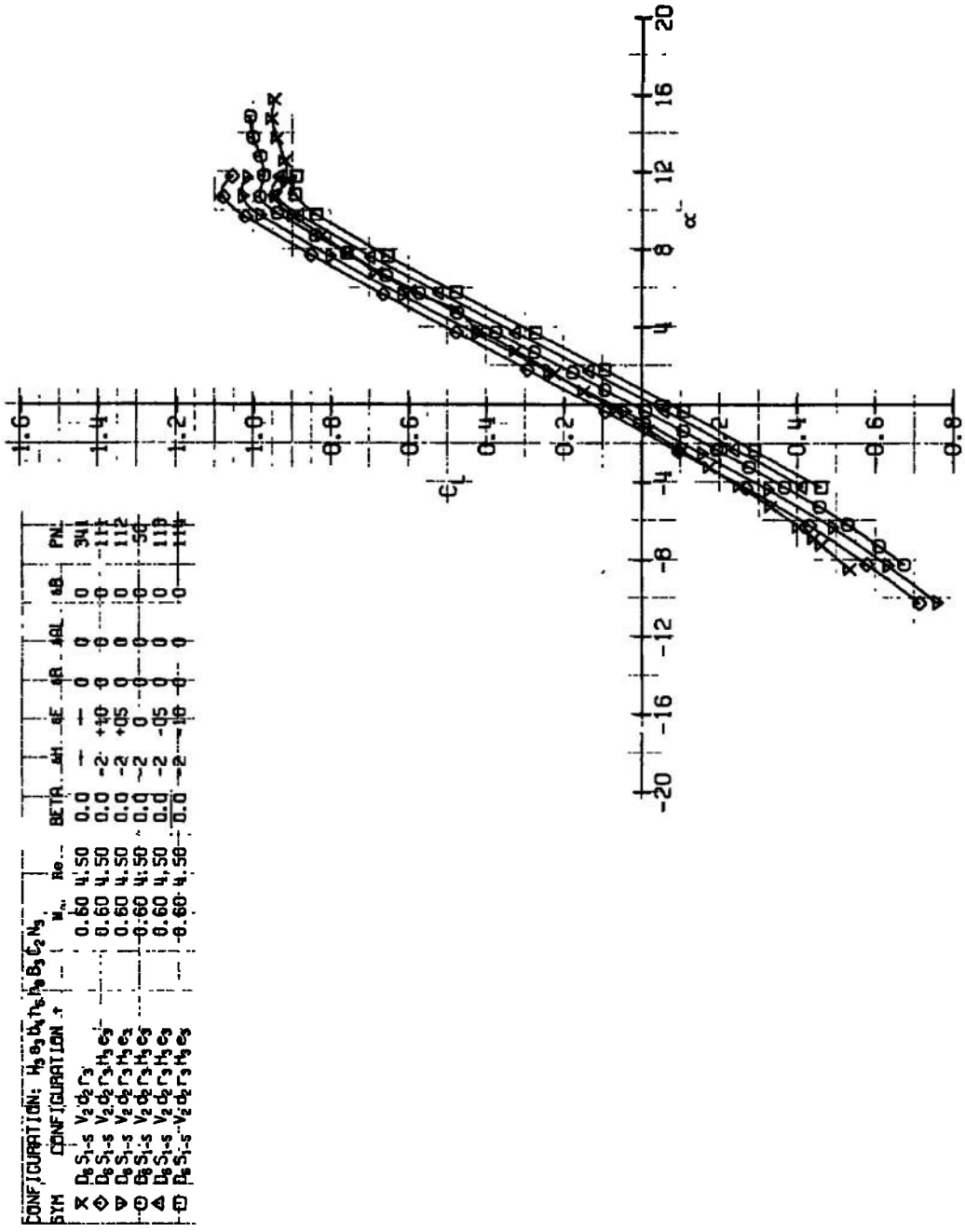

b. $M_\infty = 0.60$

Fig. 7 Continued

CONFIGURATION: $H_3 e_3 b_4 h_5 h_3 B_3 C_2 N_3$

SYM	CONFIGURATION	M_∞	Re	BETA	δ_H	δ_F	ΔR	ΔRL	ΔR	PN
⋇	$B_6 S_{14} V_2 d_2 r_3$	0.60	4.50	0.0	—	—	0	0	0	341
◇	$B_6 S_{14} V_2 d_2 r_3 H_3 e_3$	0.60	4.50	0.0	-2	+10	0	0	0	111
▽	$B_6 S_{14} V_2 d_2 r_3 H_3 e_3$	0.60	4.50	0.0	-2	+05	0	0	0	112
⊕	$B_6 S_{14} V_2 d_2 r_3 H_3 e_3$	0.60	4.50	0.0	-2	0	0	0	0	50
△	$B_6 S_{14} V_2 d_2 r_3 H_3 e_3$	0.60	4.50	0.0	-2	-05	0	0	0	113
⊞	$B_6 S_{14} V_2 d_2 r_3 H_3 e_3$	0.60	4.50	0.0	-2	-10	0	0	0	114

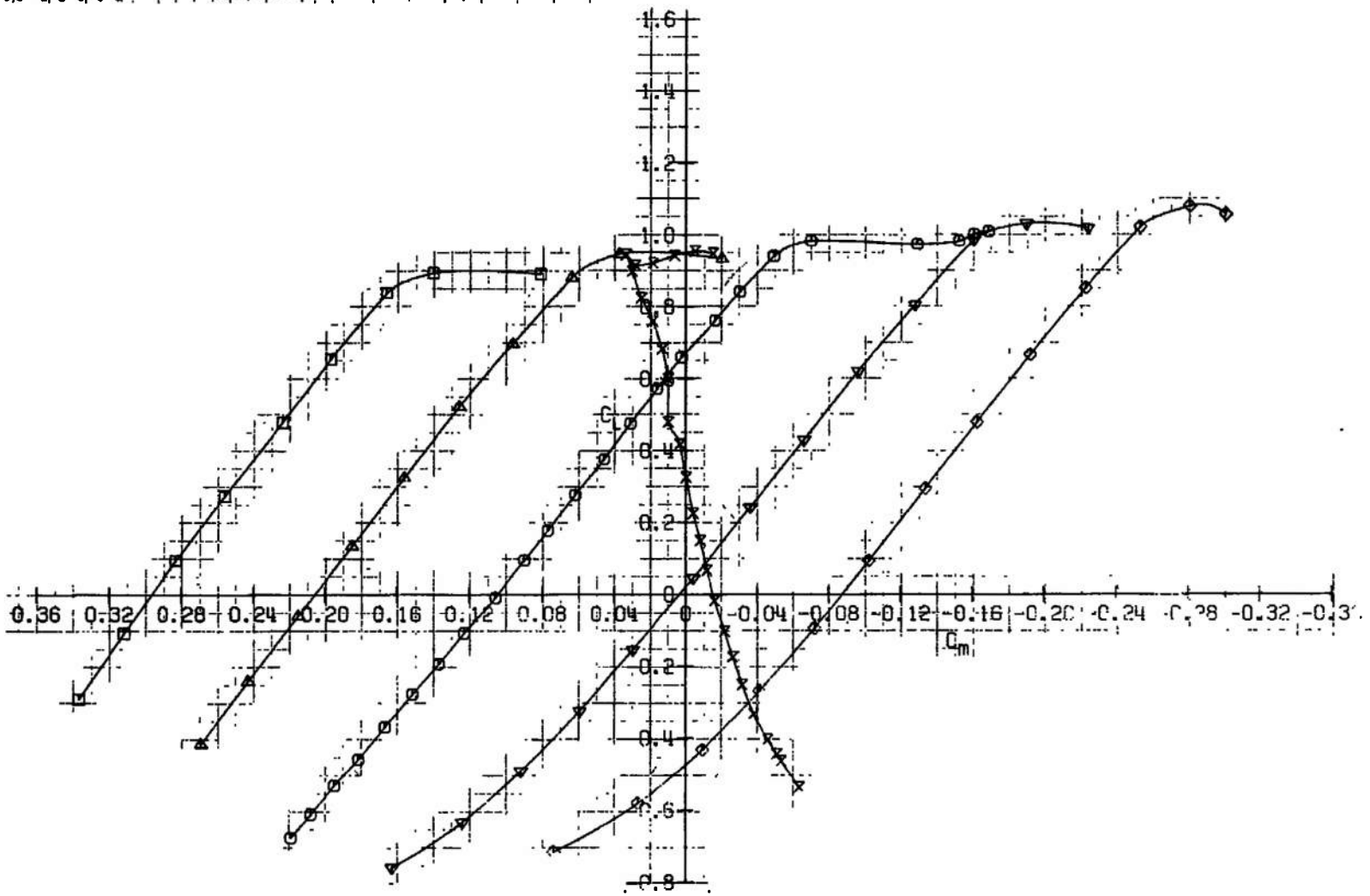

b. Continued

Fig. 7 Continued

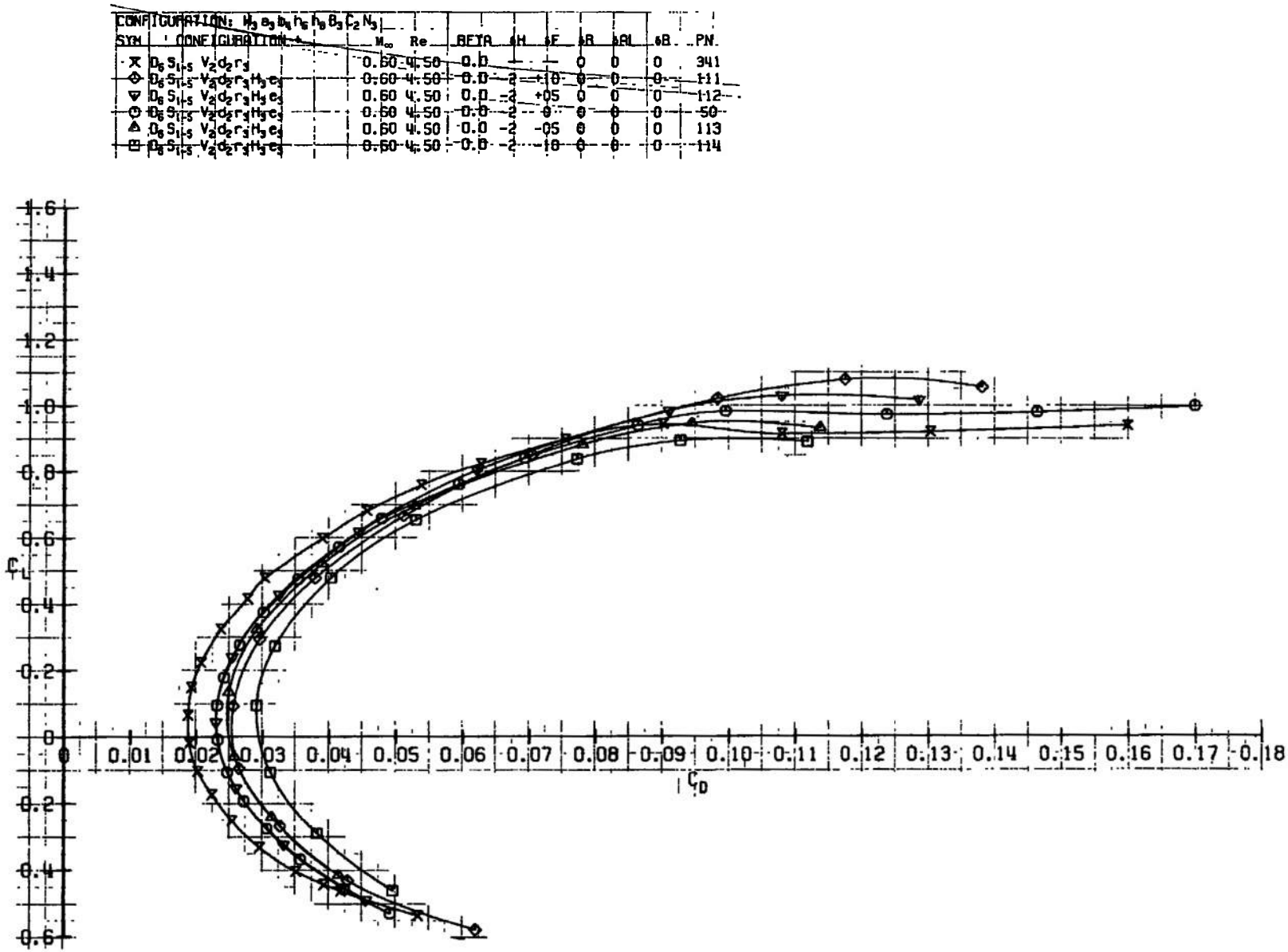

b. Concluded

Fig. 7 Continued

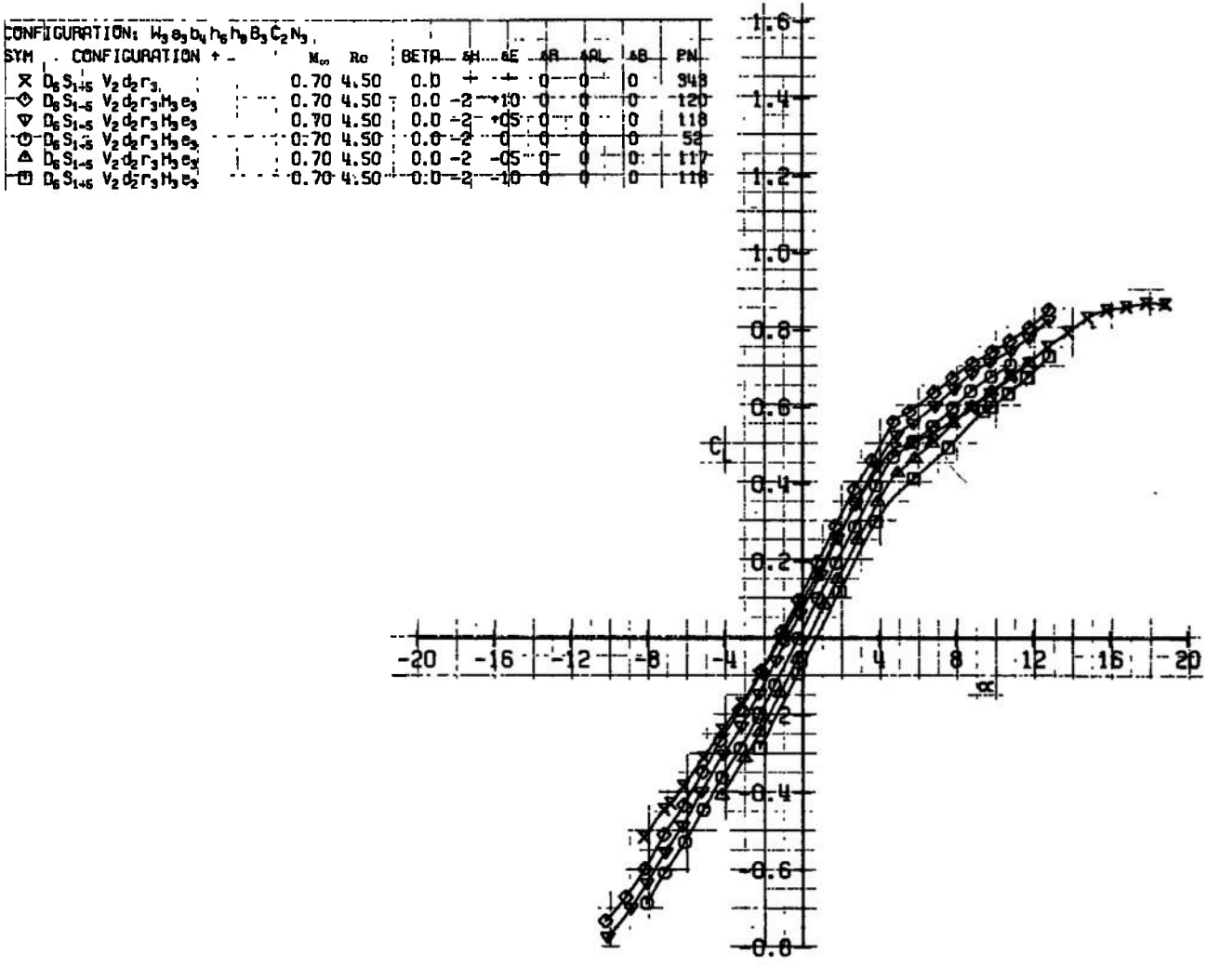

c. $M_\infty = 0.70$

Fig. 7 Continued

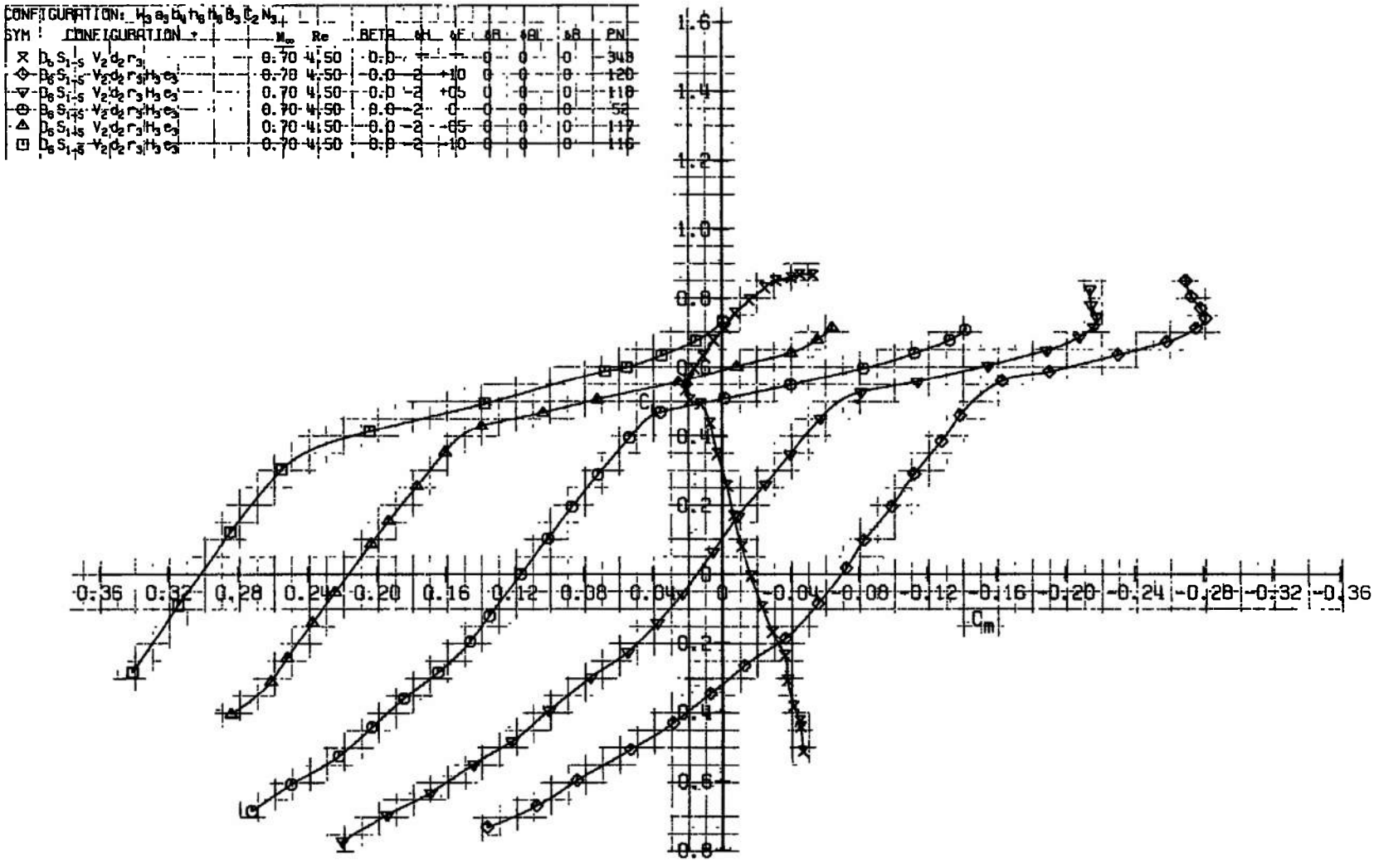

c. Continued

Fig. 7 Continued

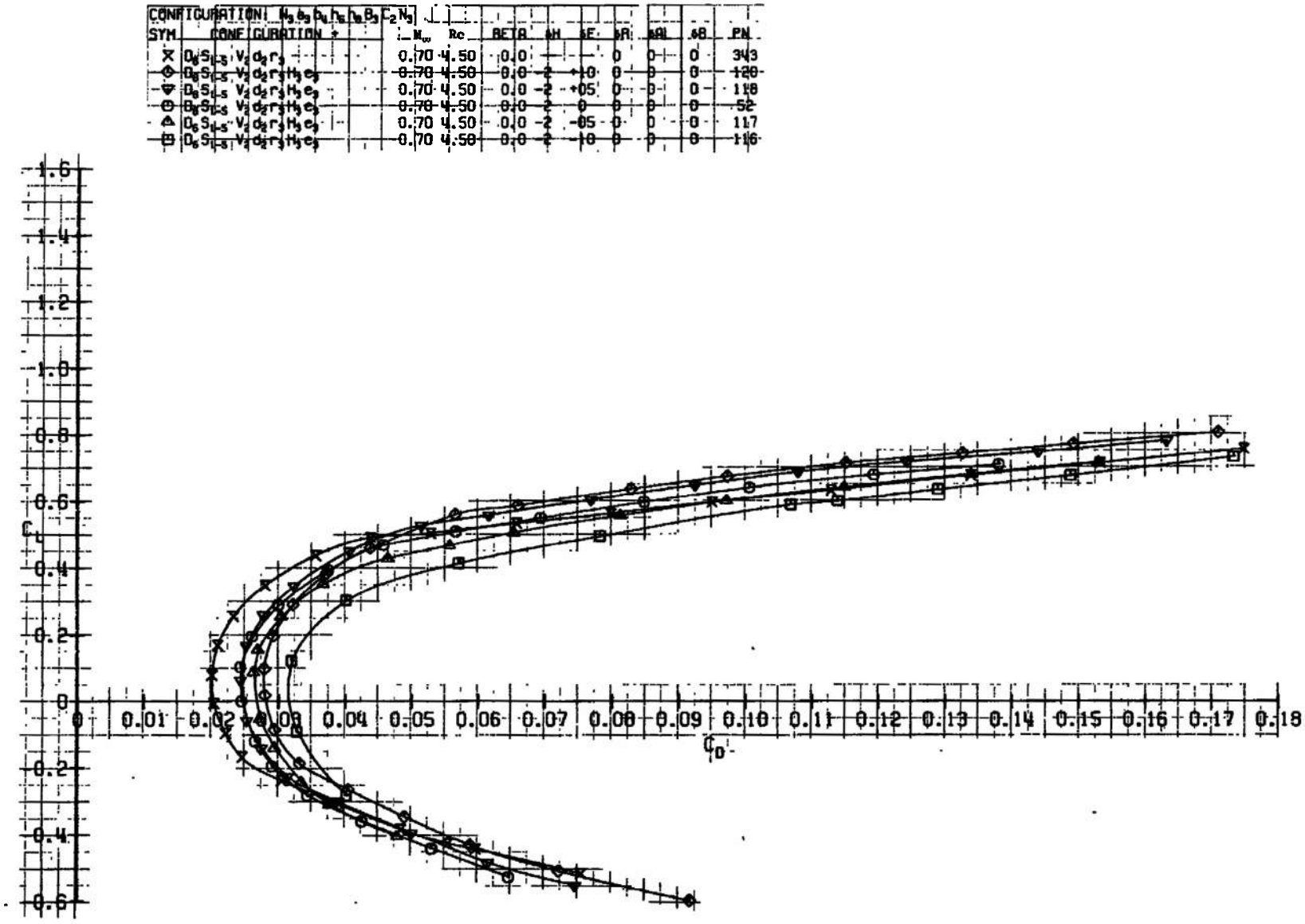

c. Concluded

Fig. 7 Continued

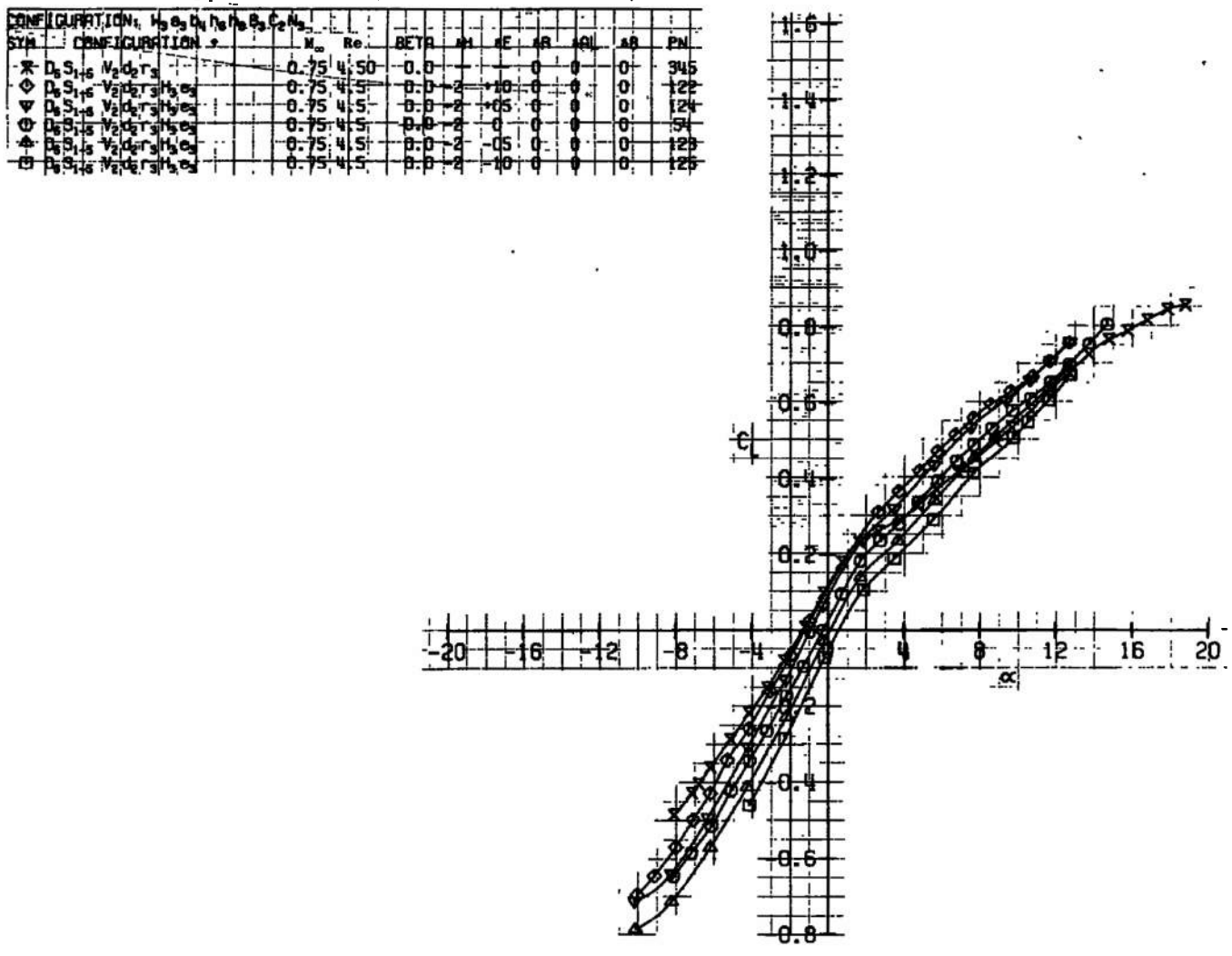

d. $M_\infty = 0.75$

Fig. 7 Continued

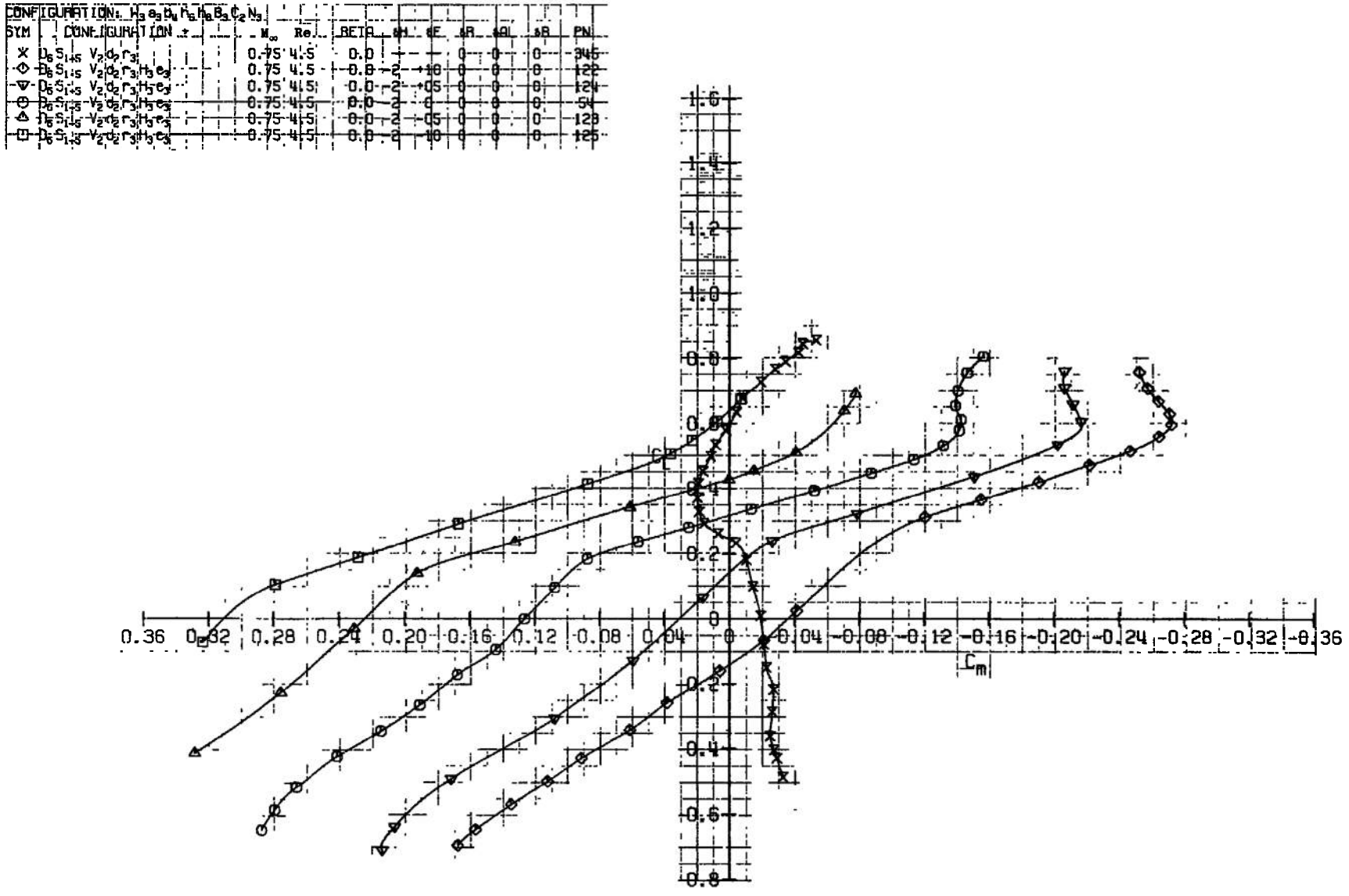

d. Continued
Fig. 7 Continued

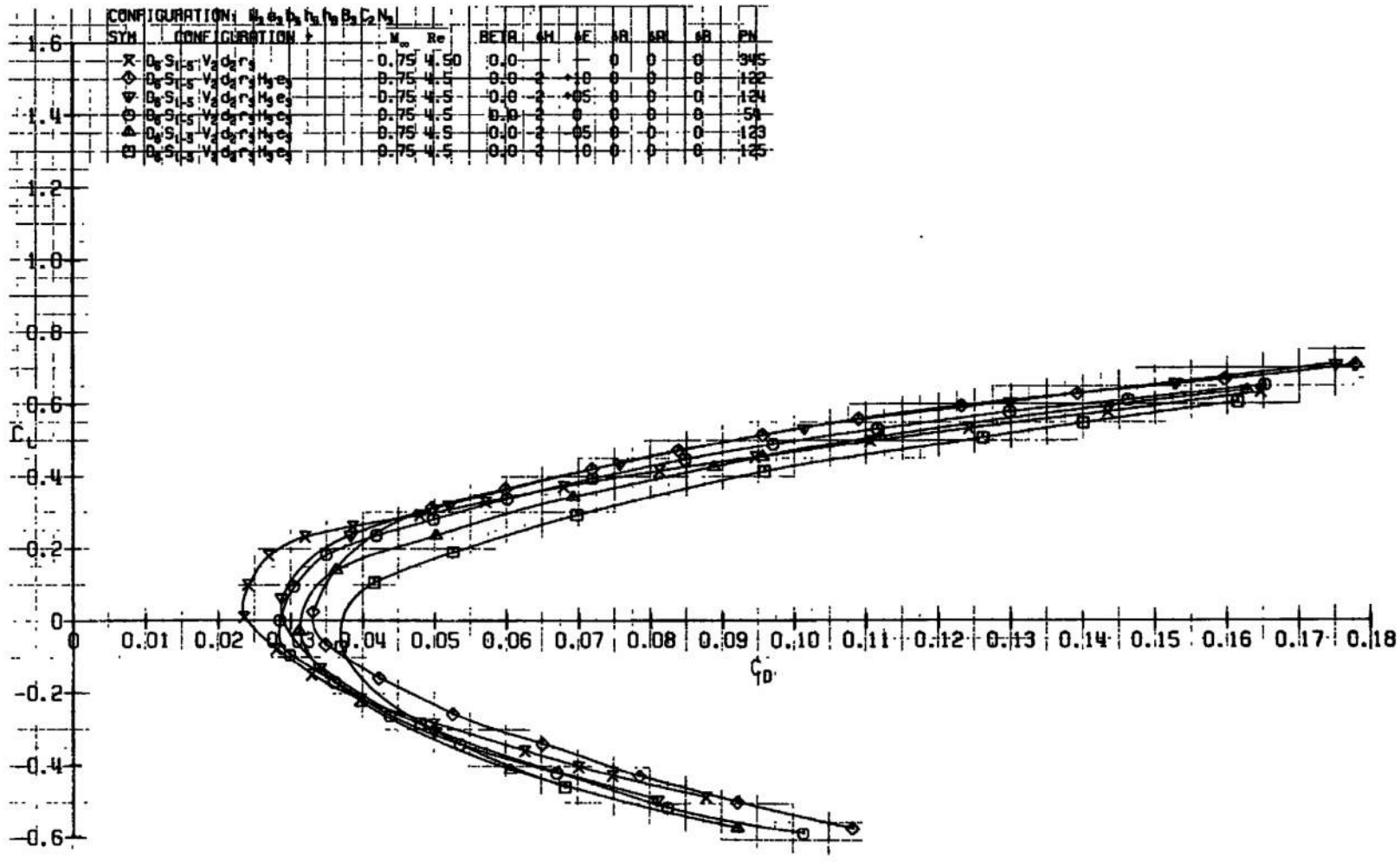

d. Concluded
Fig. 7 Continued

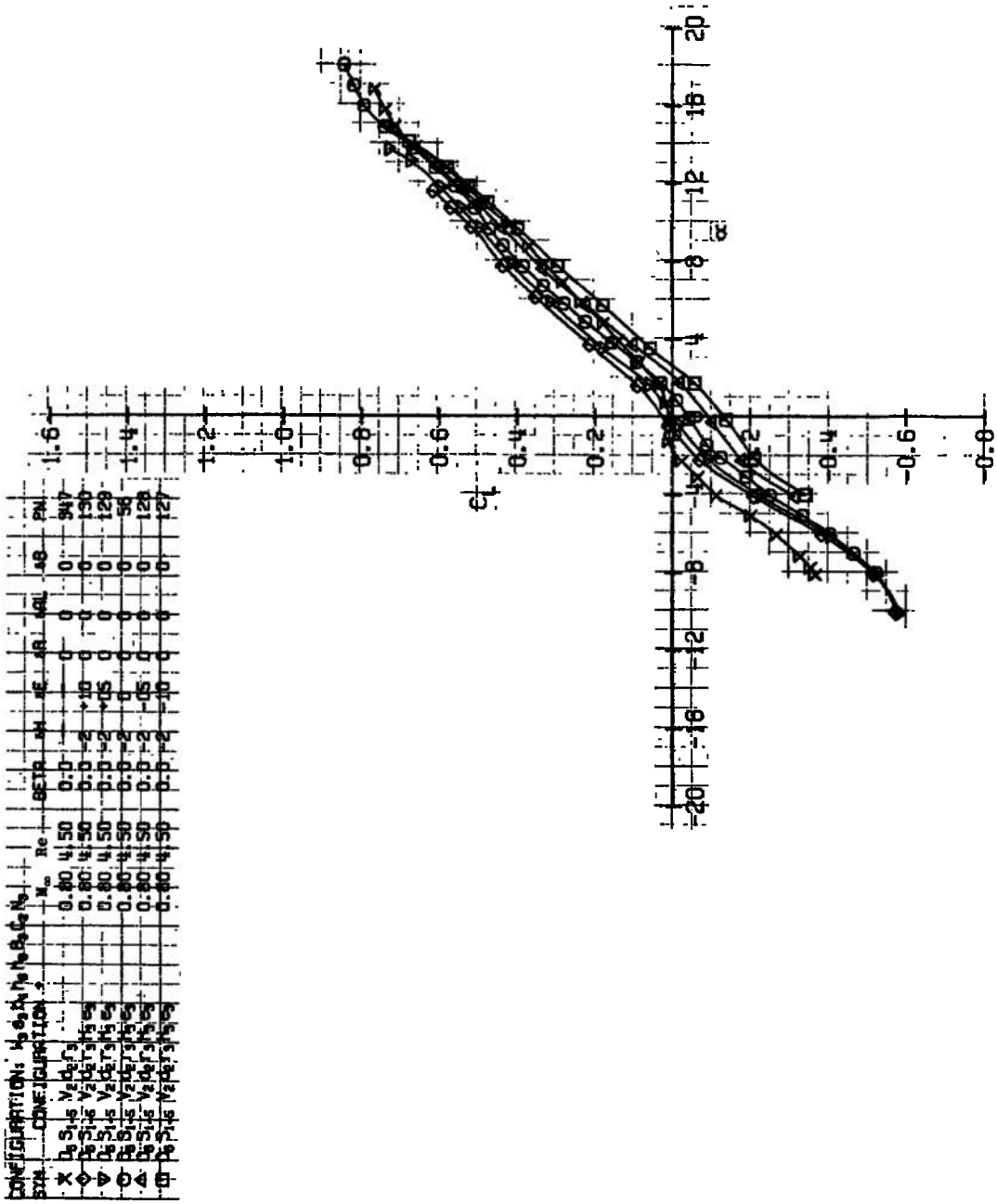

e. $M_\infty = 0.80$
Fig. 7 Continued

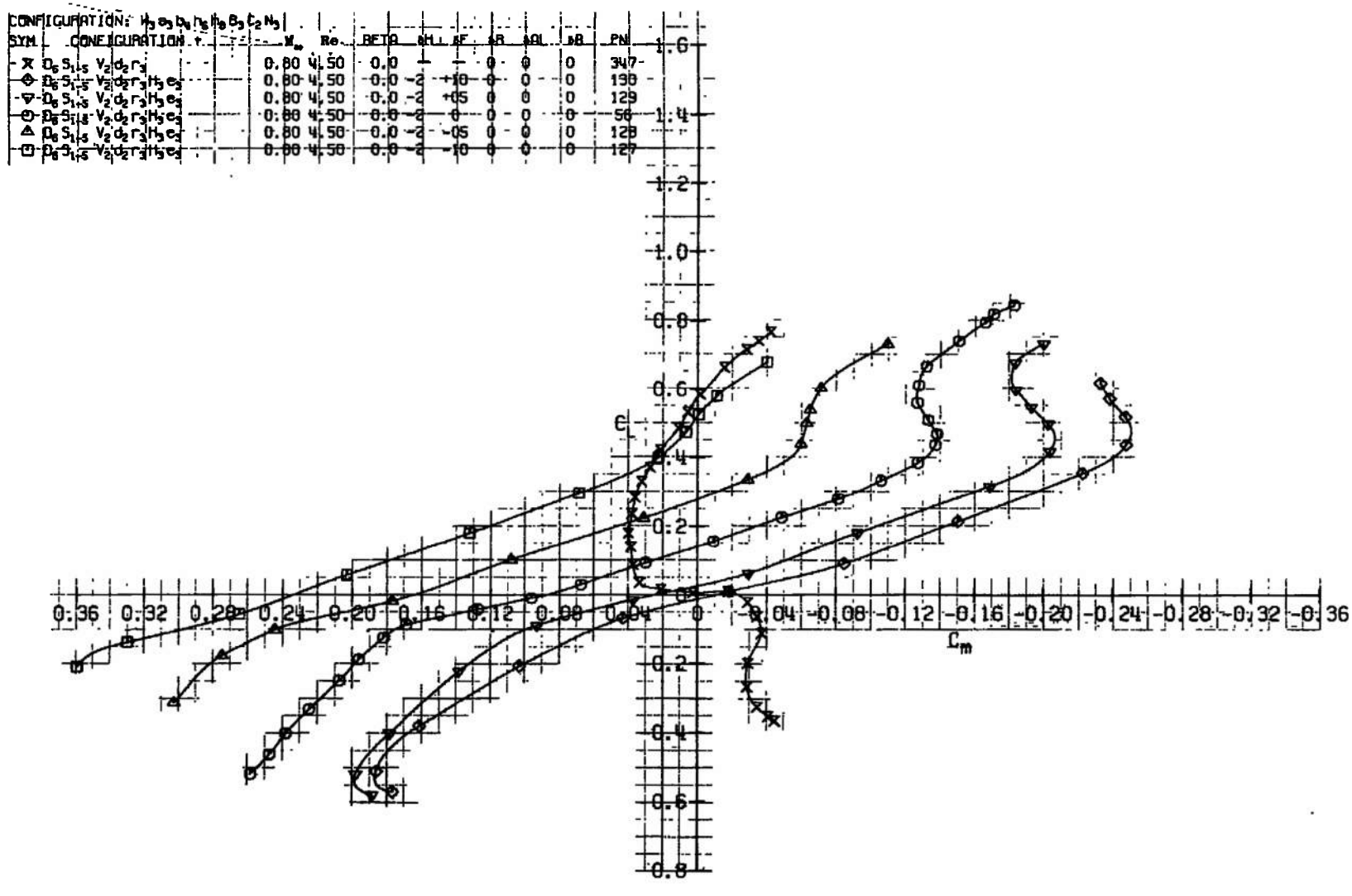

e. Continued

Fig. 7 Continued

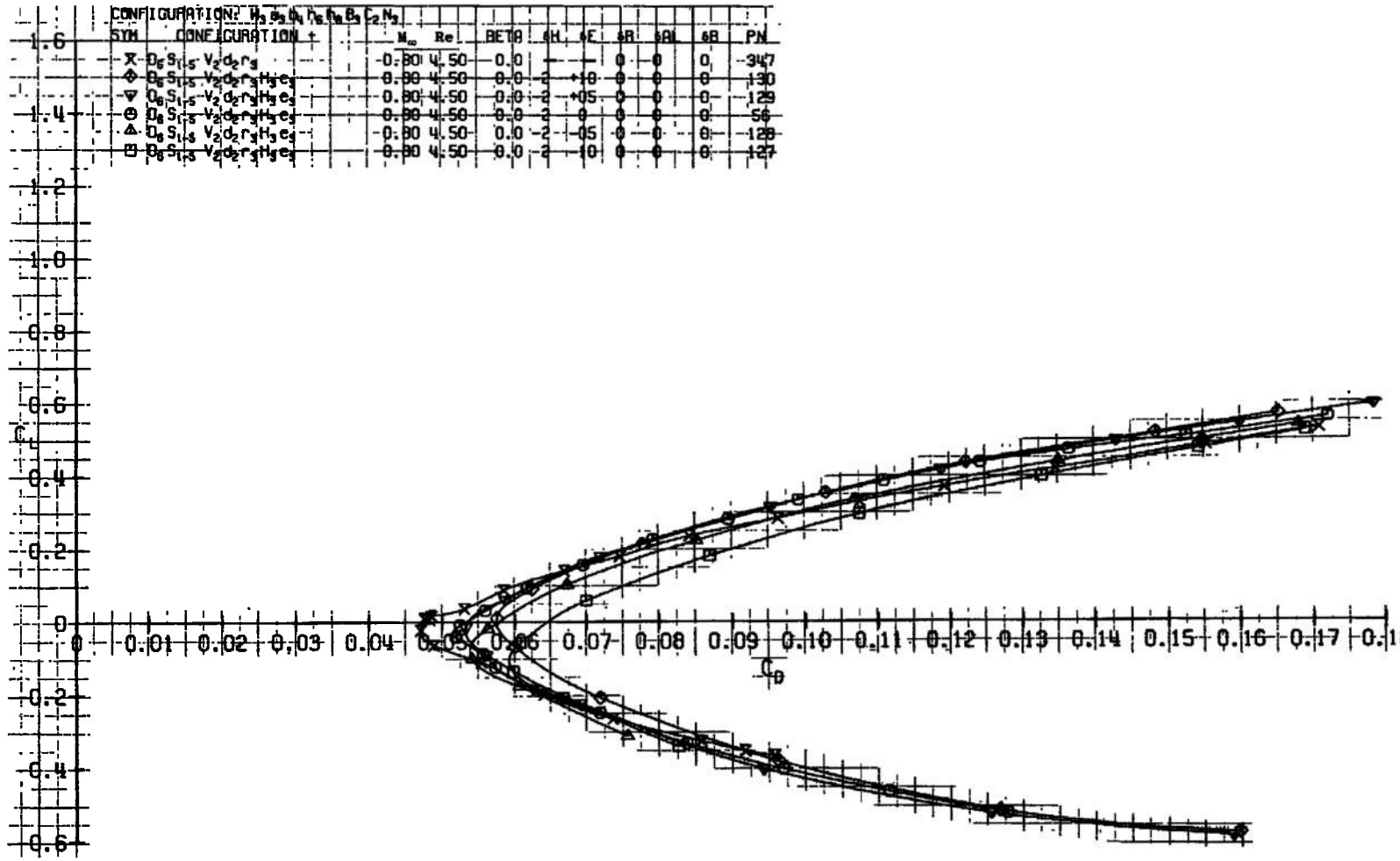

e. Concluded

Fig. 7 Concluded

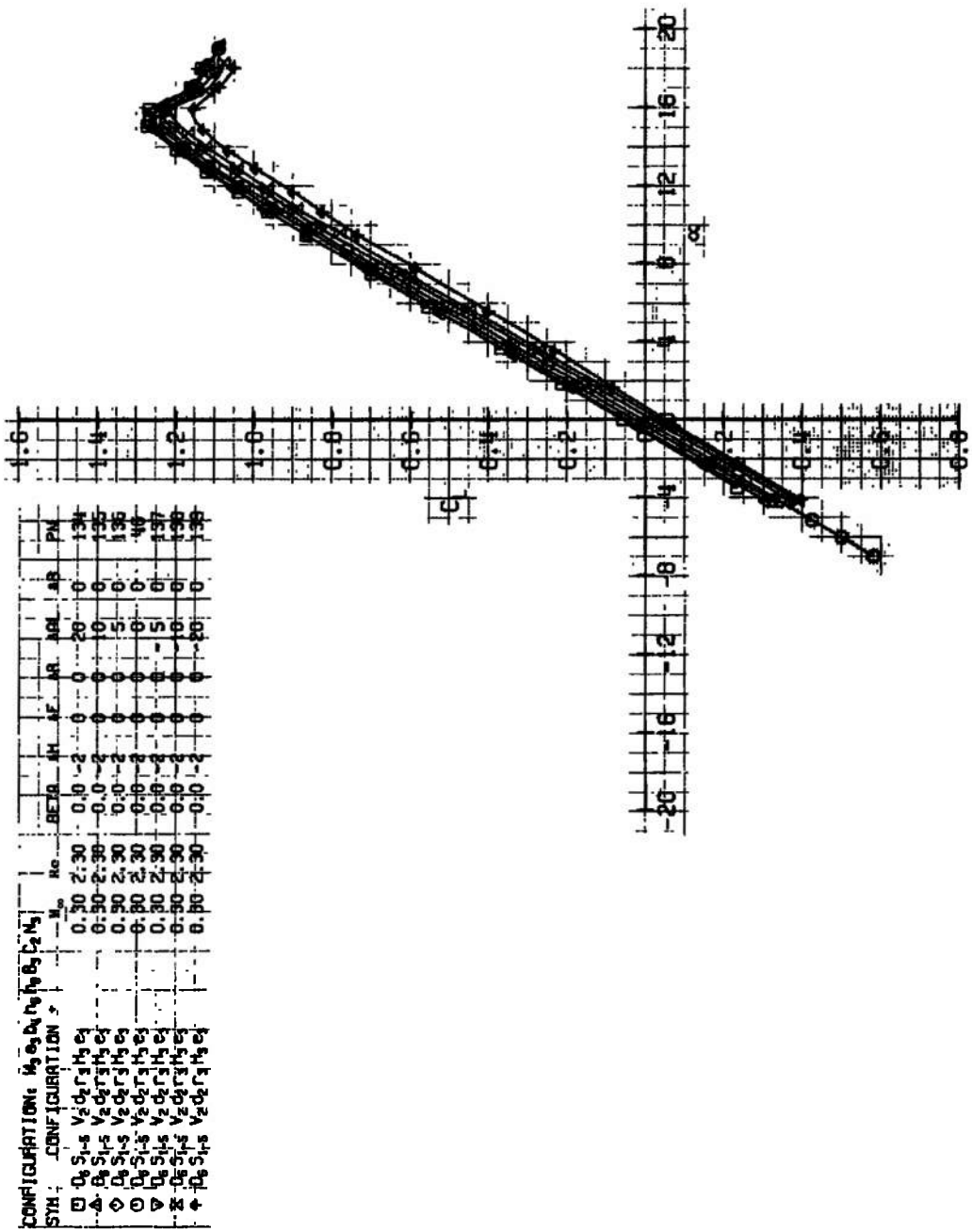

a. $M_\infty = 0.30$

Fig. 8 Aileron Effectiveness

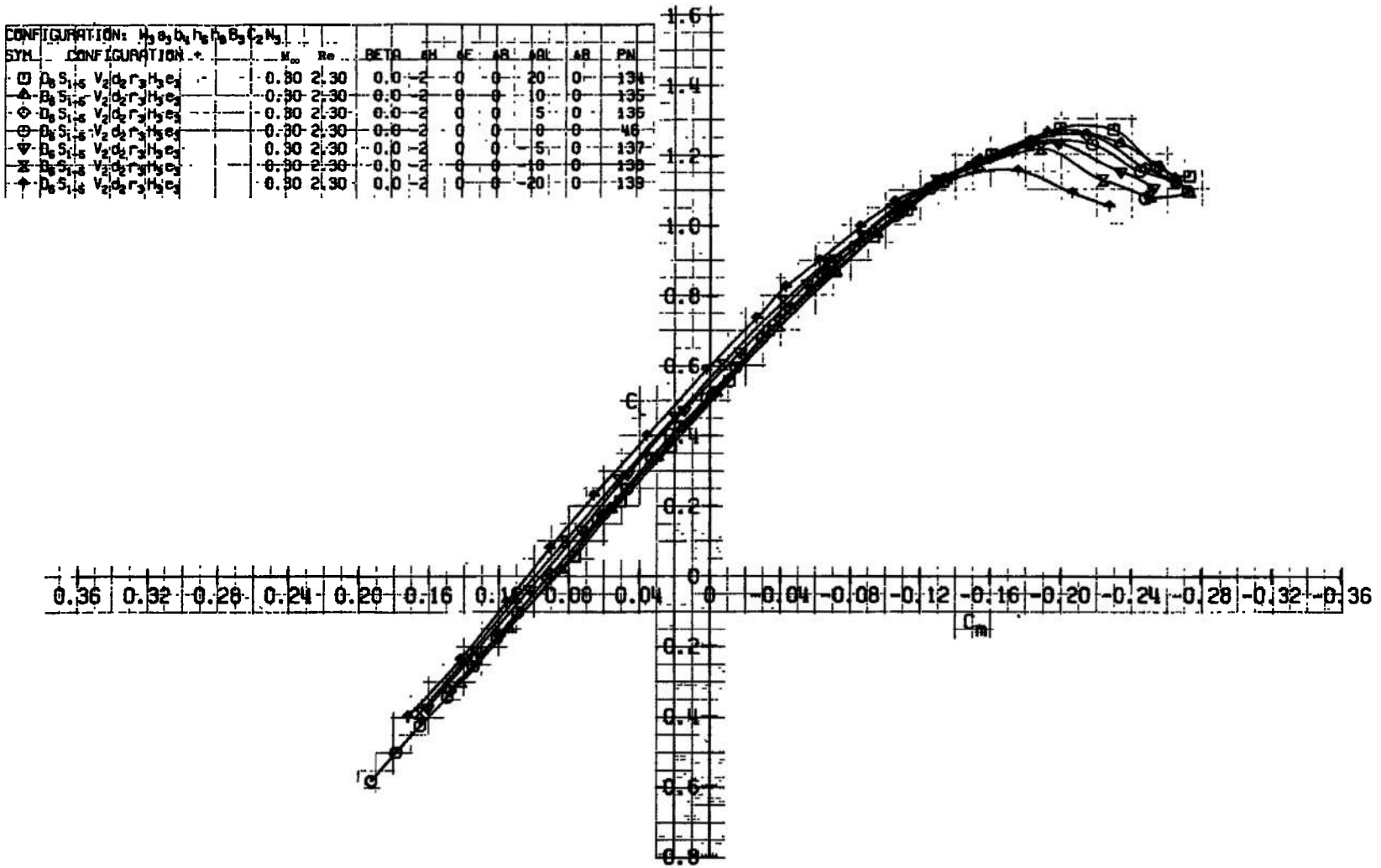

a. Continued

Fig. 8 Continued

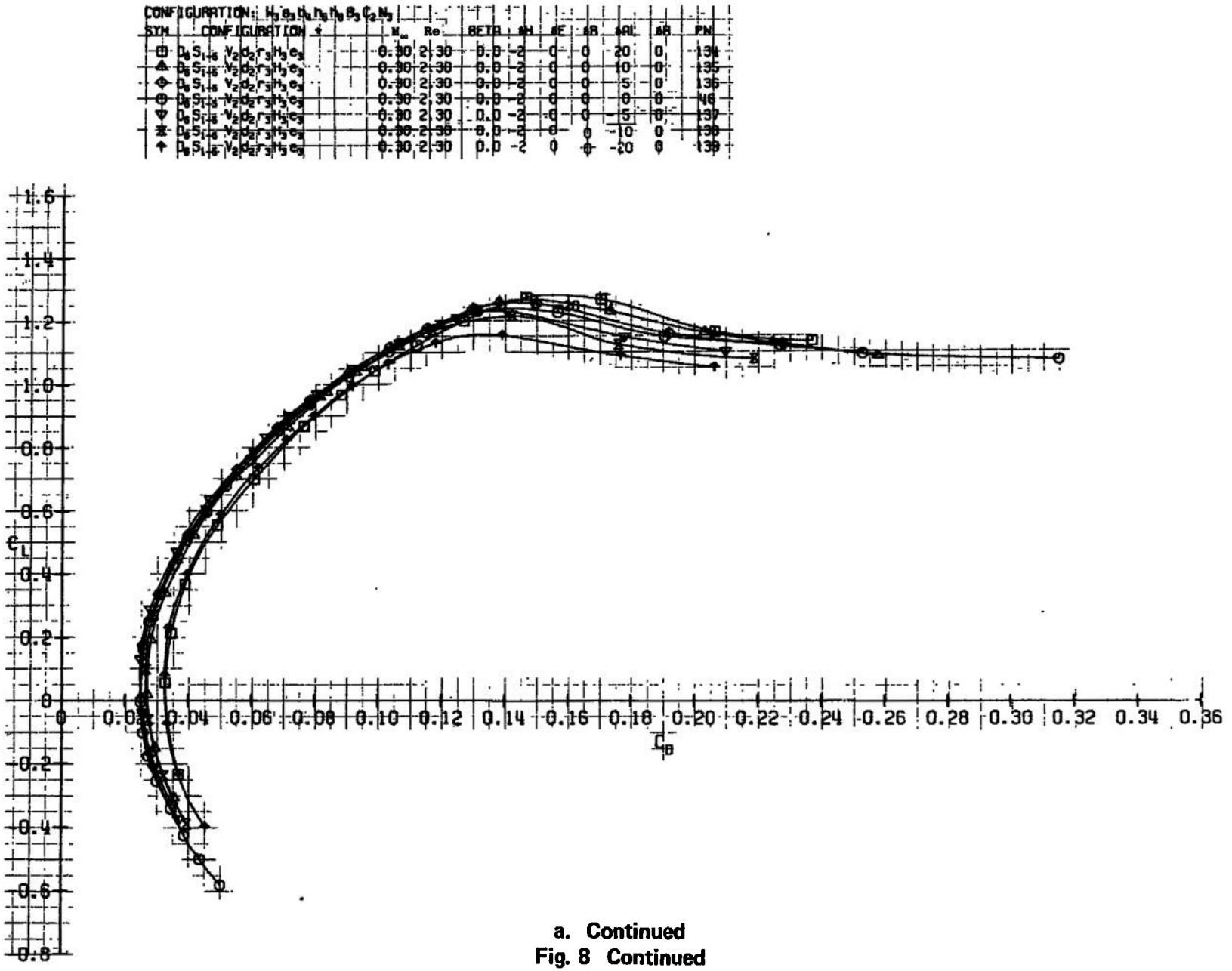

a. Continued

Fig. 8 Continued

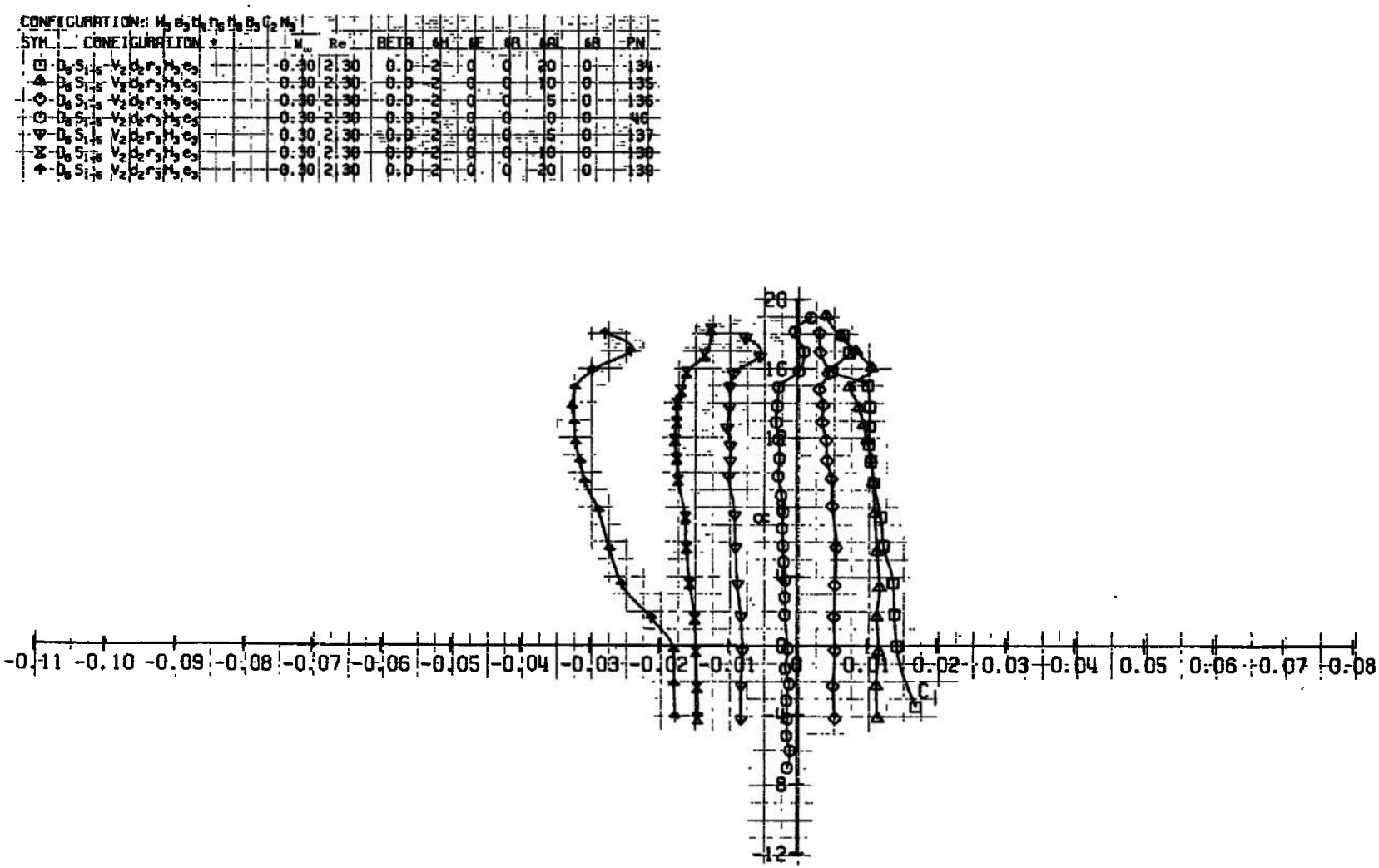

a. Concluded

Fig. 8 Continued

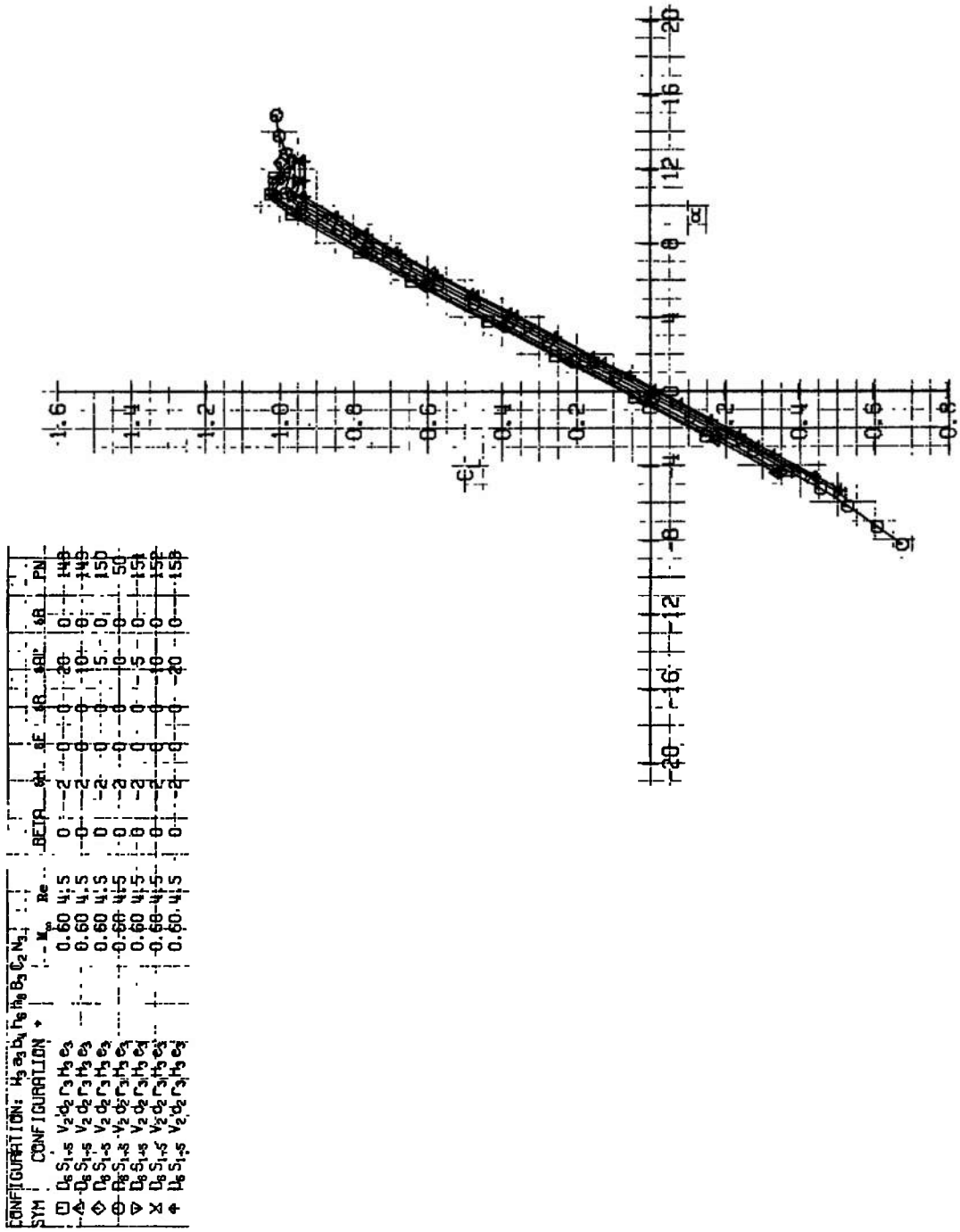

b. $M_\infty = 0.60$
Fig. 8 Continued

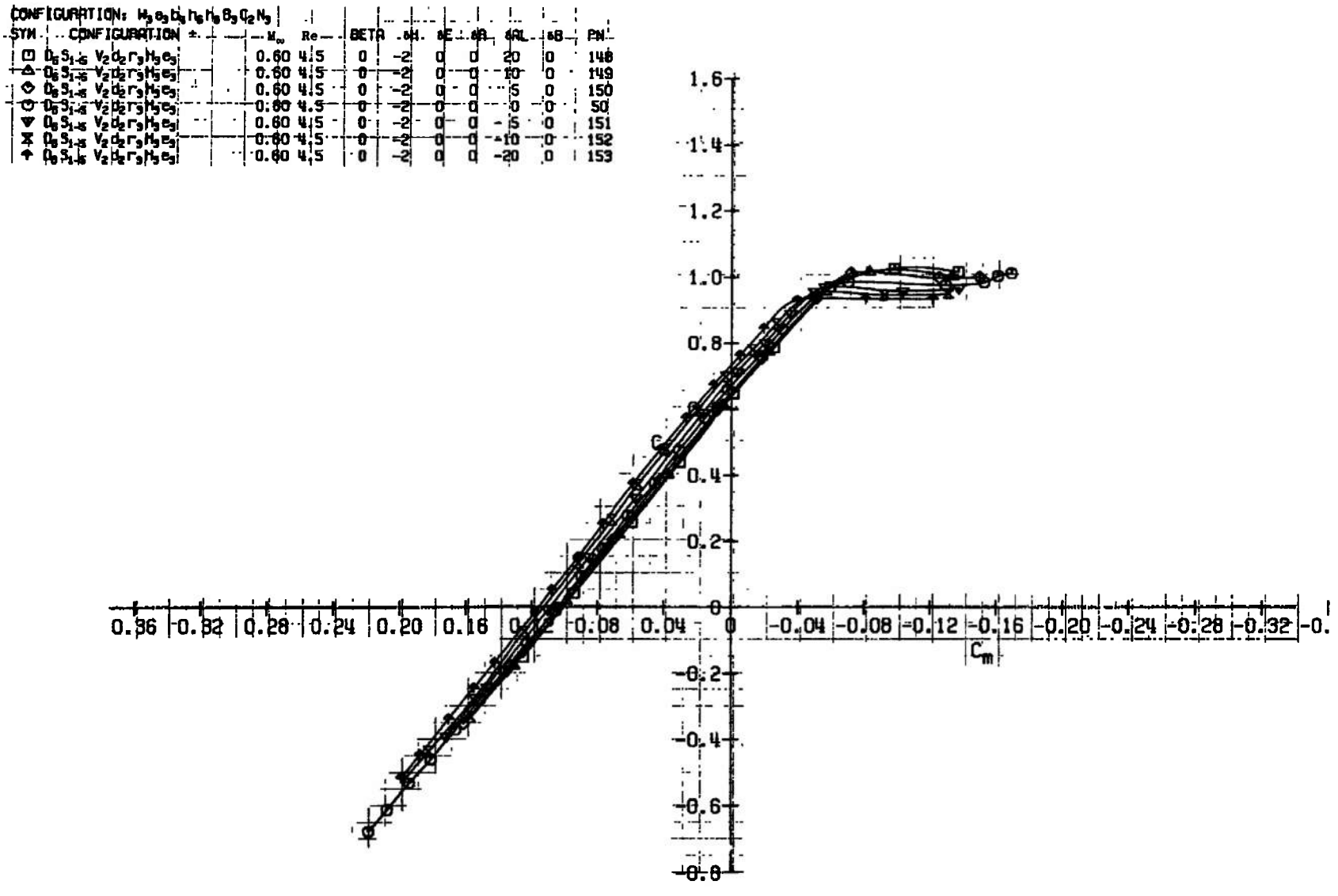

b. Continued

Fig. 8 Continued

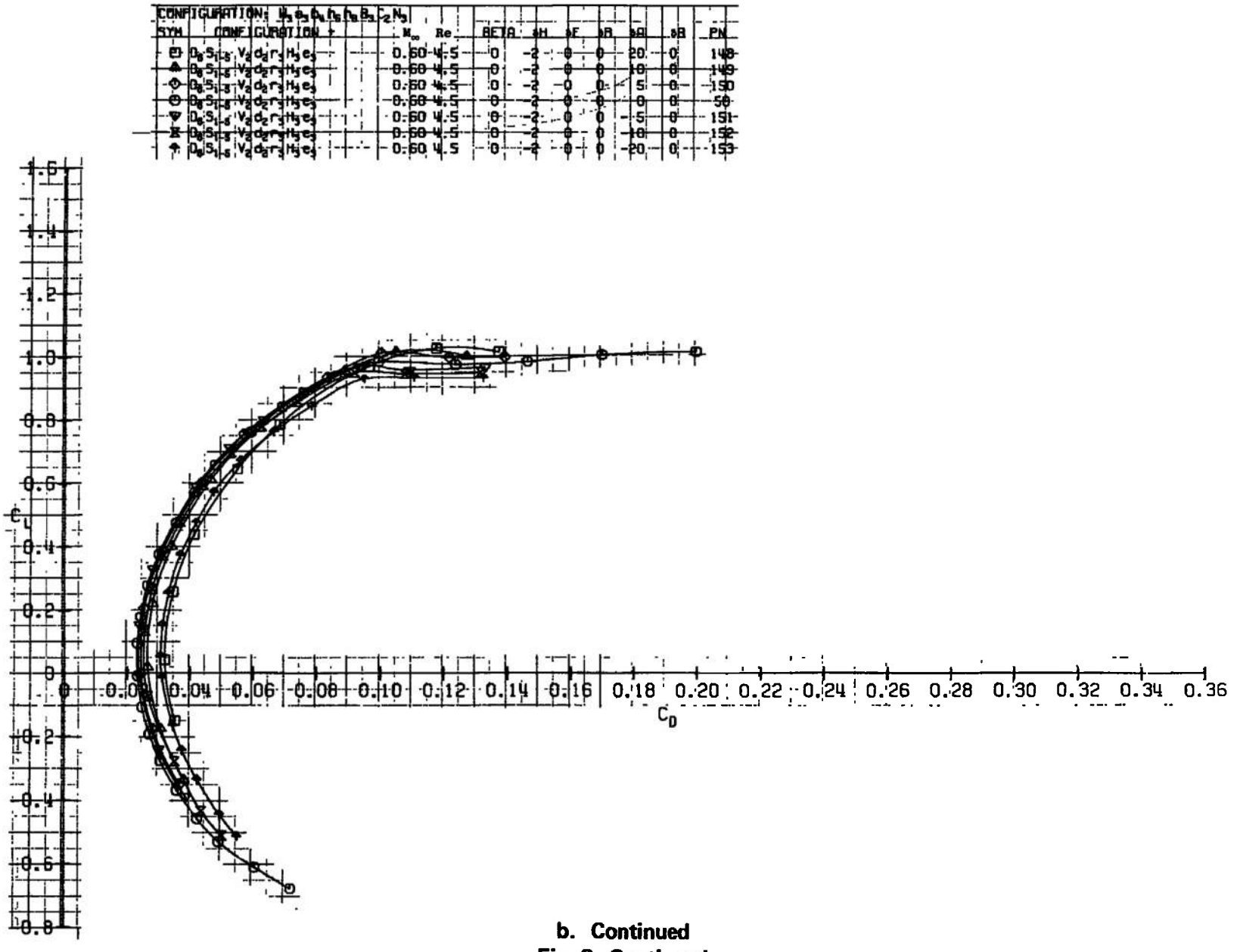

b. Continued

Fig. 8 Continued

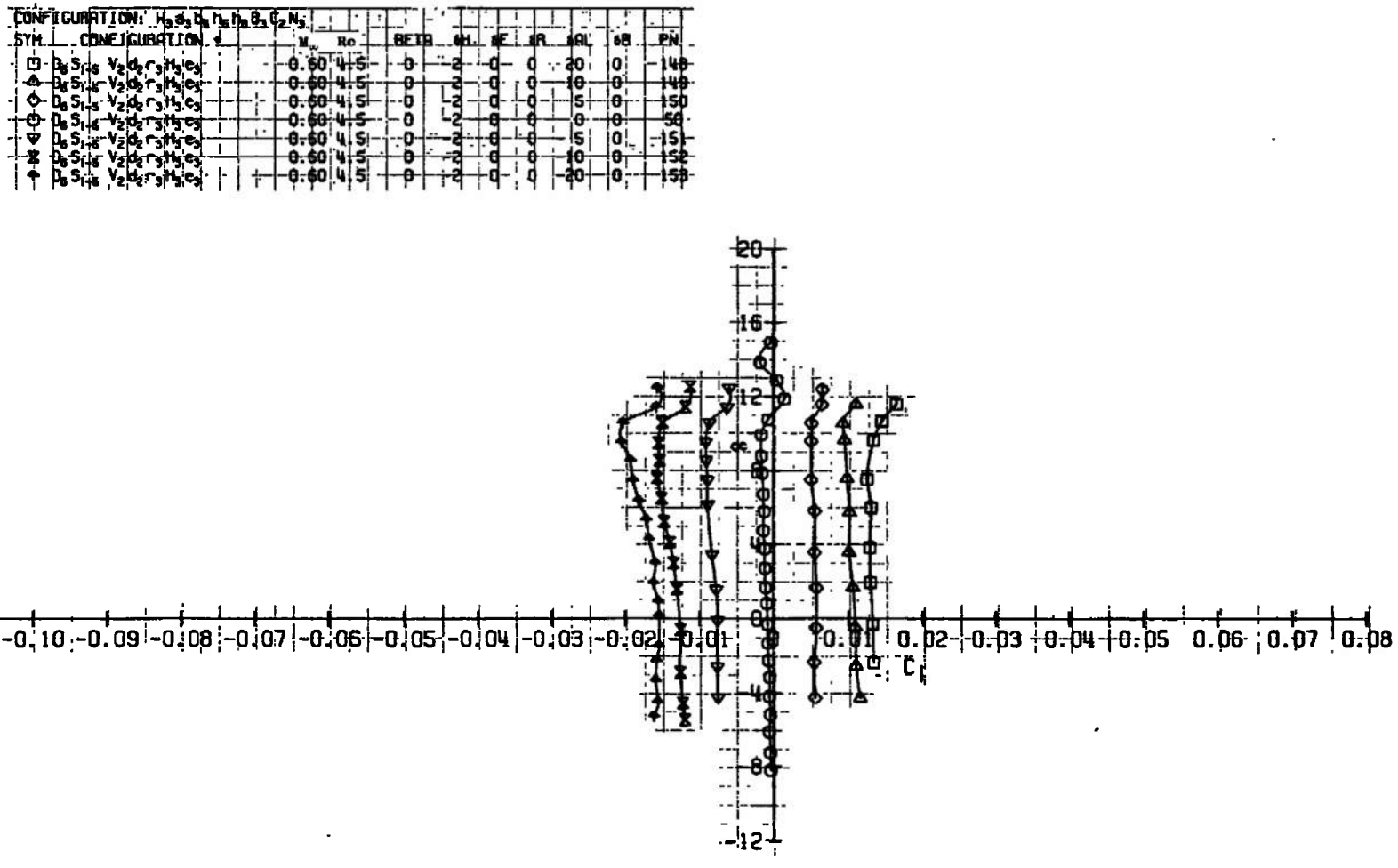

b. Concluded
Fig. 8 Continued

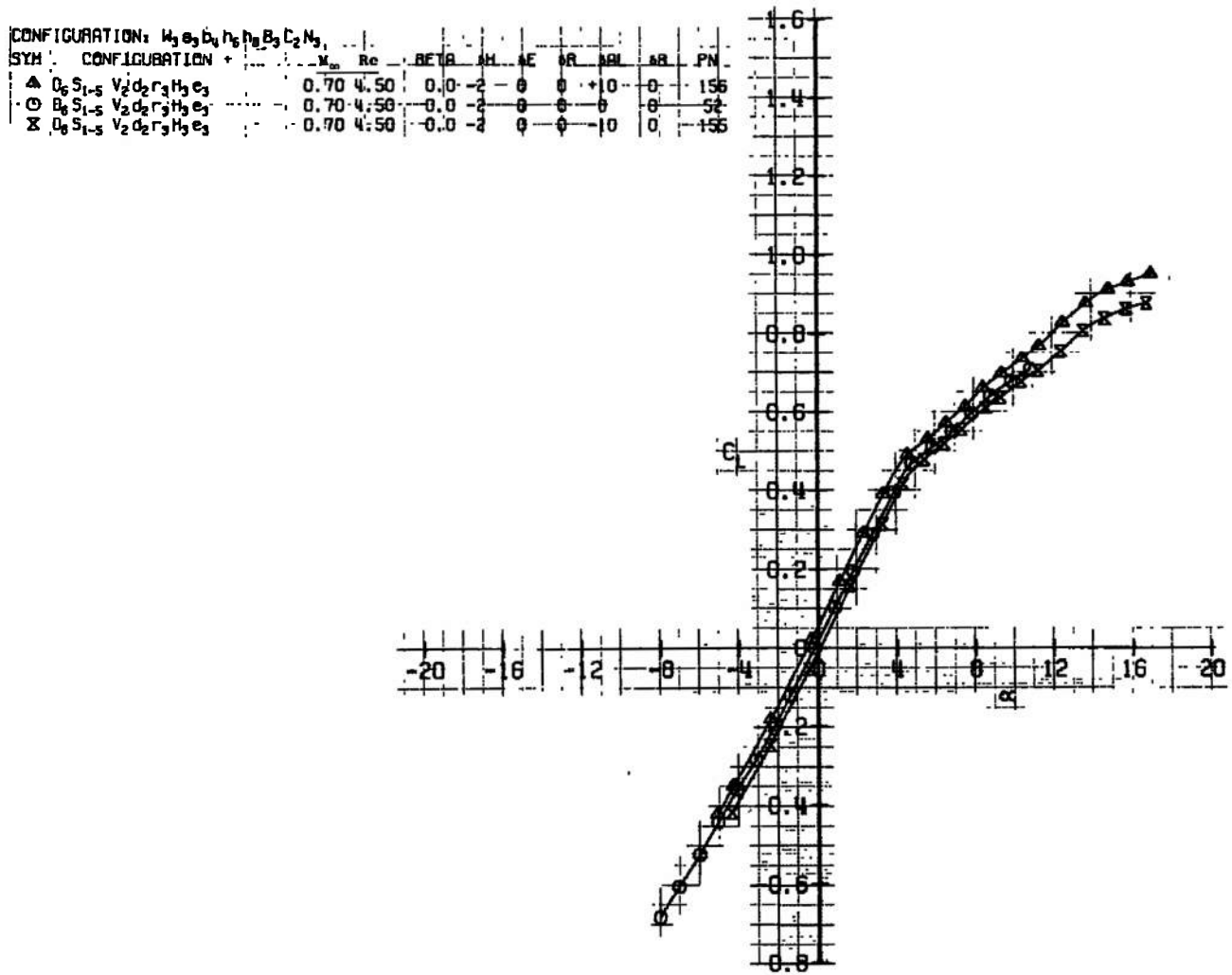

c. $M_\infty = 0.70$

Fig. 8 Continued

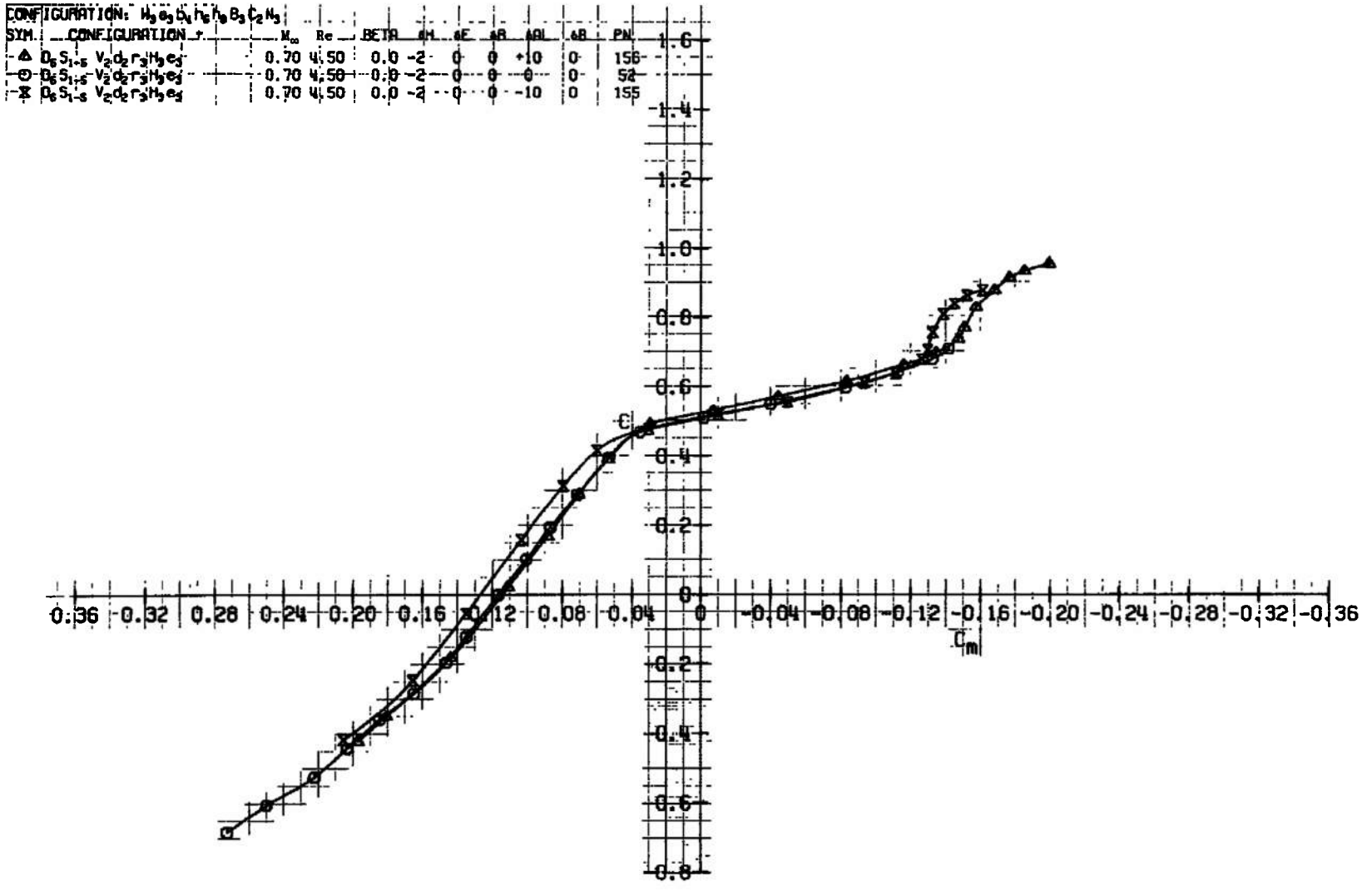

c. Continued

Fig. 8 Continued

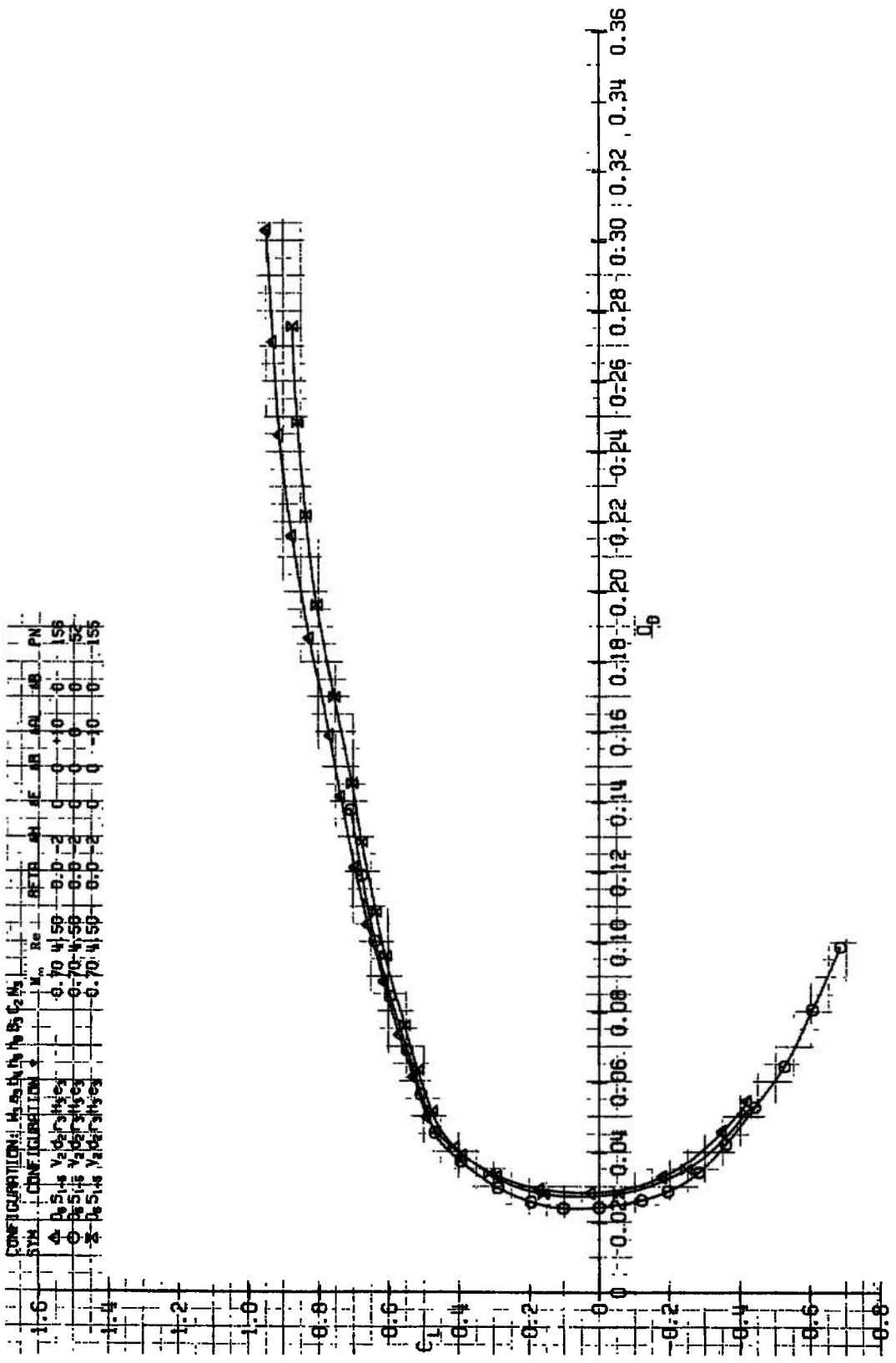

c. Continued
Fig. 8 Continued

CONFIGURATION: $M_3B_3M_6n_5n_6B_3C_2N_3$

SYM.	CONFIGURATION	M_∞	Re	BETA	ϕ_H	ϕ_F	ϕ_R	ϕ_{RL}	ϕ_B	PN
△	$D_6S_{1.6}V_2d_2r_3H_3e_3$	0.70	4.50	0.0	-2	0	0	+10	0	156
○	$D_6S_{1.6}V_2d_2r_3H_3e_3$	0.70	4.50	0.0	-2	0	0	0	0	52
✕	$D_6S_{1.6}V_2d_2r_3H_3e_3$	0.70	4.50	0.0	-2	0	0	-10	0	155

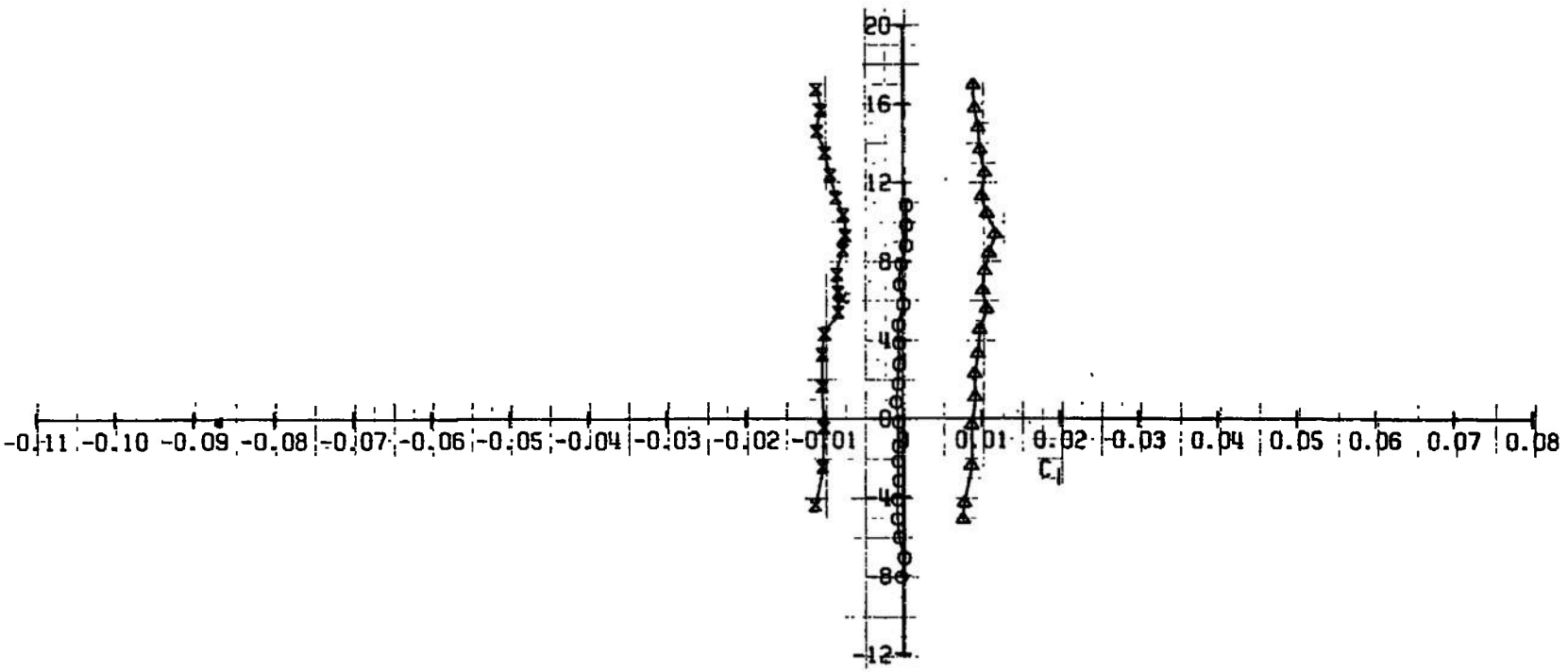

c. Concluded

Fig. 8 Continued

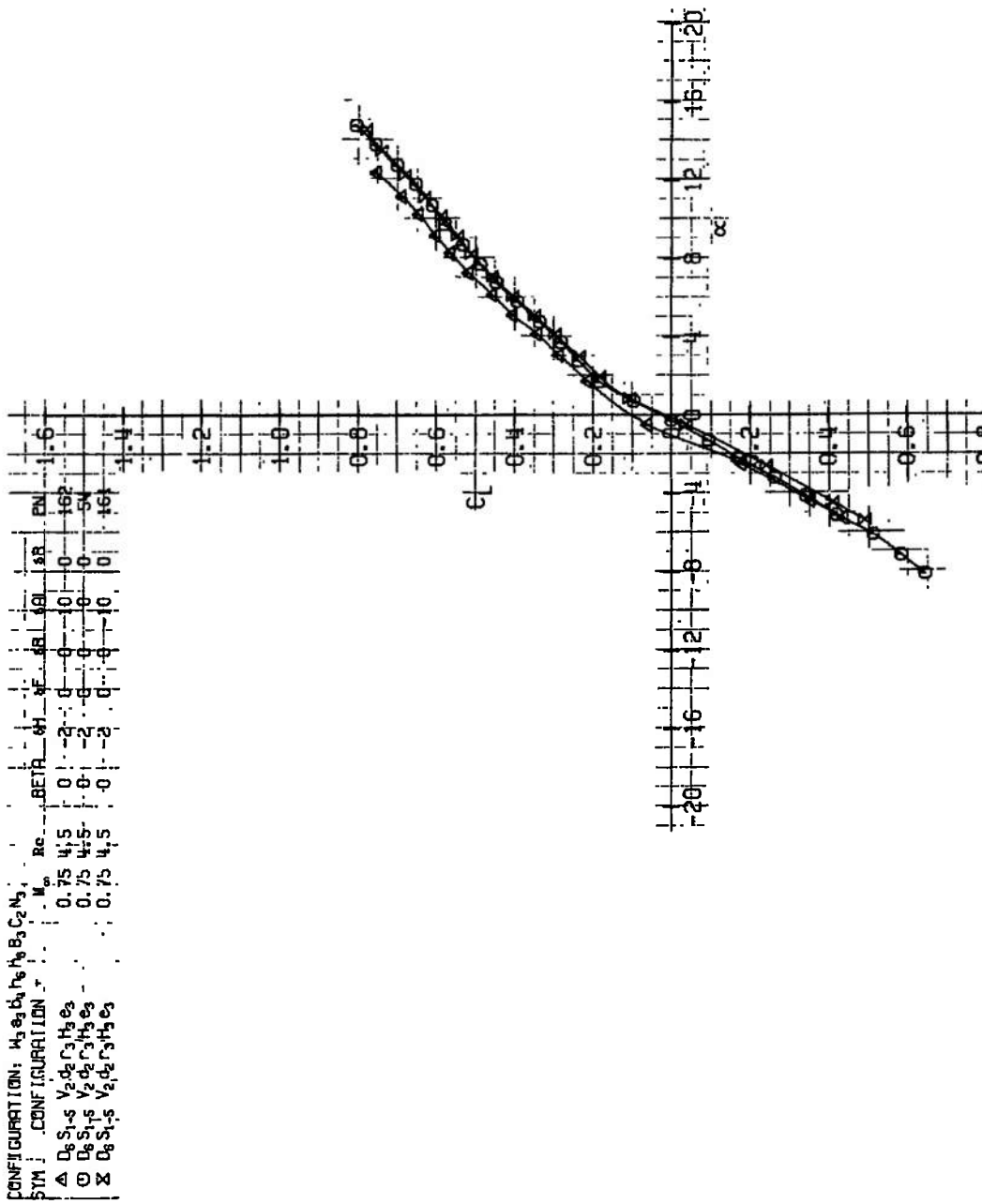

d. $M_\infty = 0.75$
Fig. 8 Continued

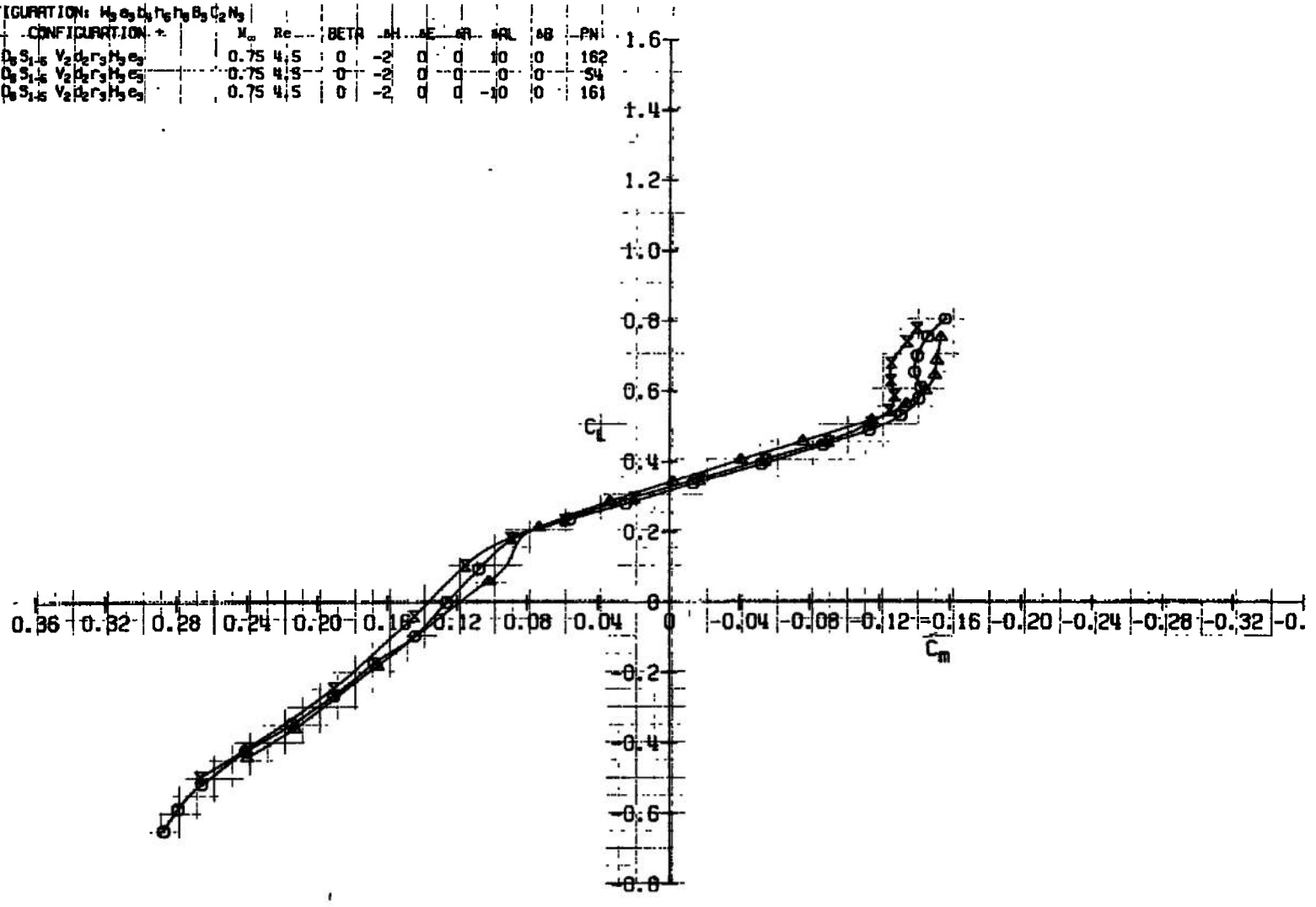

d. Continued

Fig. 8 Continued

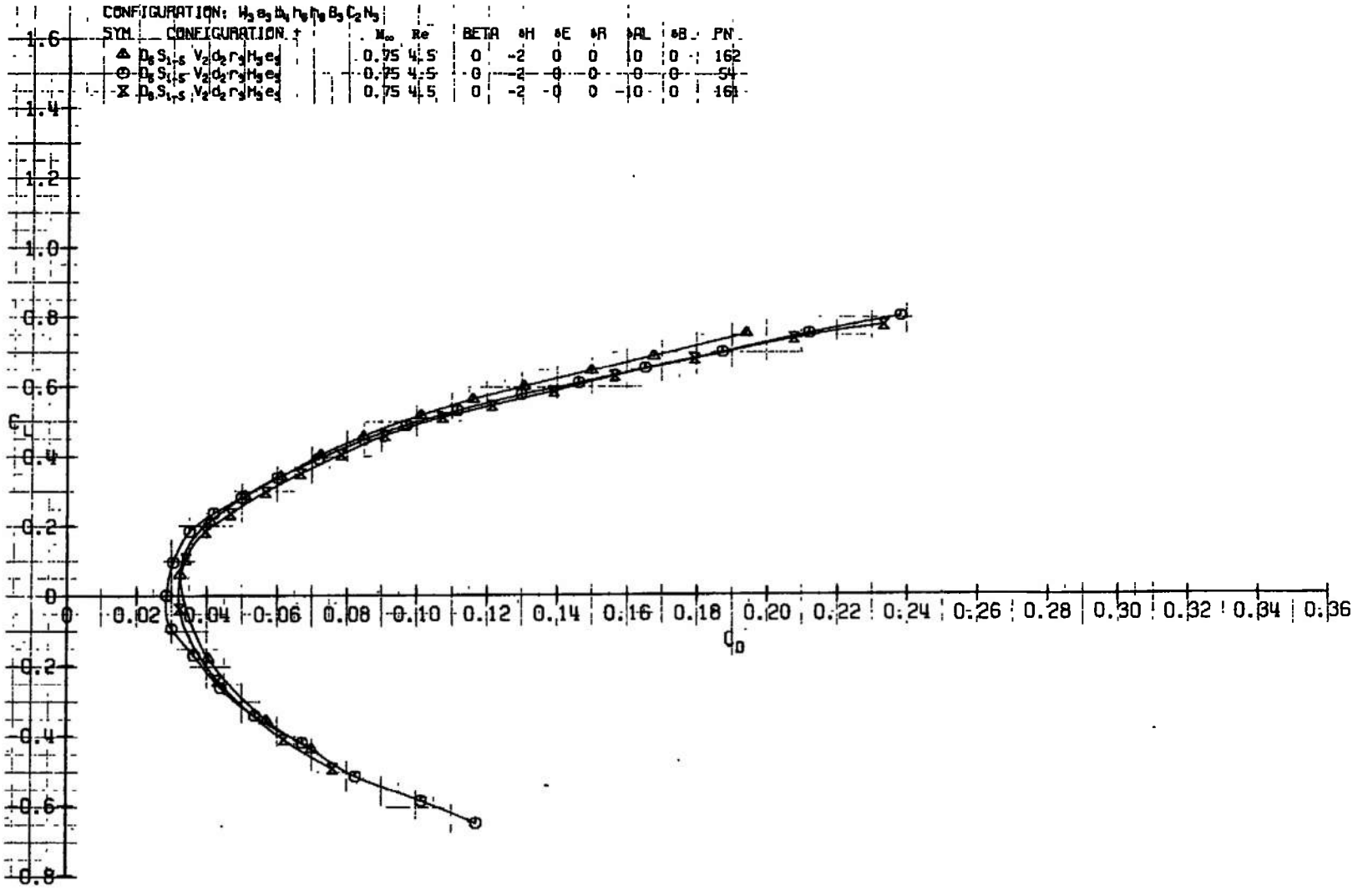

d. Continued

Fig. 8 Continued

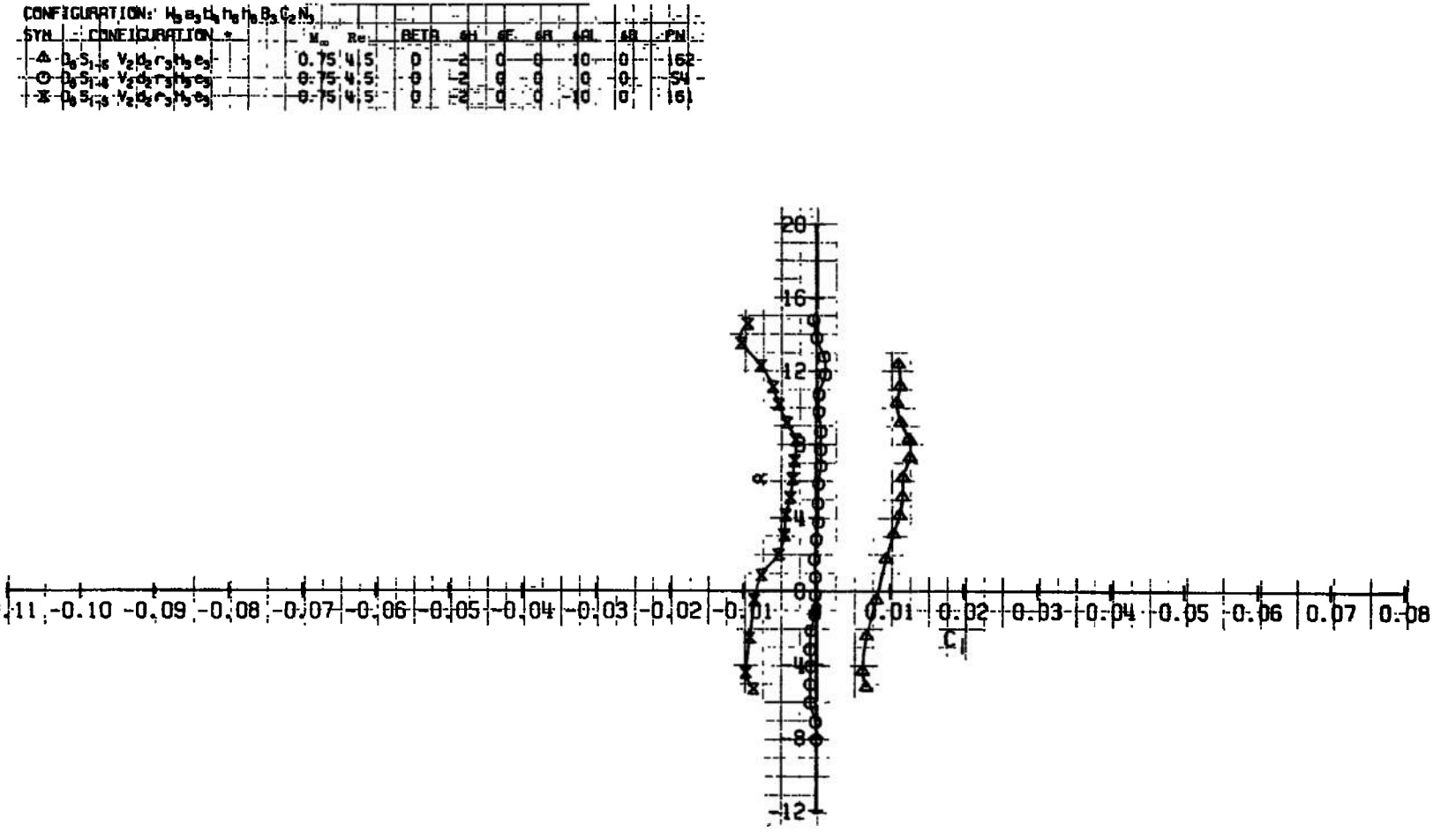

d. Concluded

Fig. 8 Continued

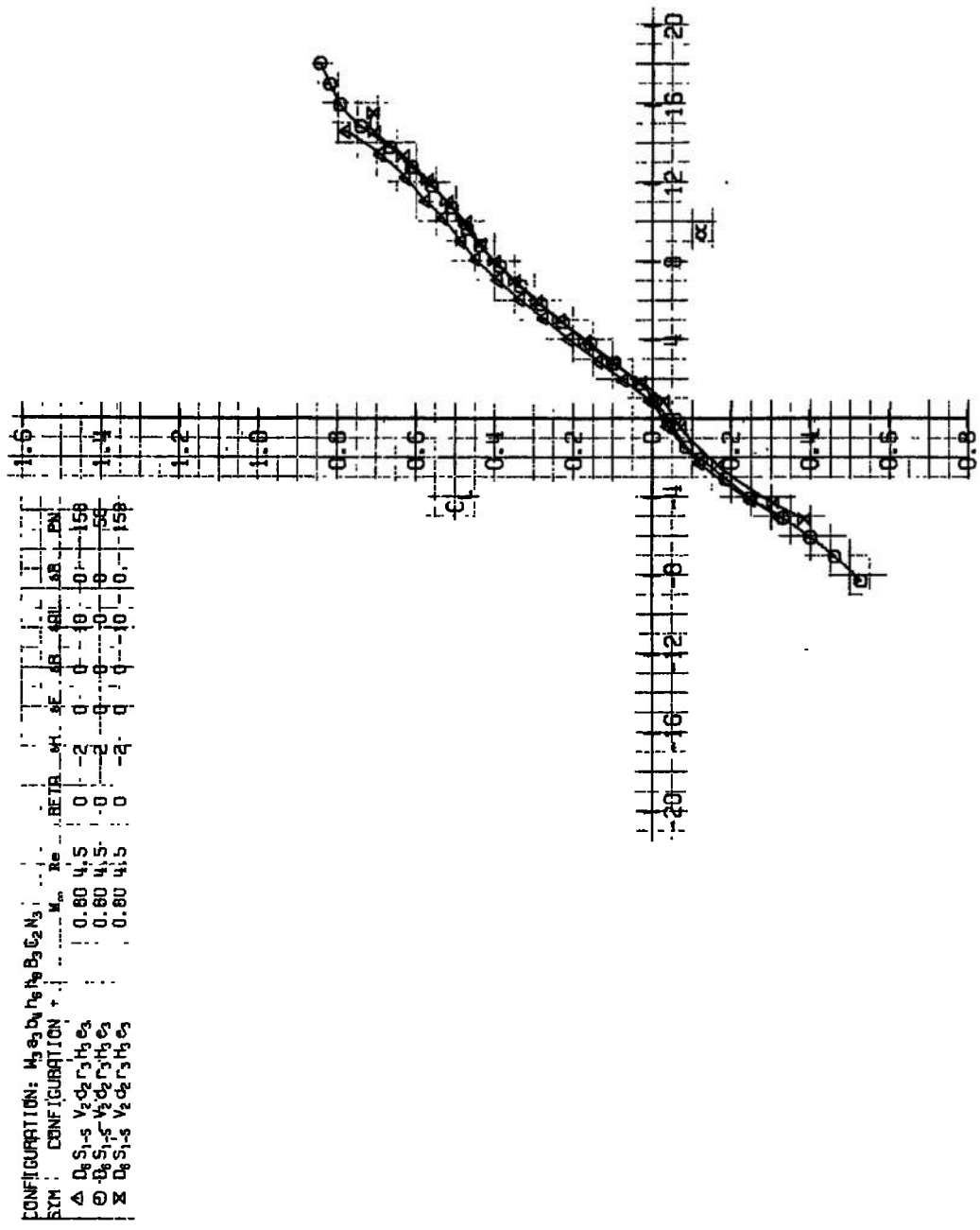

e. $M_\infty = 0.80$

Fig. 8 Continued

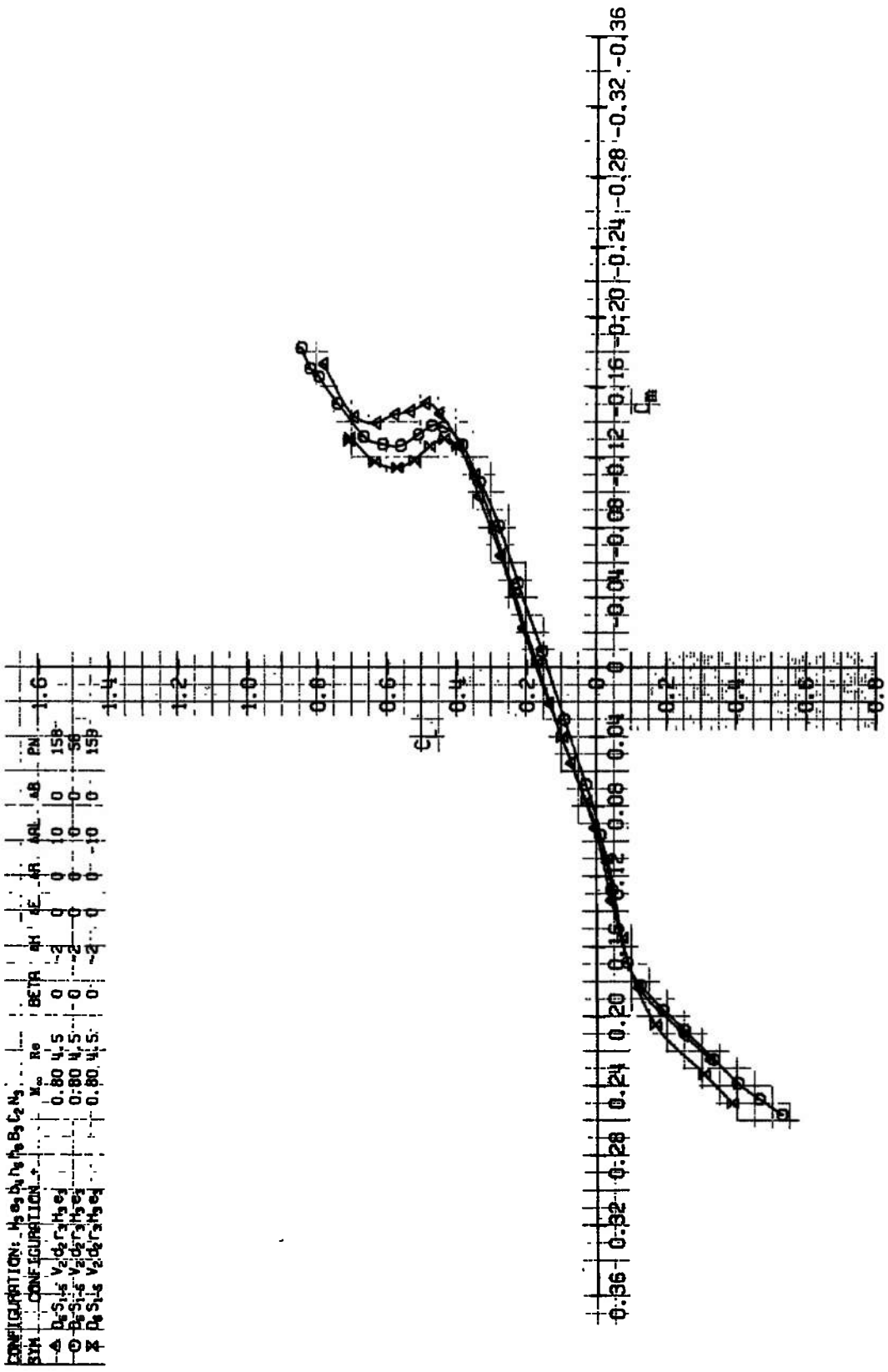

e. Continued
Fig. 8 Continued

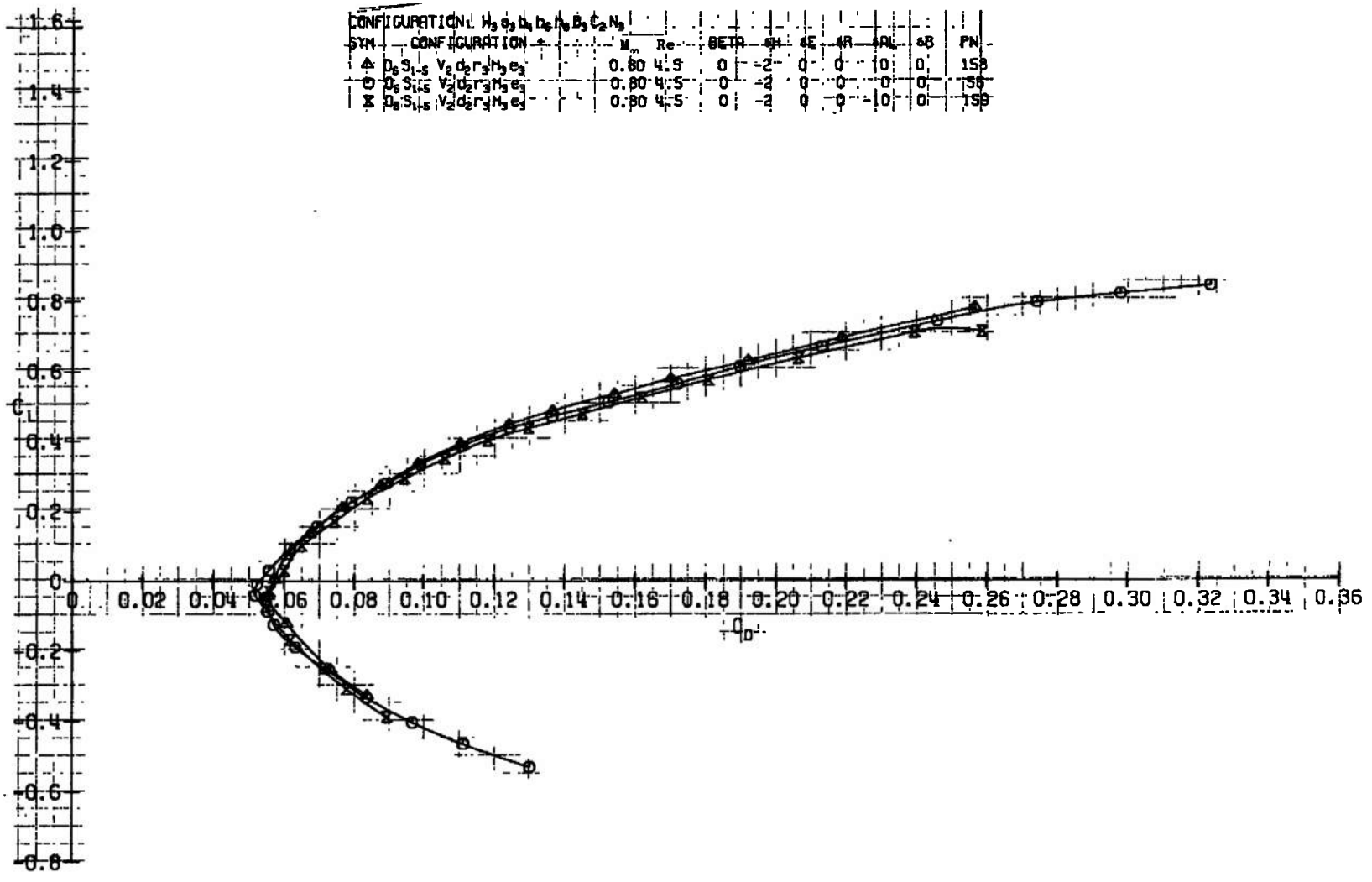

e. Continued

Fig. 8 Continued

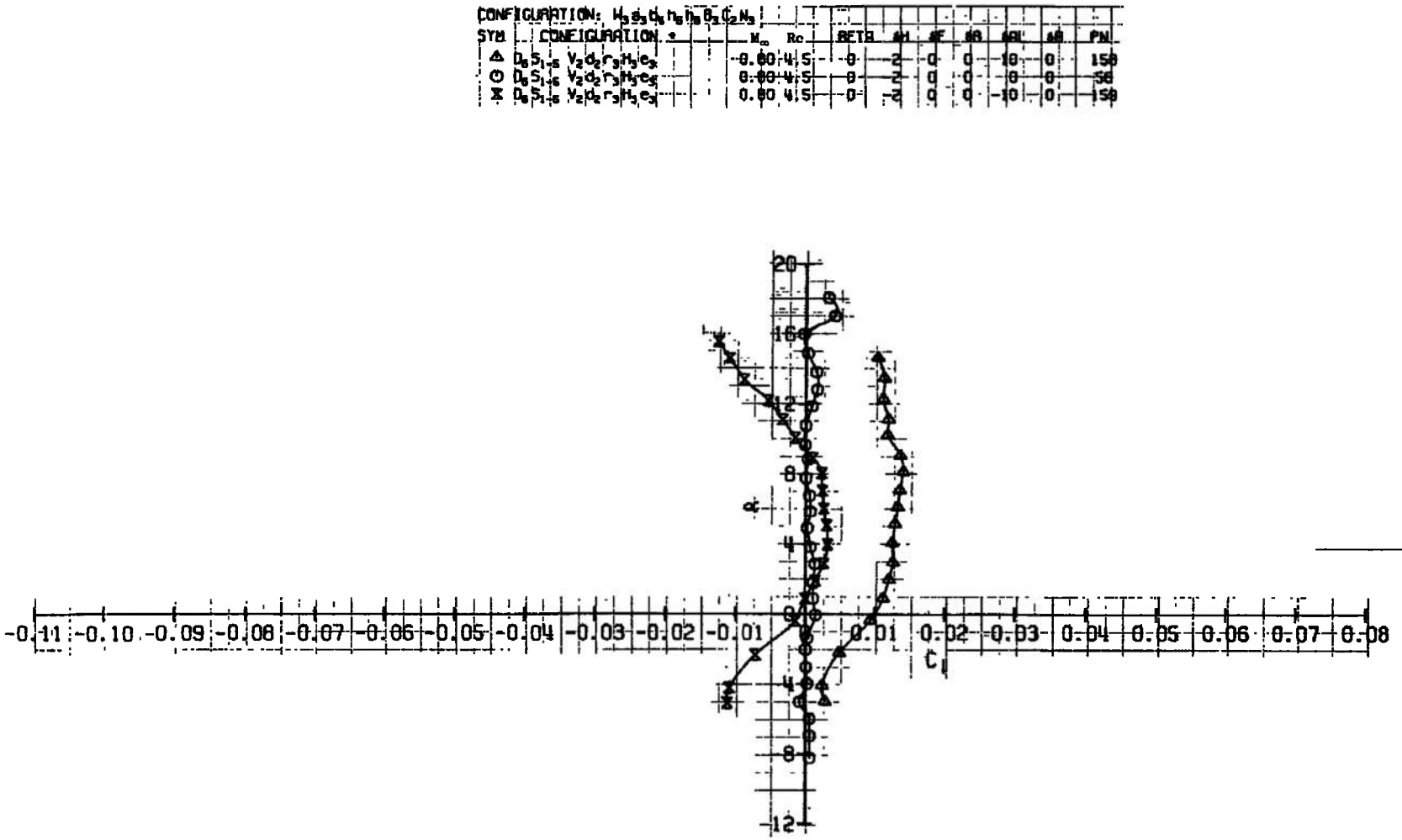

e. Concluded

Fig. 8 Continued

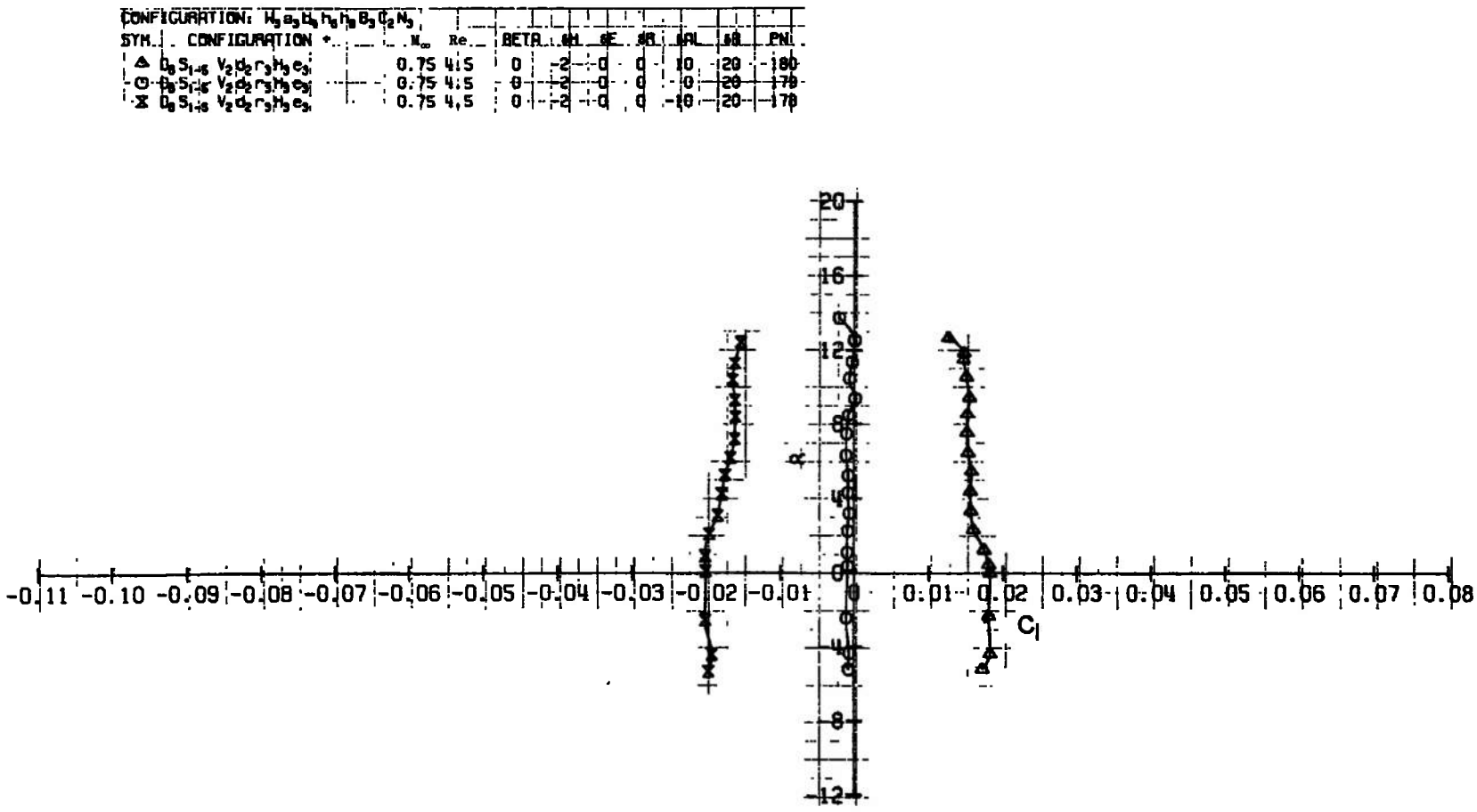

f. $M_\infty = 0.75$

Fig. 8 Continued

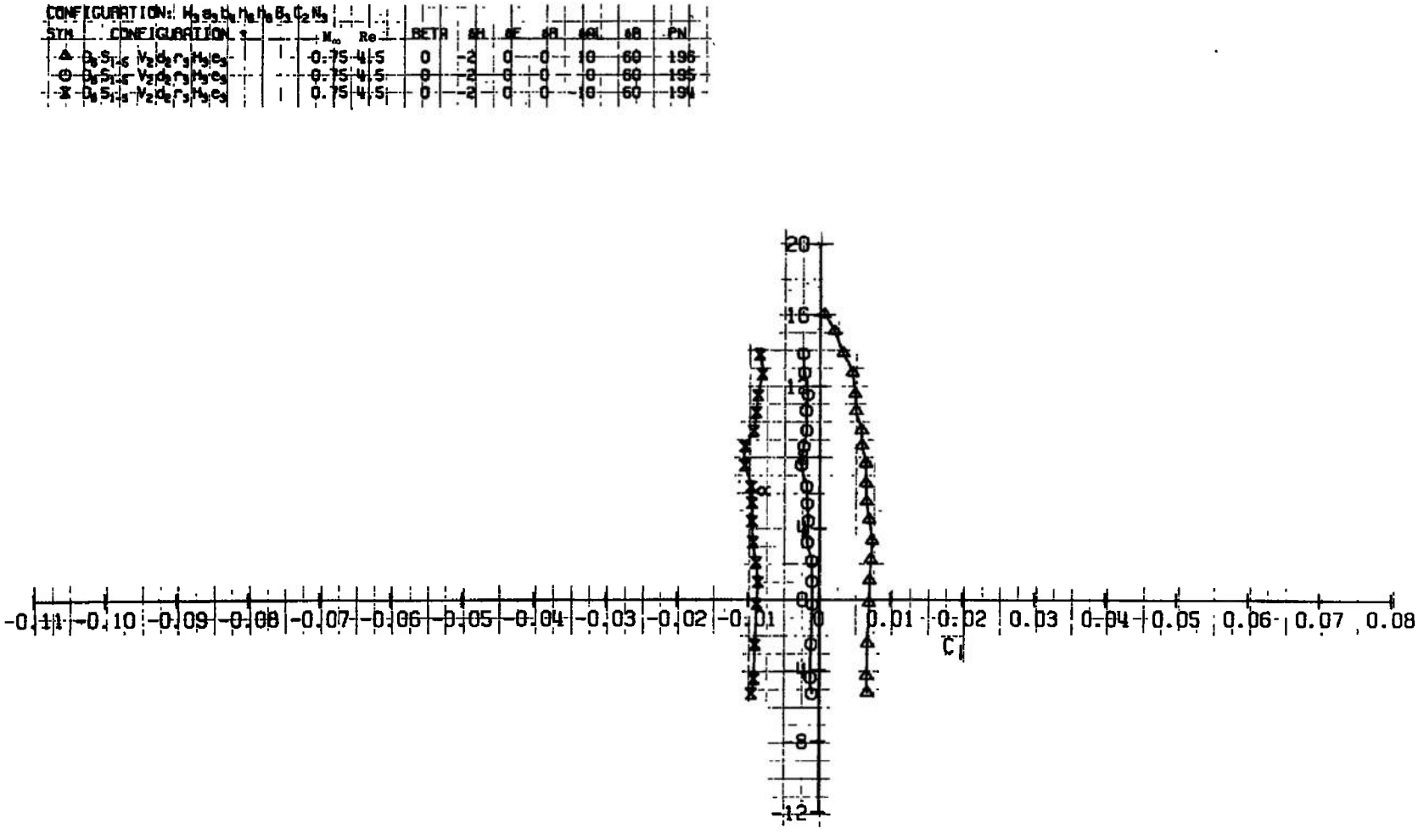

f. Concluded
Fig. 8 Continued

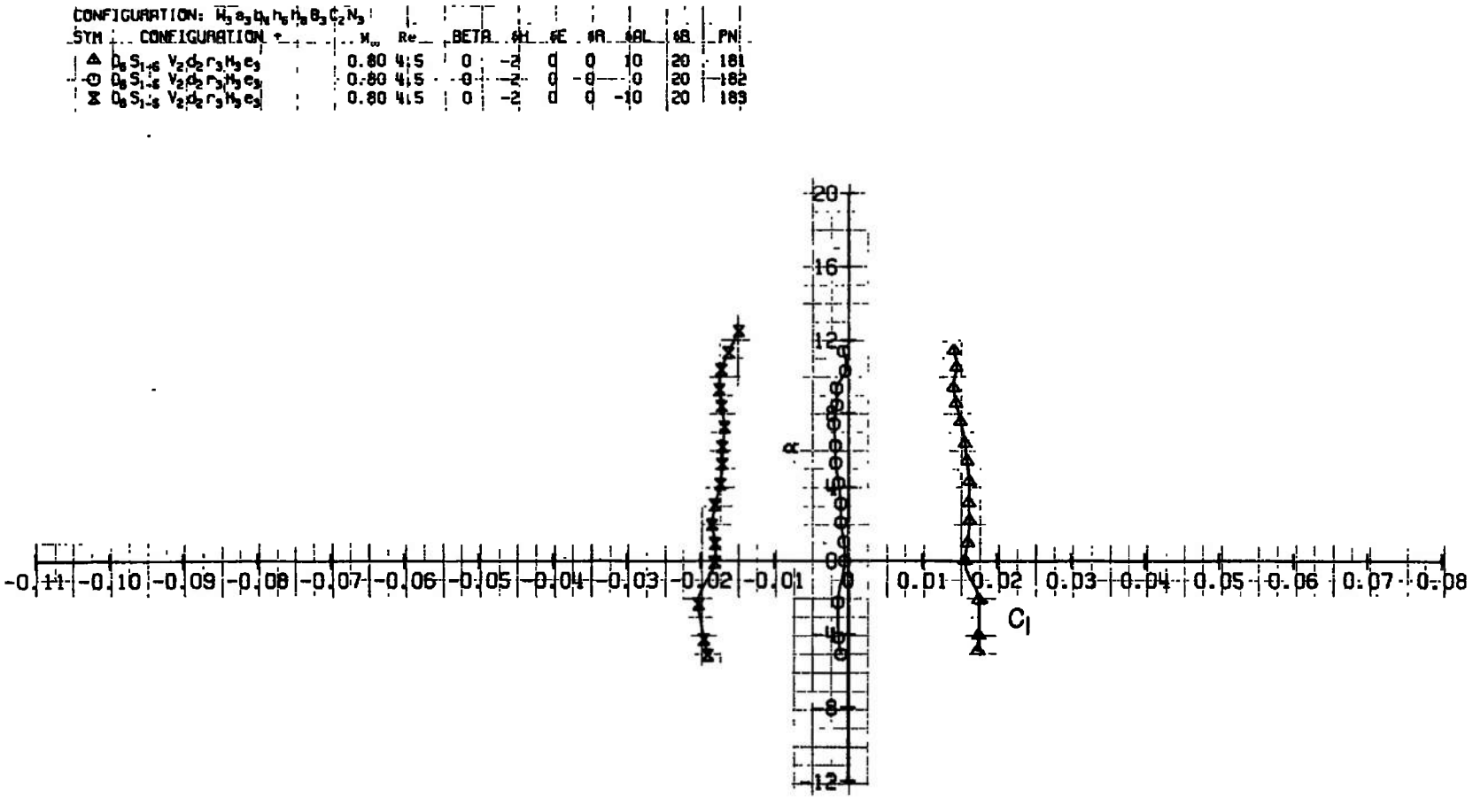

g. M_∞ = 0.80
Fig. 8 Continued

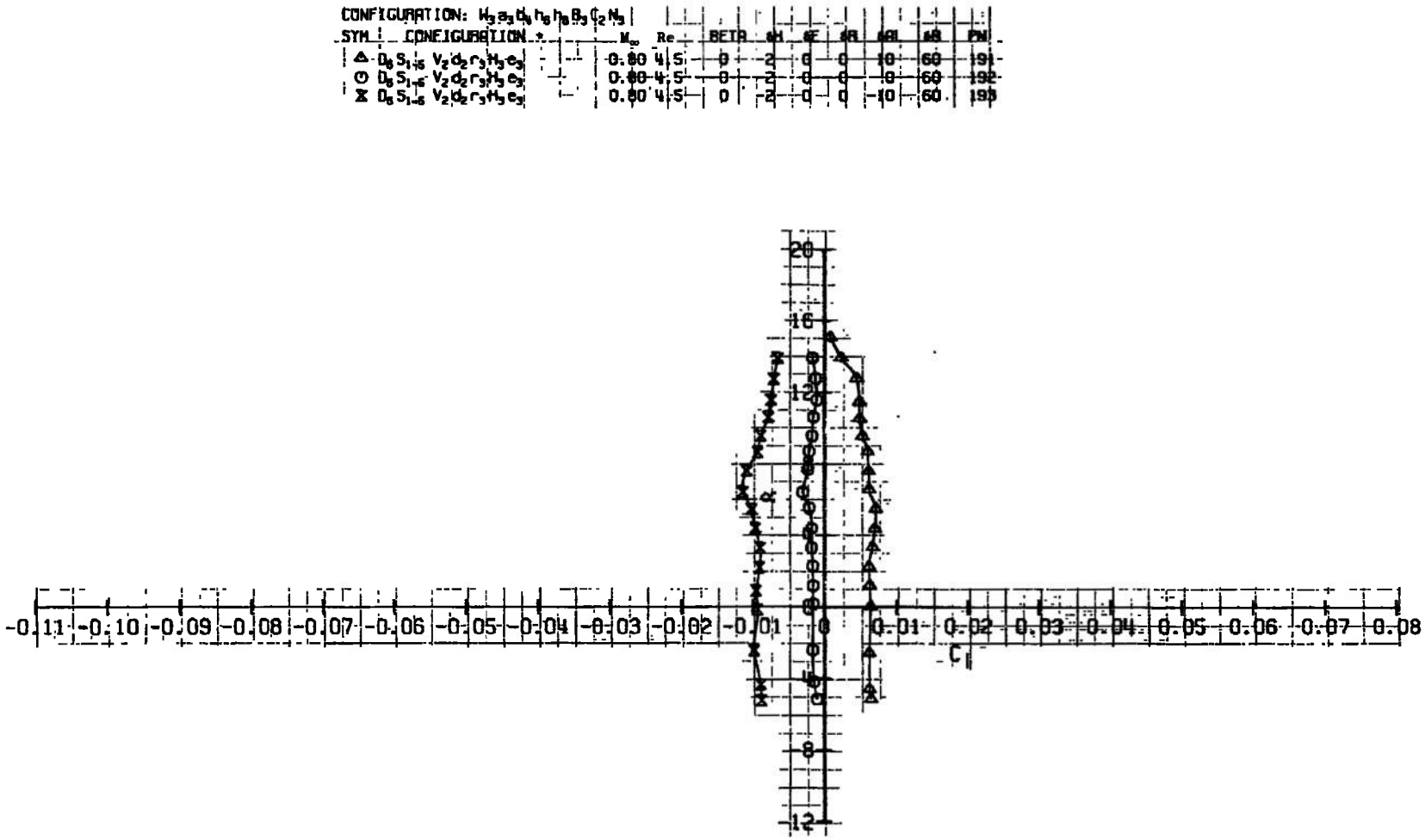

g. Concluded

Fig. 8 Concluded

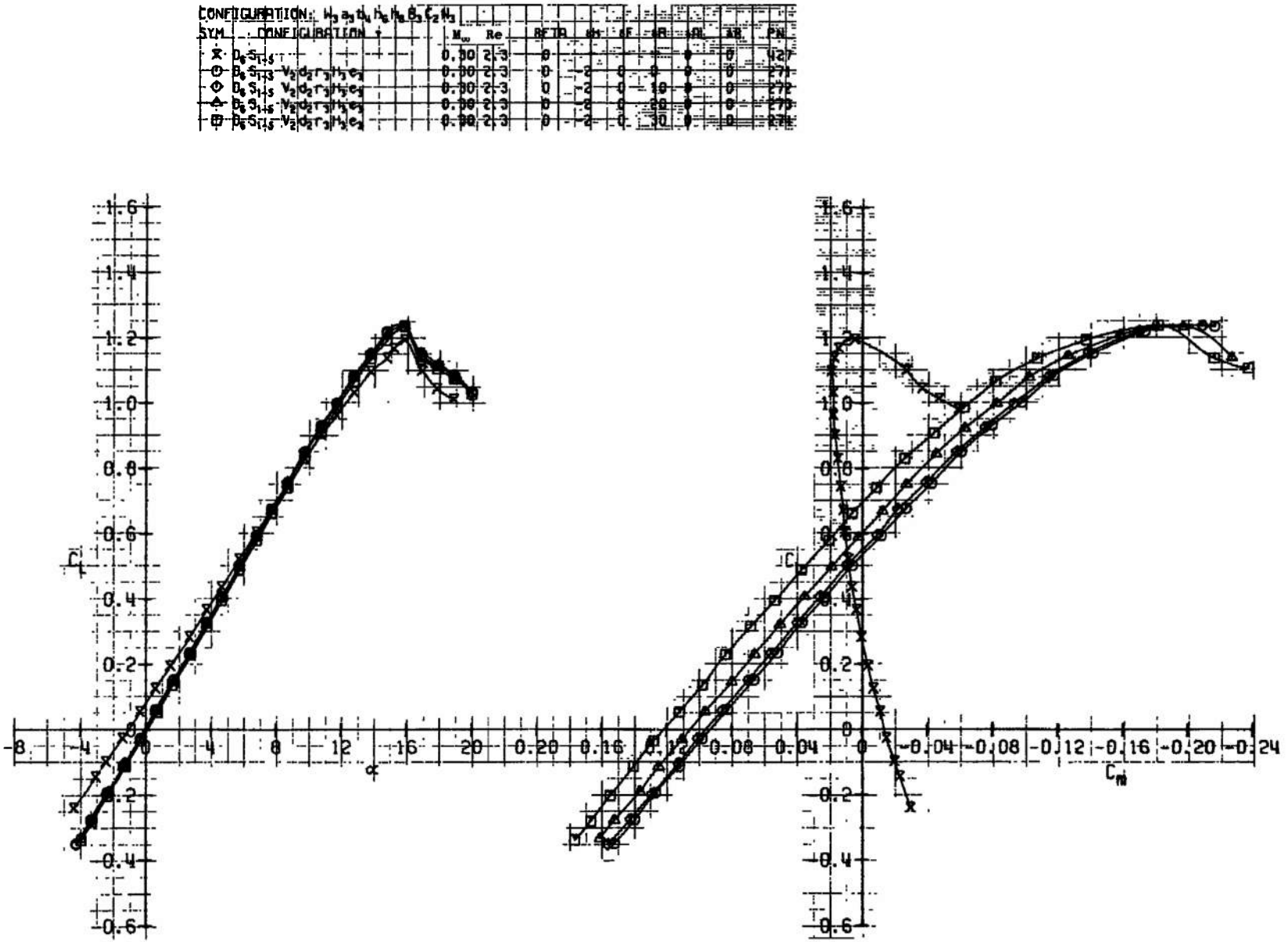

a. $M_\infty = 0.30$

Fig. 9 Rudder Effectiveness

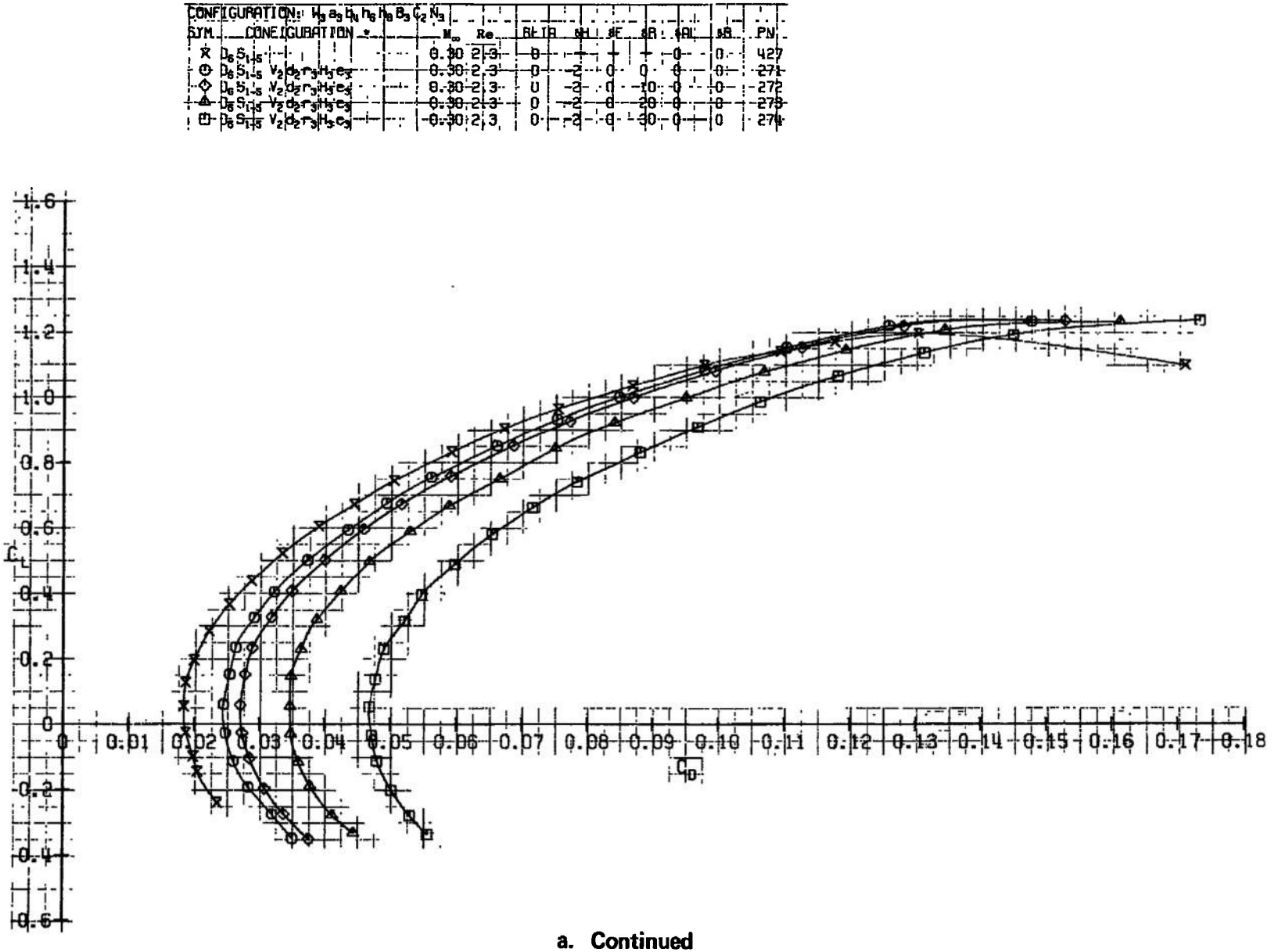

a. Continued

Fig. 9 Continued

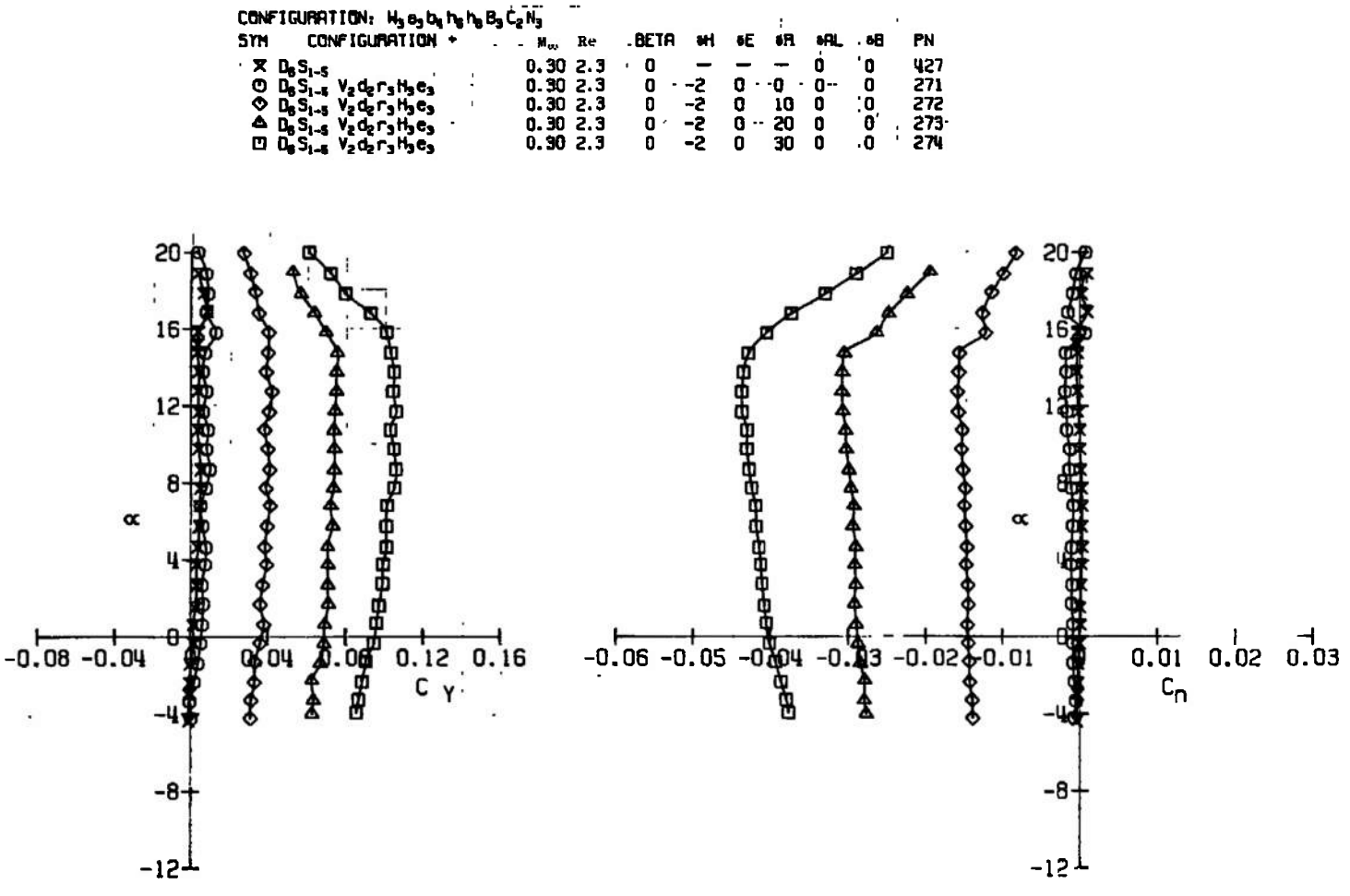

a. Continued

Fig. 9 Continued

CONFIGURATION: $W_3 e_3 b_6 h_6 h_8 B_3 C_2 N_3$

SYM	CONFIGURATION +	M_∞	Re	BETA	δH	δE	δR	δRL	δB	PN
✕	$D_6 S_{1-5}$	0.30	2.3	0	—	—	—	0	0	427
⊙	$D_6 S_{1-5} V_2 d_2 r_3 H_3 e_3$	0.30	2.3	0	-2	0	0	0	0	271
◇	$D_6 S_{1-5} V_2 d_2 r_3 H_3 e_3$	0.30	2.3	0	-2	0	10	0	0	272
△	$D_6 S_{1-5} V_2 d_2 r_3 H_3 e_3$	0.30	2.3	0	-2	0	20	0	0	273
□	$D_6 S_{1-5} V_2 d_2 r_3 H_3 e_3$	0.30	2.3	0	-2	0	30	0	0	274

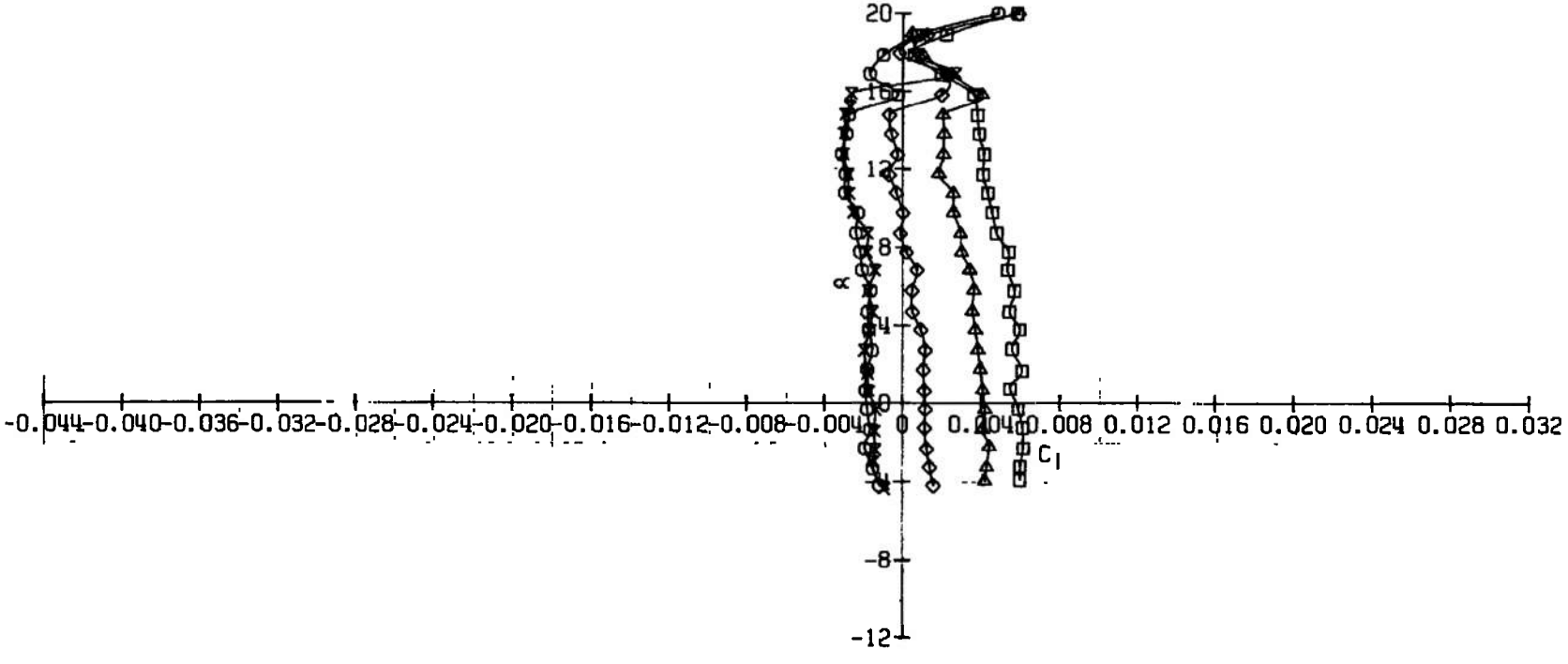

a. Concluded

Fig. 9 Continued

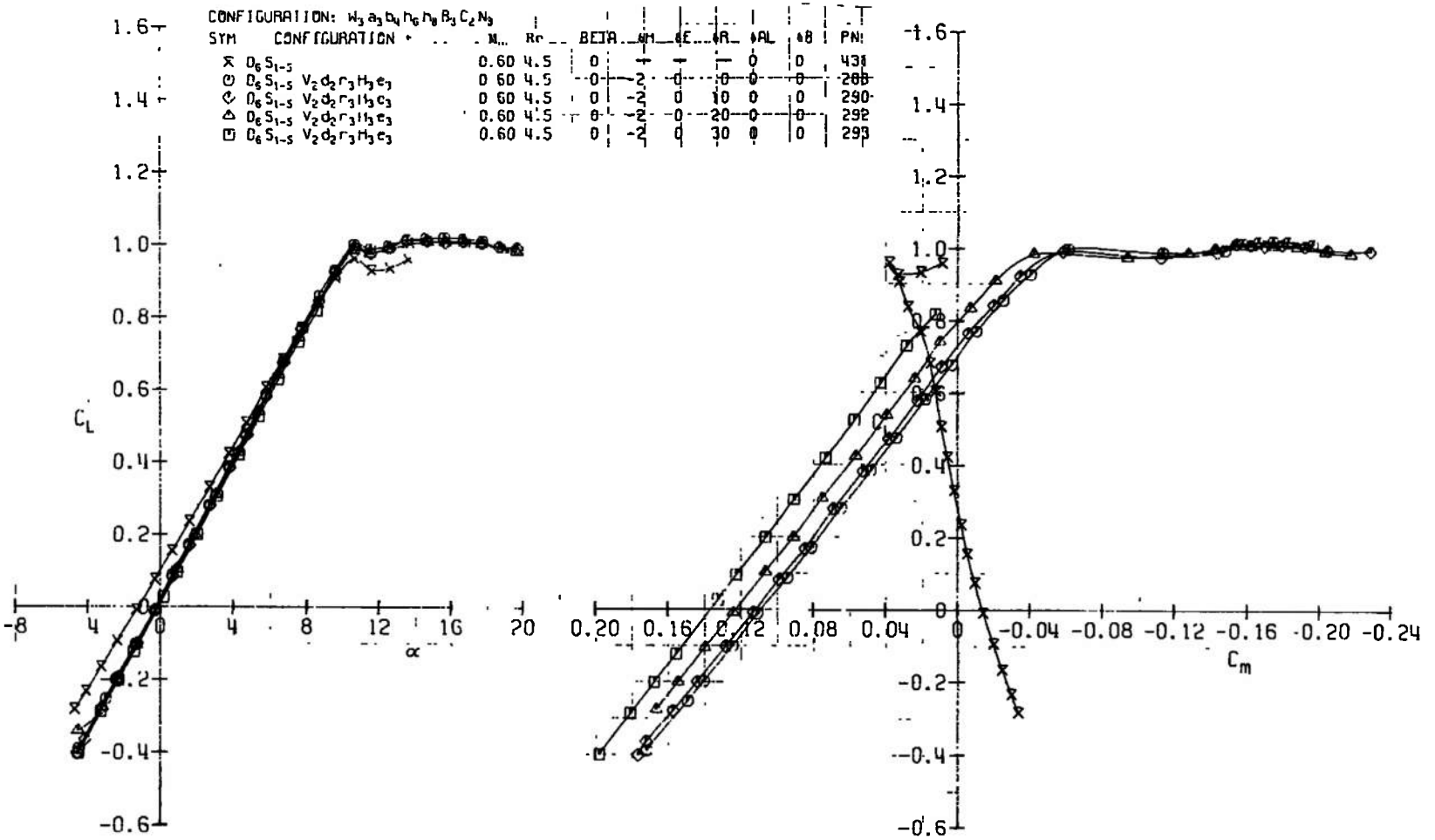

b. $M_\infty = 0.60$
Fig. 9 Continued

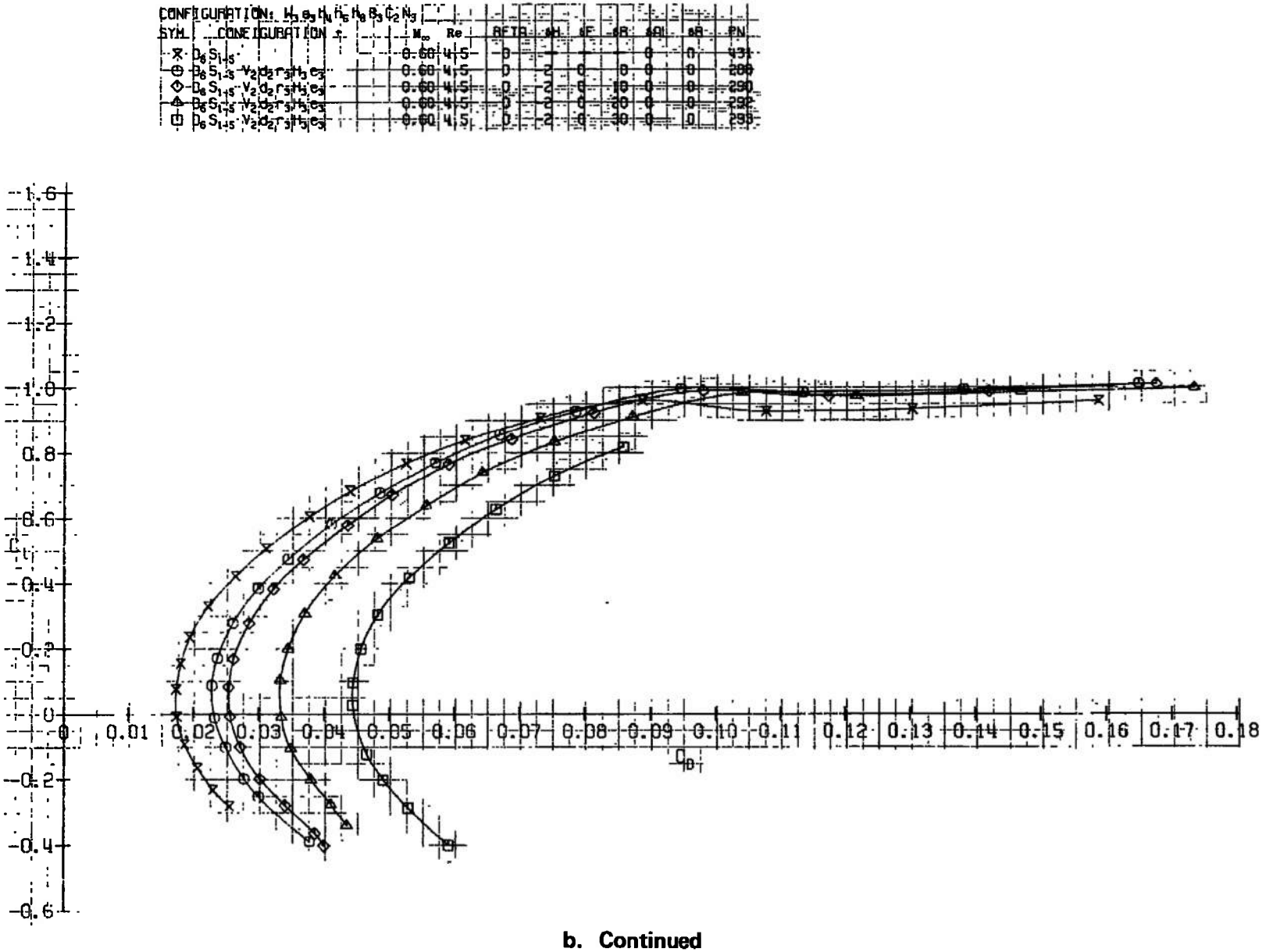

b. Continued

Fig. 9 Continued

b. Continued

Fig. 9 Continued

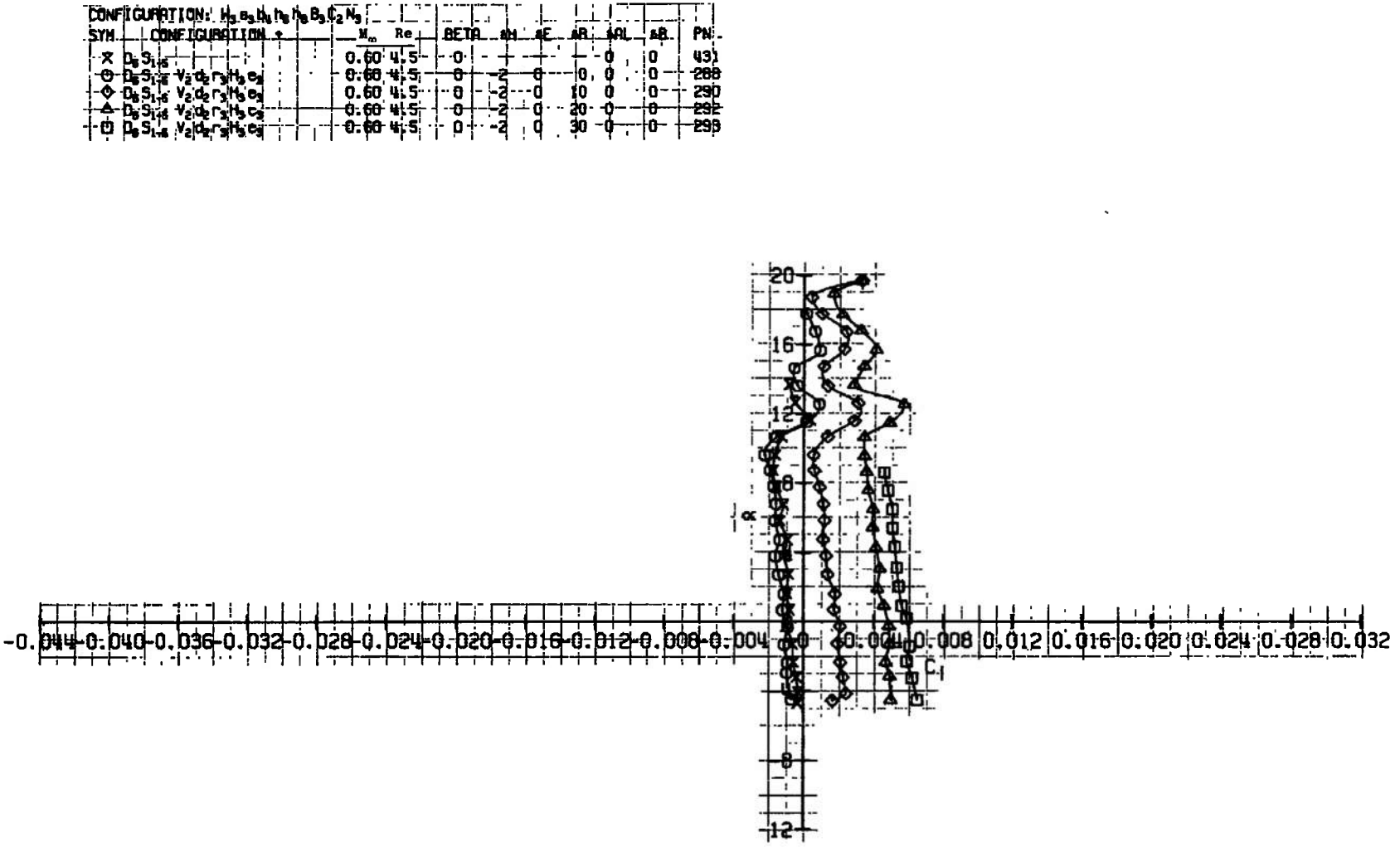

b. Concluded

Fig. 9 Continued

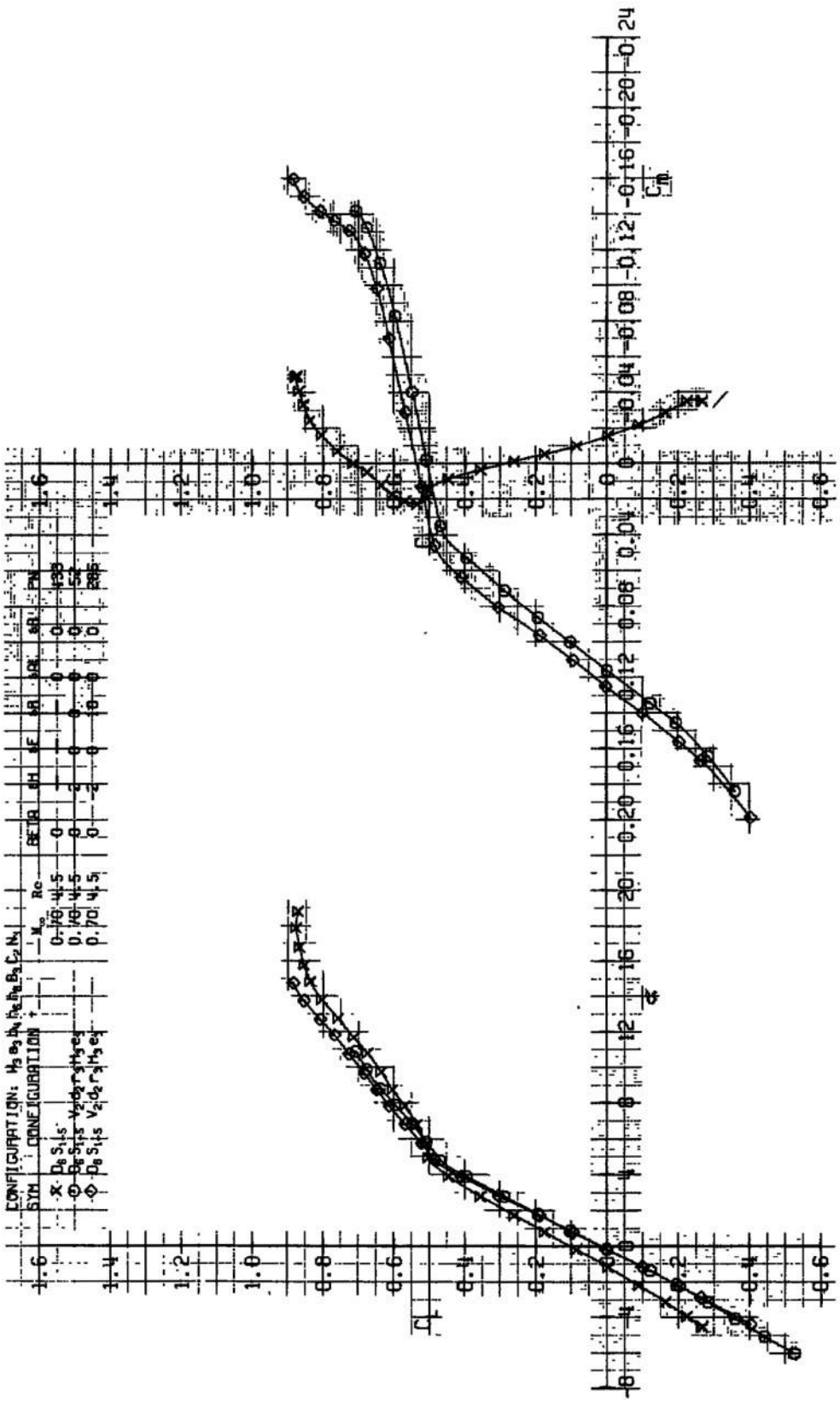

c. $M_\infty = 0.70$
Fig. 9 Continued

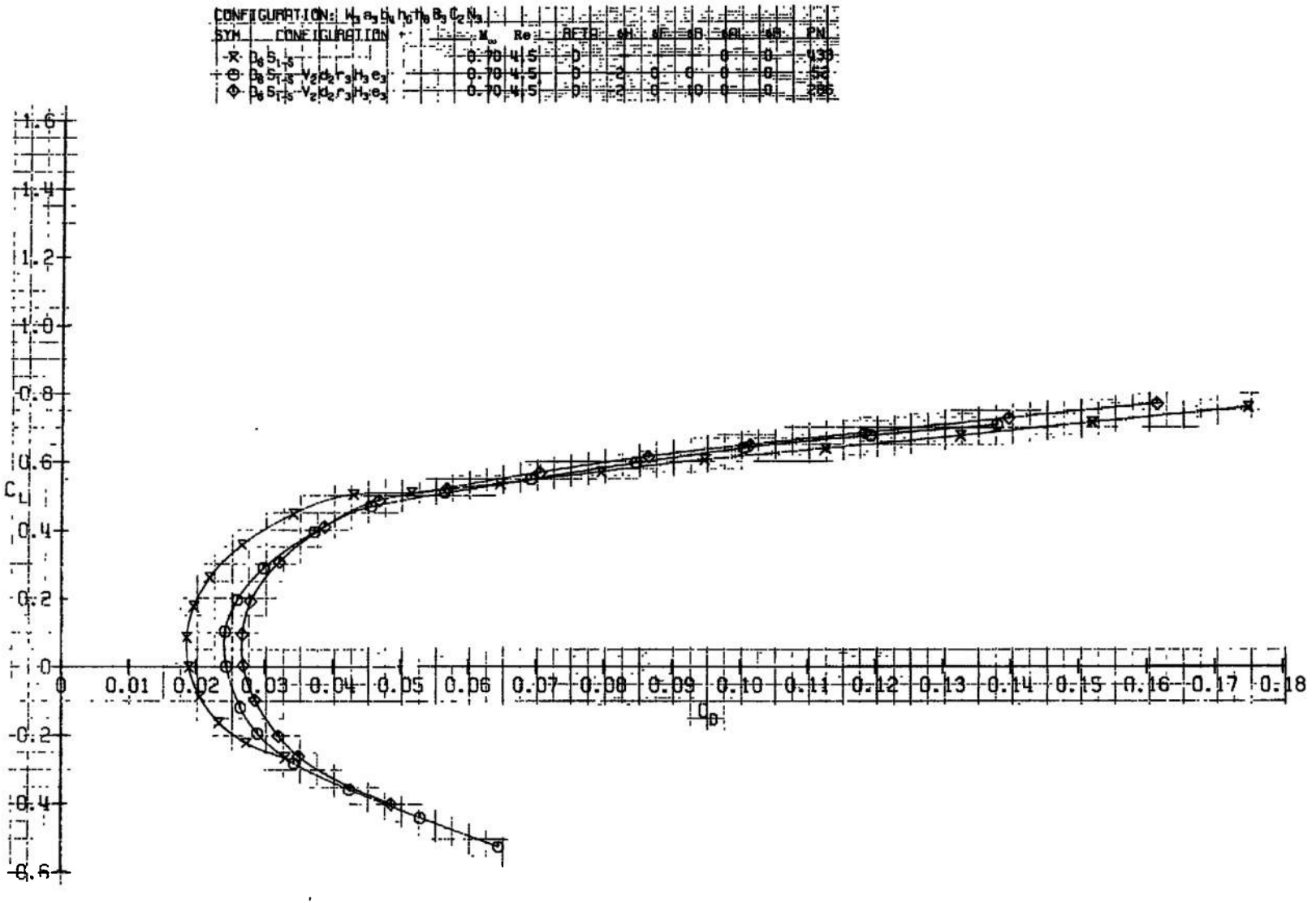

c. Continued

Fig. 9 Continued

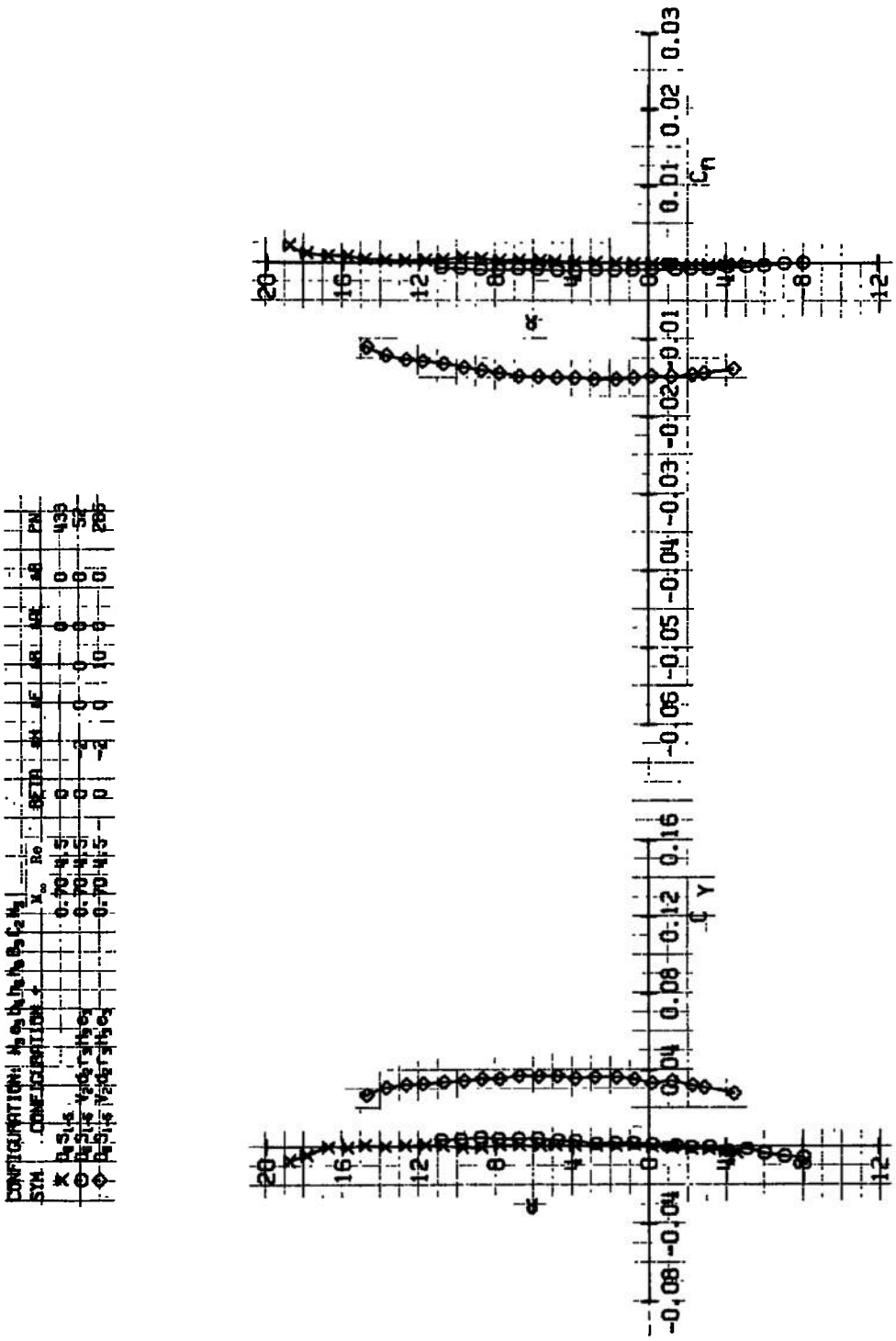

c. Continued
Fig. 9 Continued

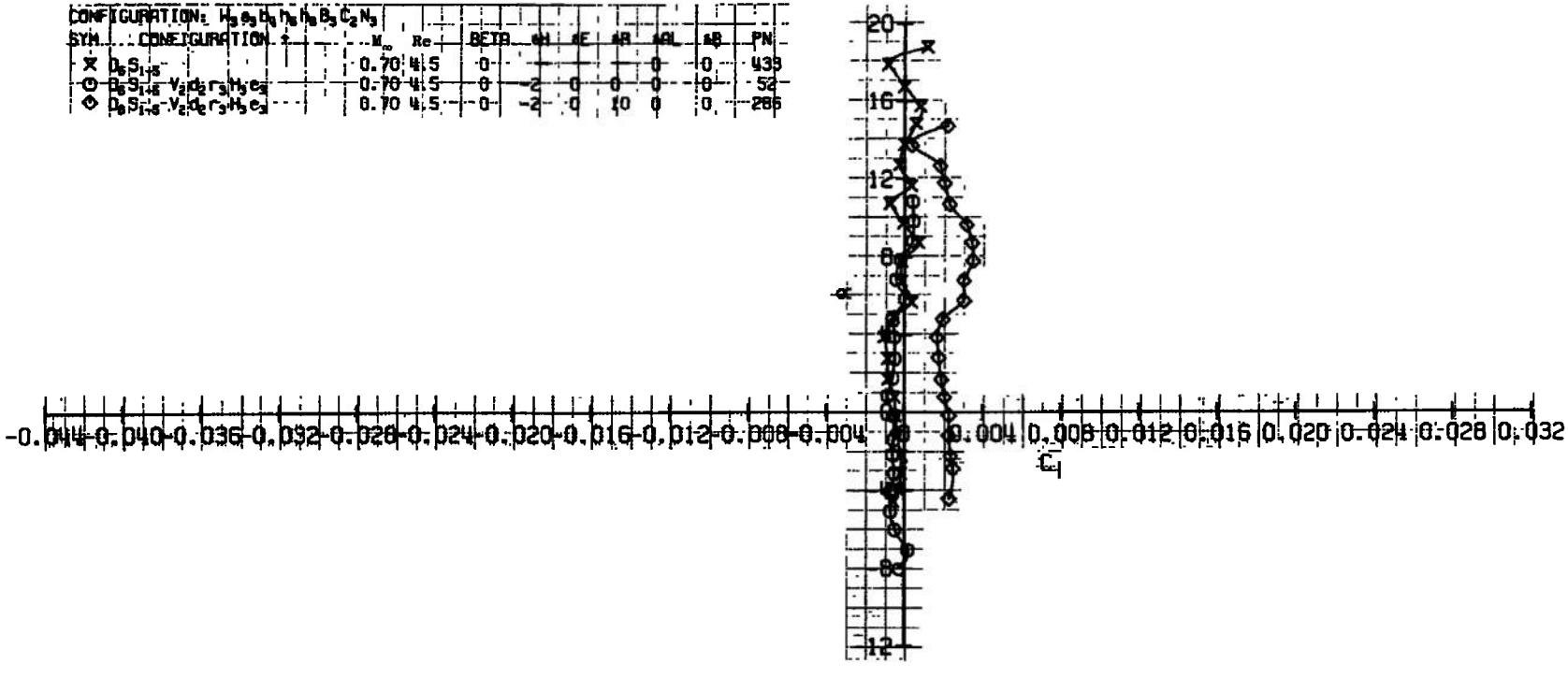

c. Concluded

Fig. 9 Continued

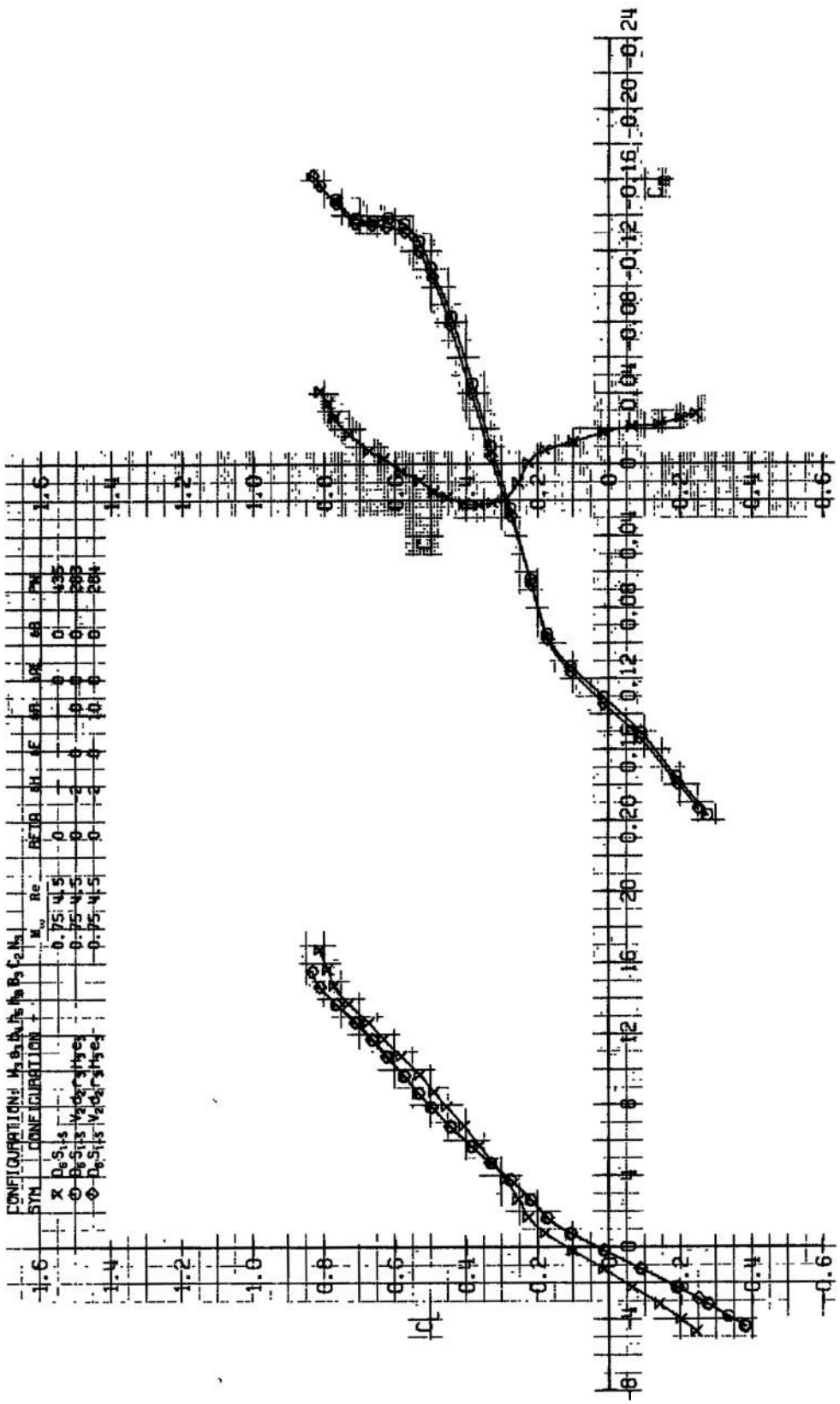

d. $M_\infty = 0.75$
Fig. 9 Continued

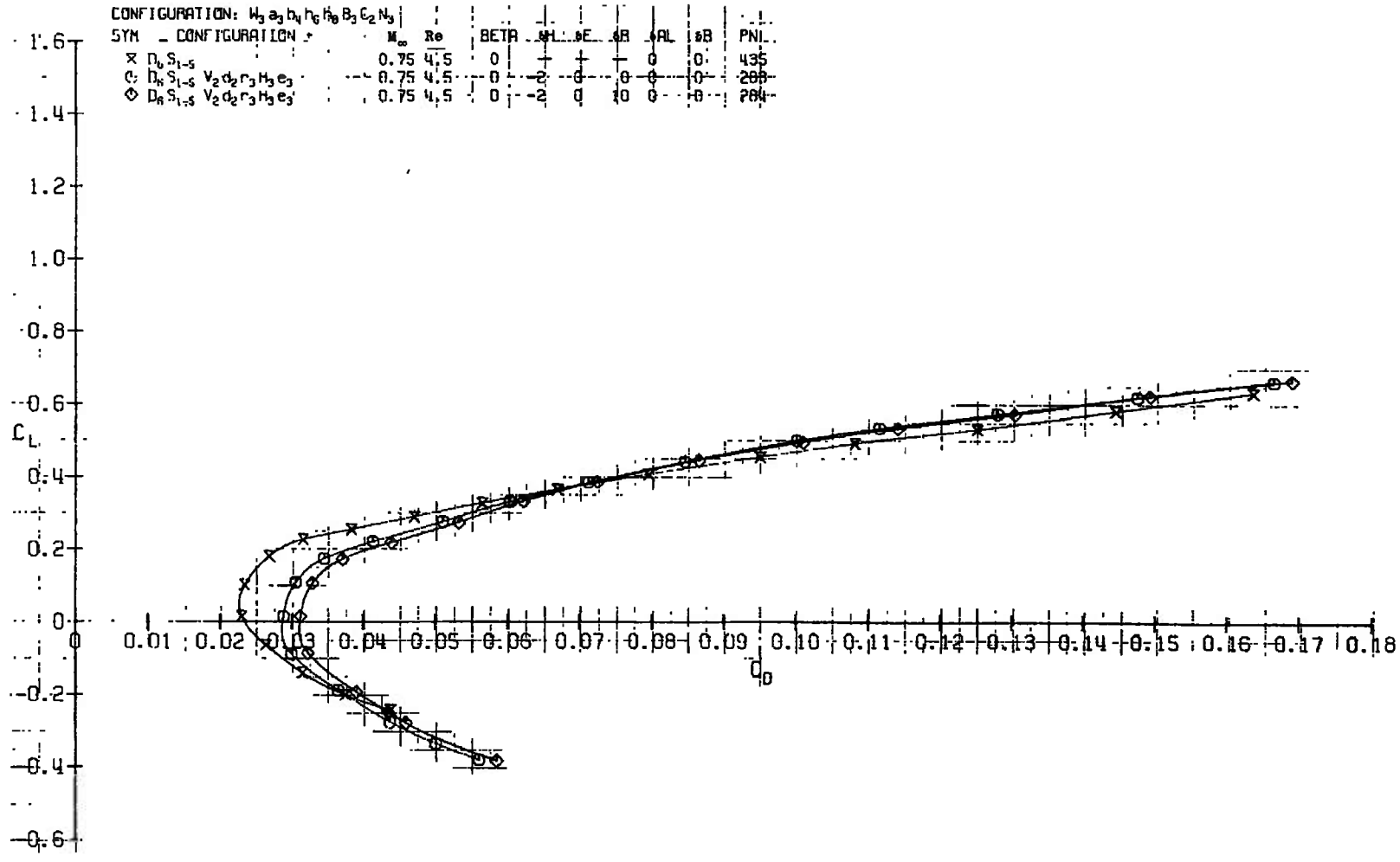

d. Continued
Fig. 9 Continued

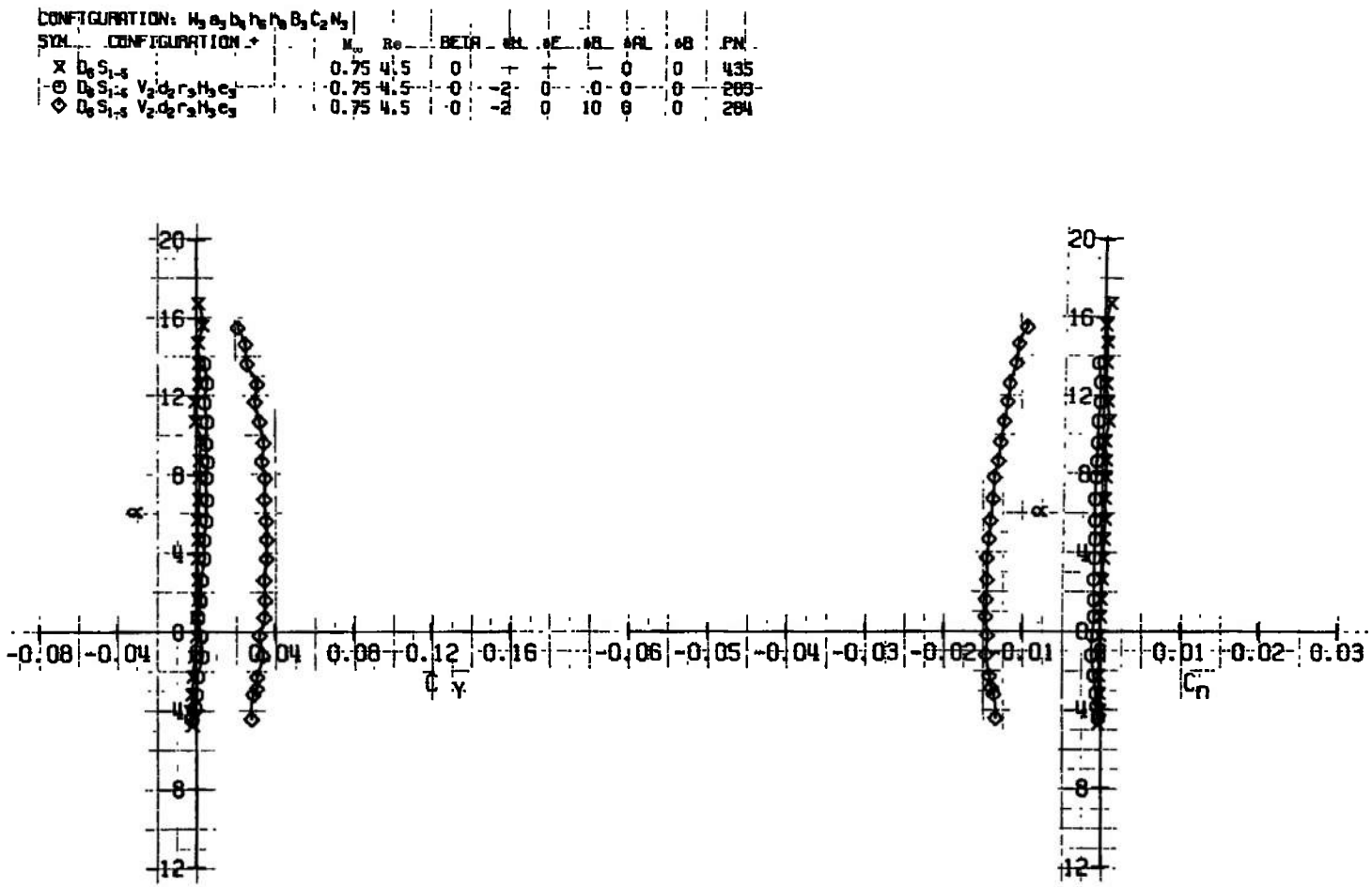

d. Continued

Fig. 9 Continued

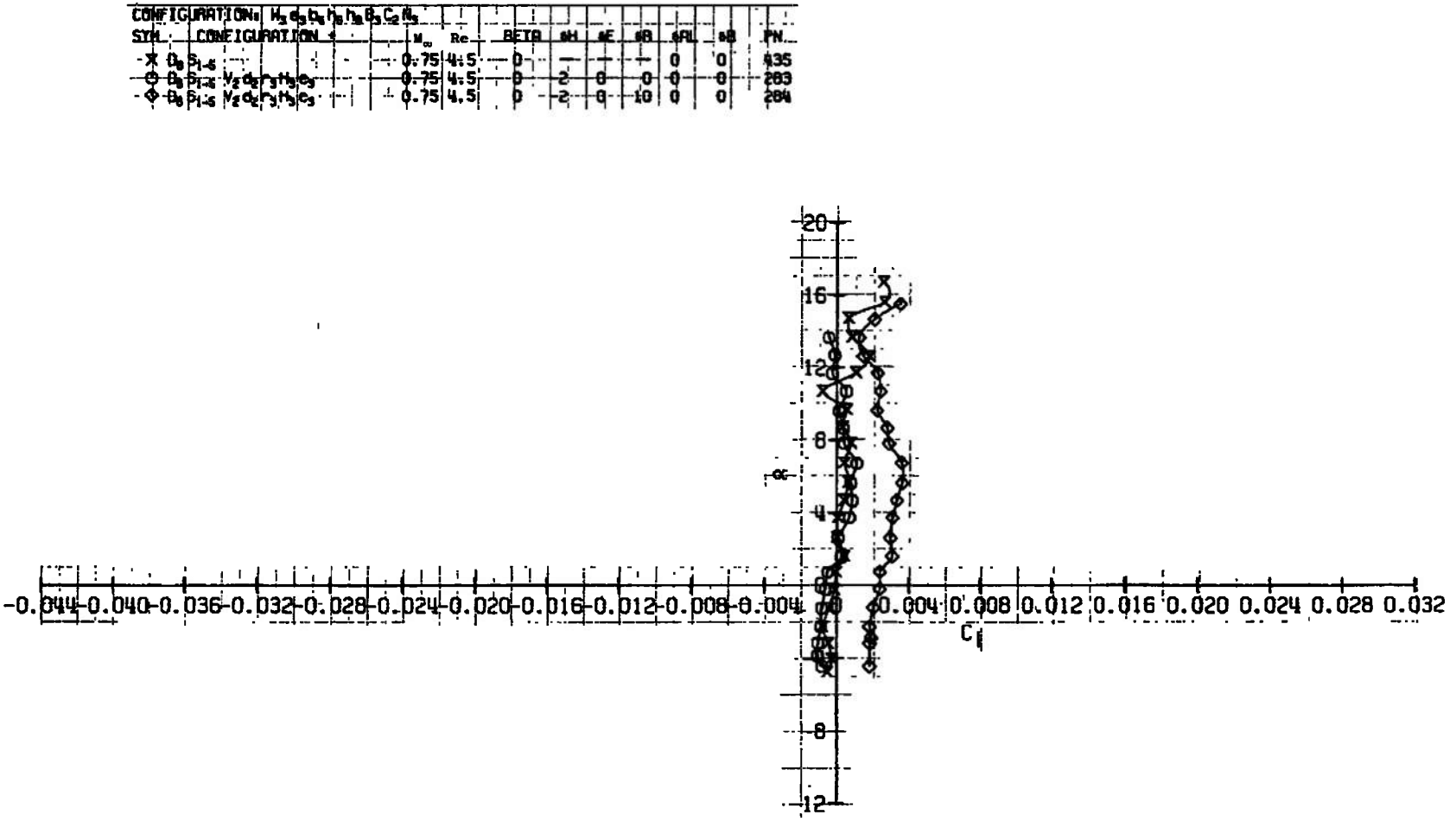

d. Concluded

Fig. 9 Continued

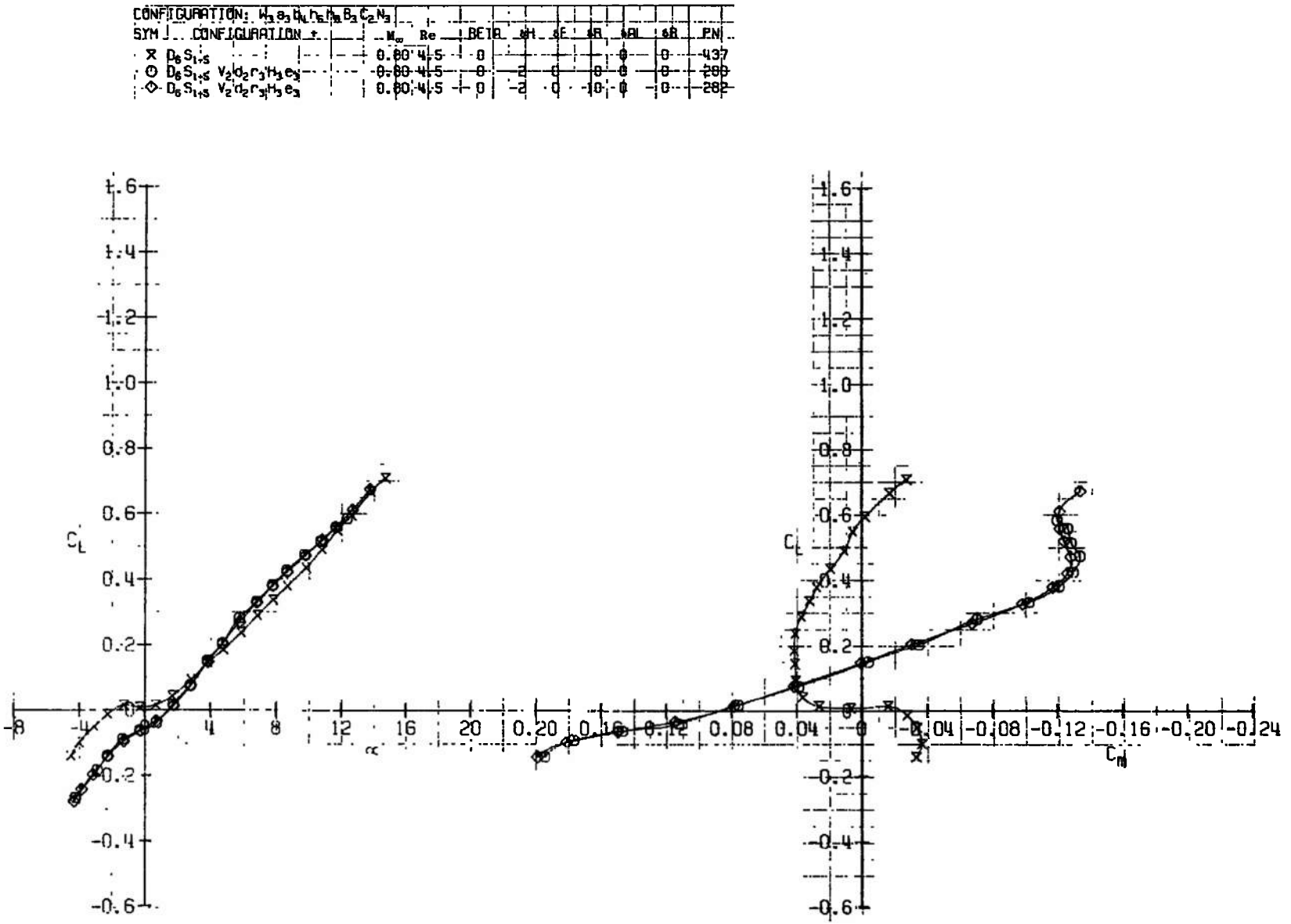

e. $M_\infty = 0.80$

Fig. 9 Continued

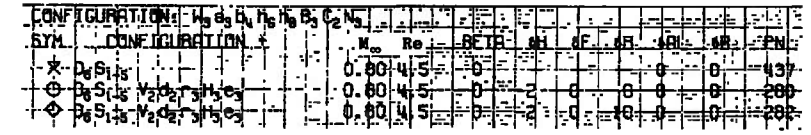

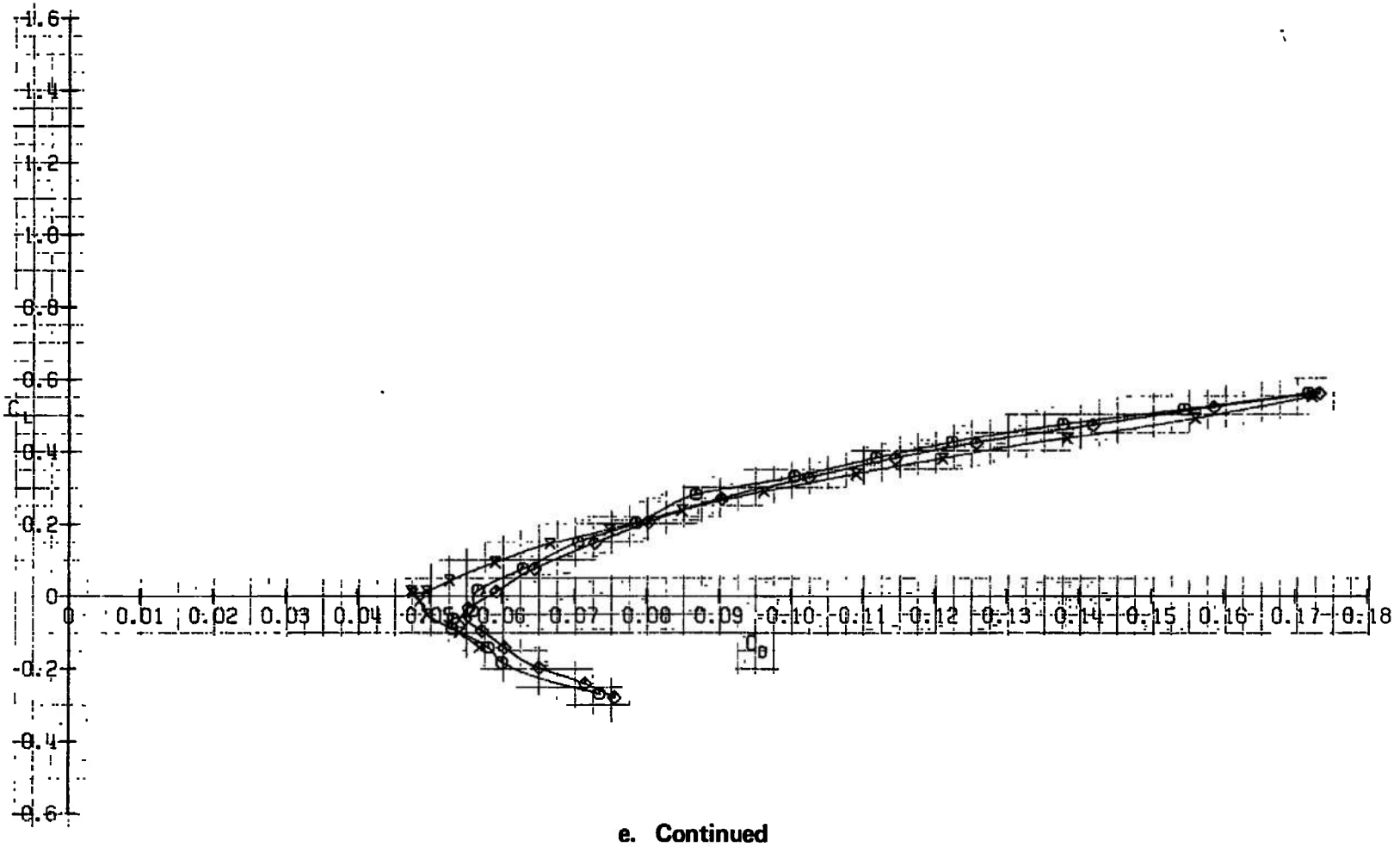

e. Continued

Fig. 9 Continued

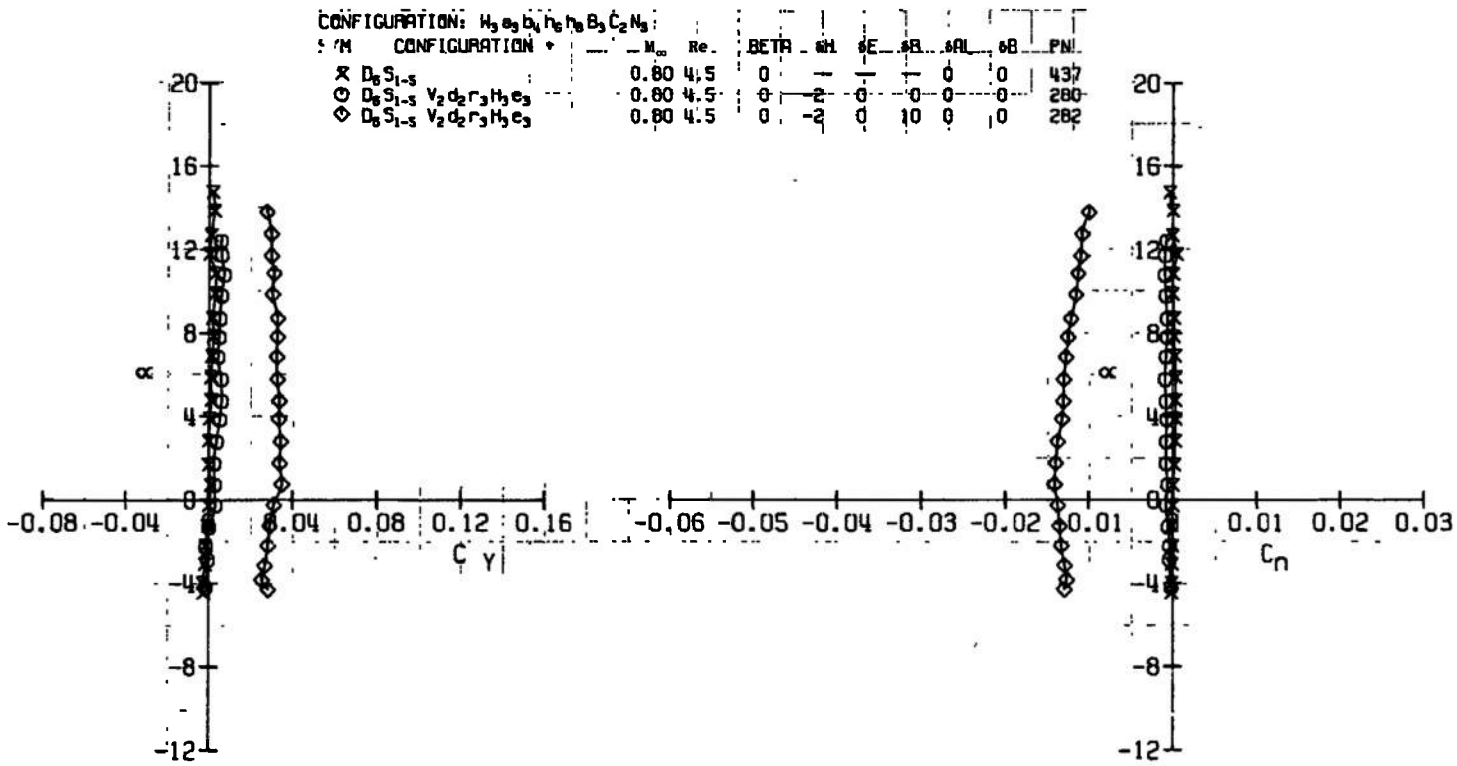

e. Continued

Fig. 9 Continued

CONFIGURATION: $W_3 e_3 b_6 h_6 h_9 B_3 C_2 N_3$

SYM	CONFIGURATION	M_∞	Re.	BETA	δH	δE	δR	δAL	δB	PN
⊠	$D_6 S_{1-5}$	0.80	4.5	0	—	—	—	0	0	437
⊙	$D_6 S_{1-5}$ $V_2 d_2 r_3 H_3 e_3$	0.80	4.5	0	-2	0	0	0	0	280
◇	$D_6 S_{1-5}$ $V_2 d_2 r_3 H_3 e_3$	0.80	4.5	0	-2	0	10	0	0	282

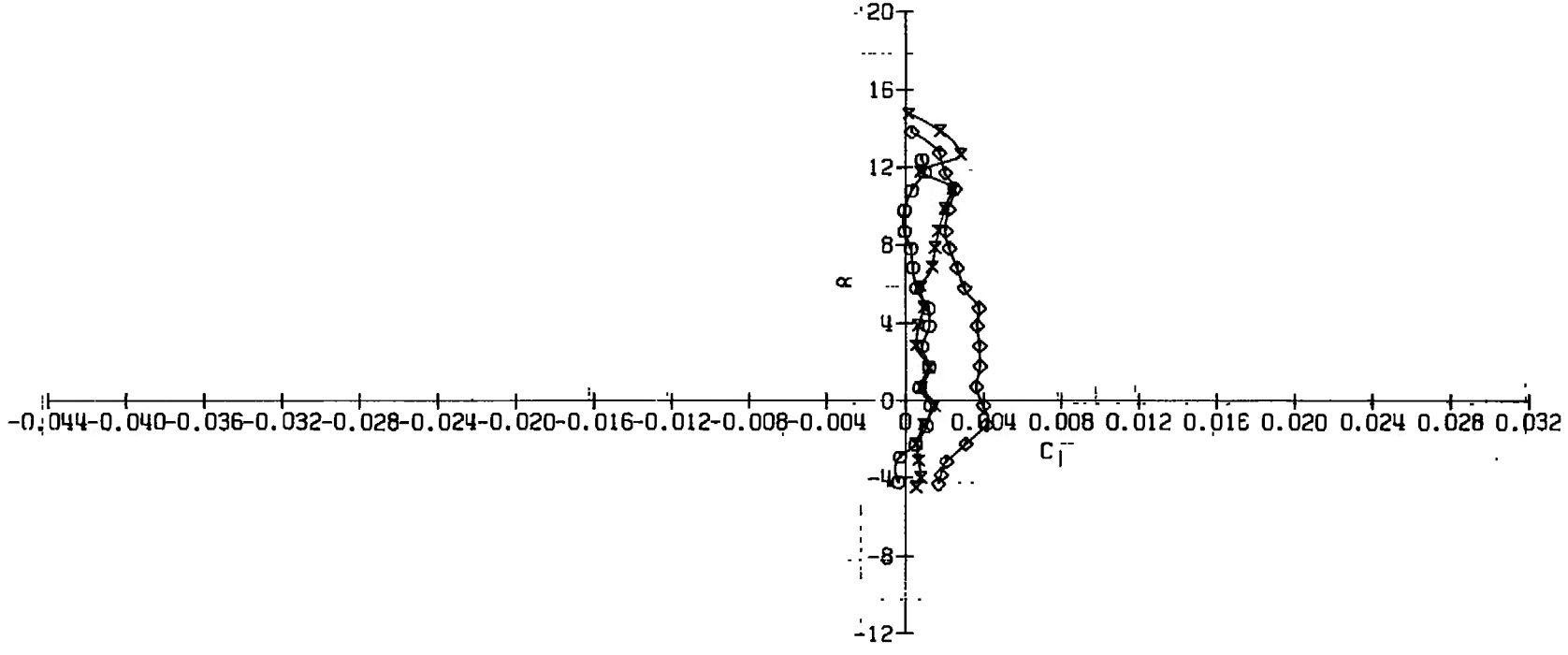

e. Concluded

Fig. 9 Concluded

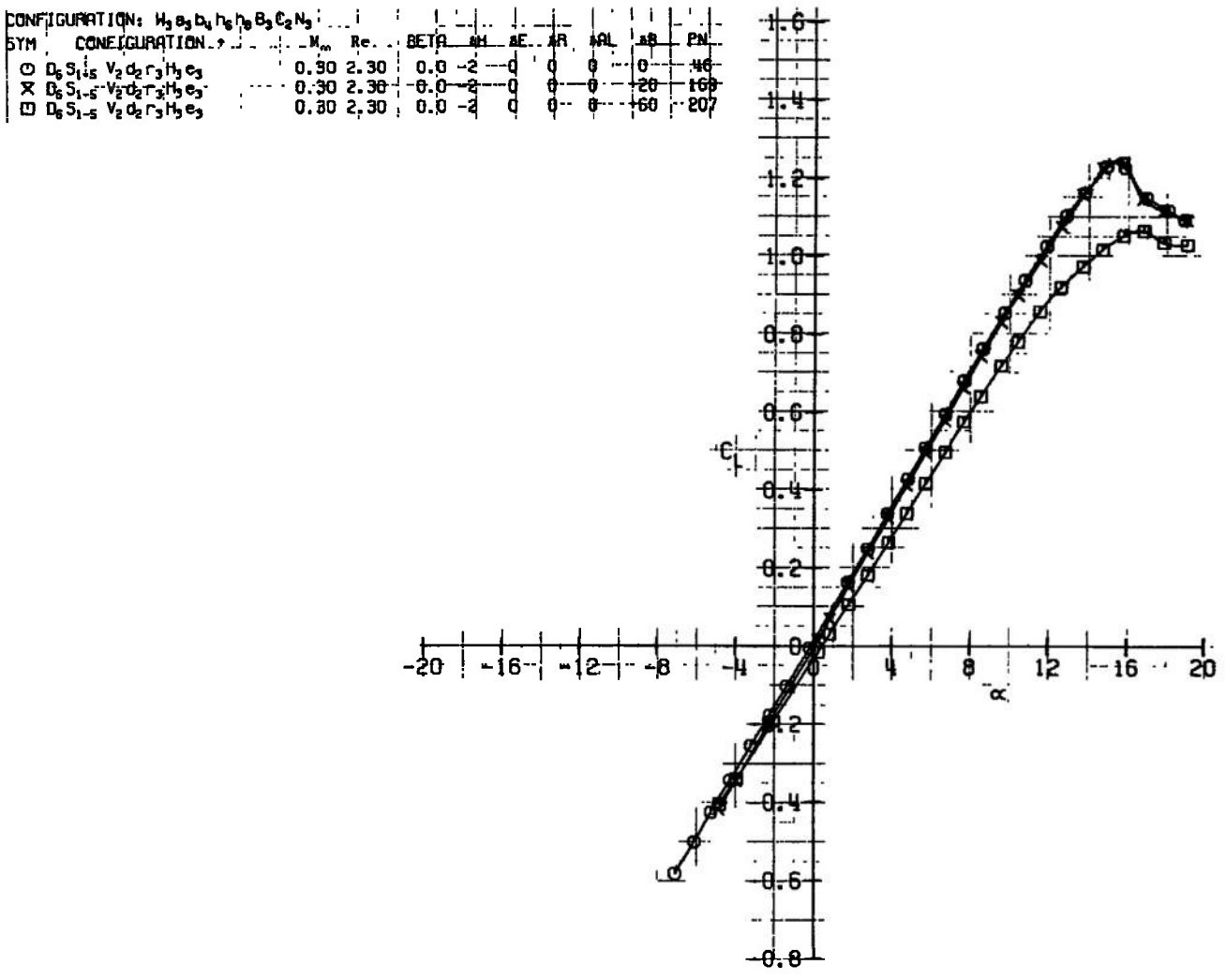

a. $M_\infty = 0.30$

Fig. 10 Speed Brake Effectiveness

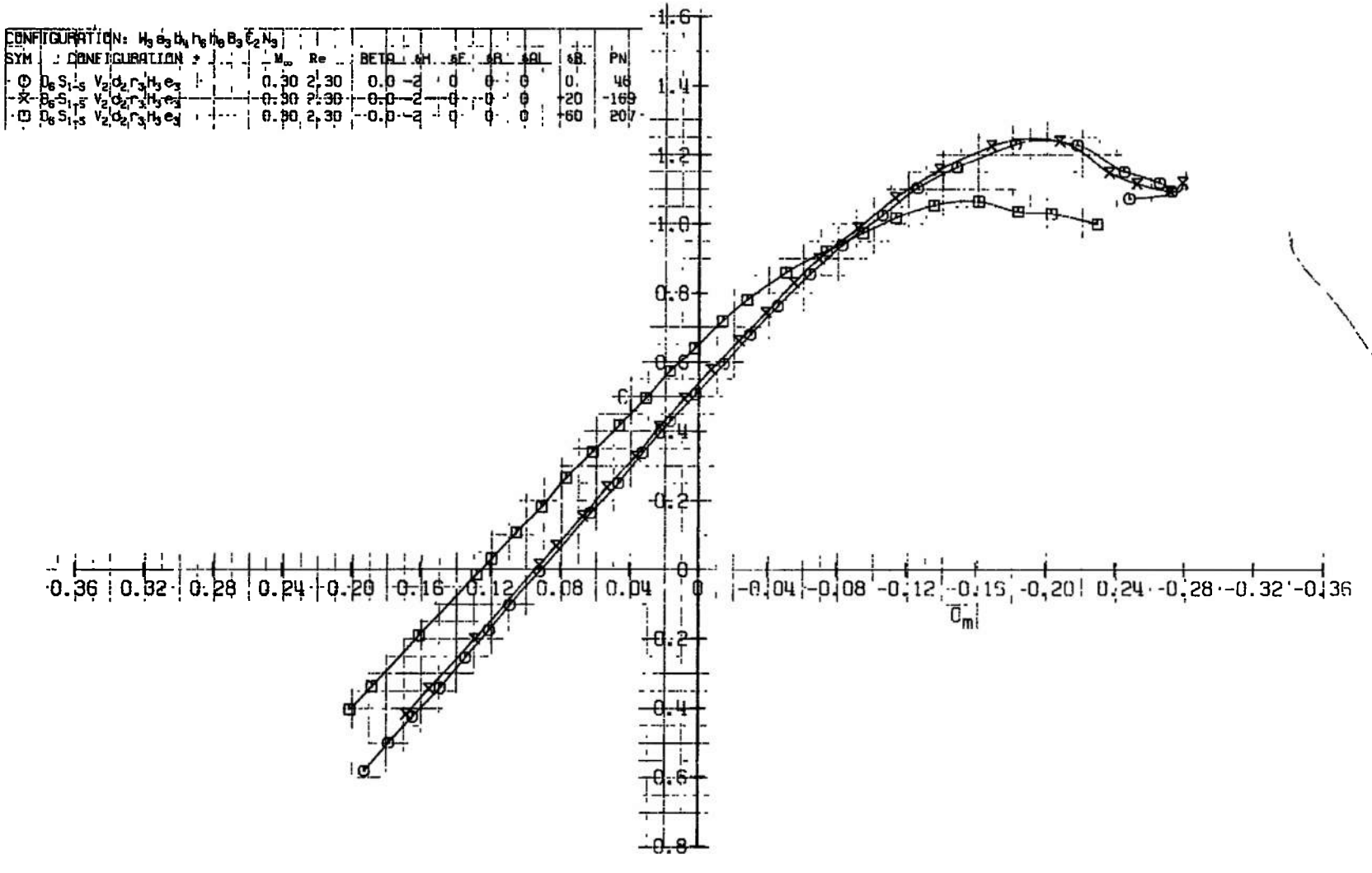

a. Continued

Fig. 10 Continued

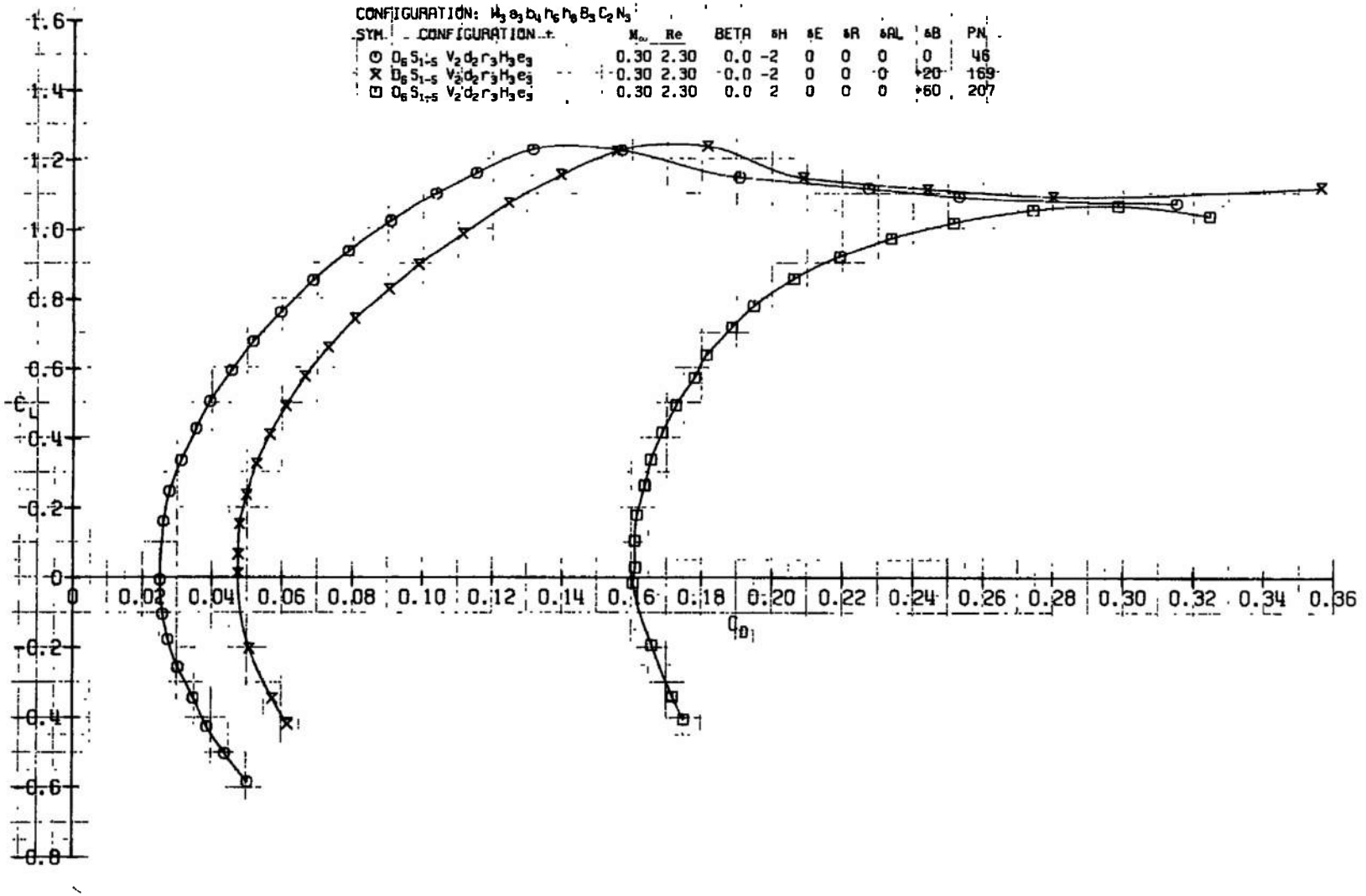

a. Concluded

Fig. 10 Continued

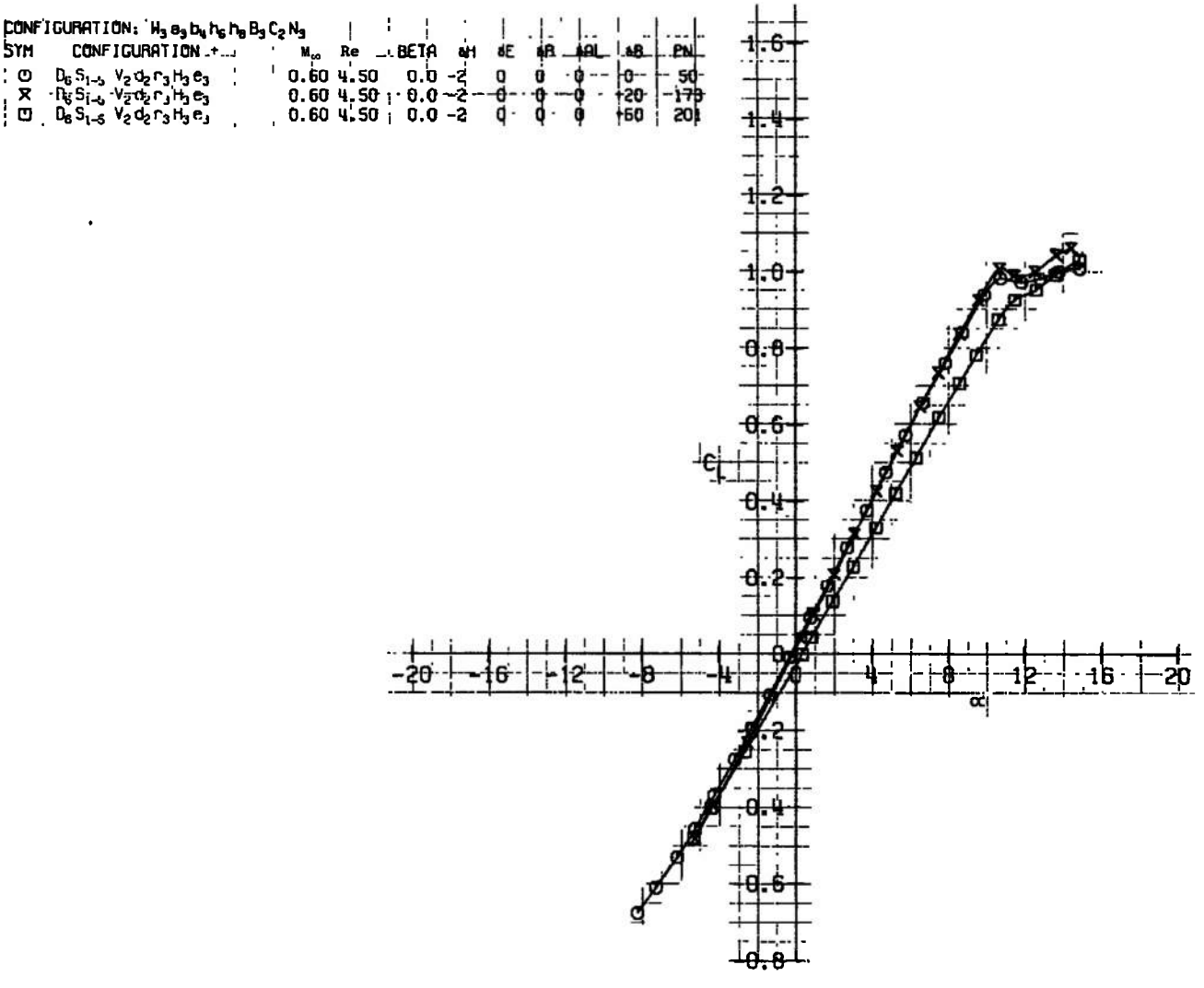

b. $M_\infty = 0.60$

Fig. 10 Continued

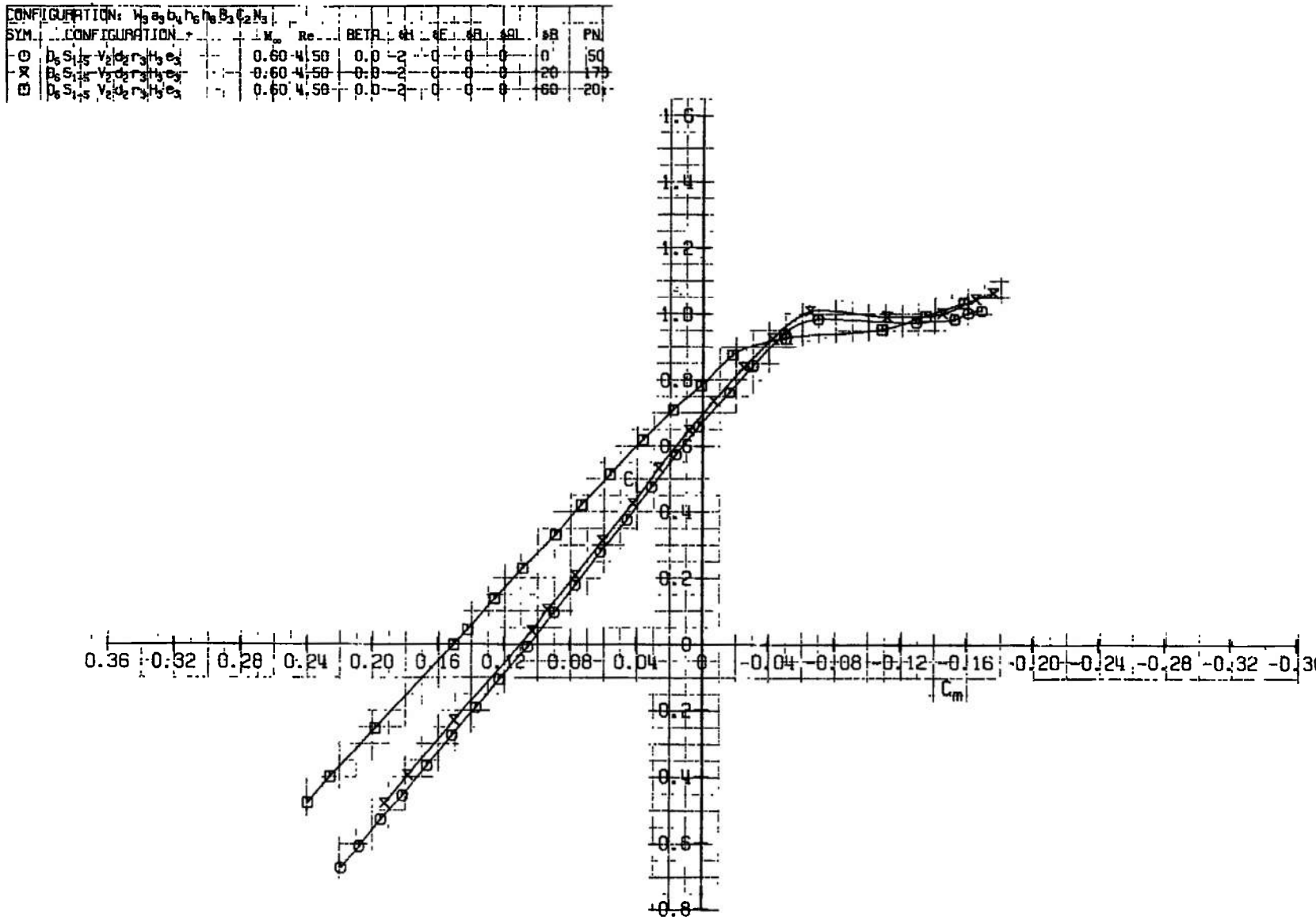

b. Continued
Fig. 10 Continued

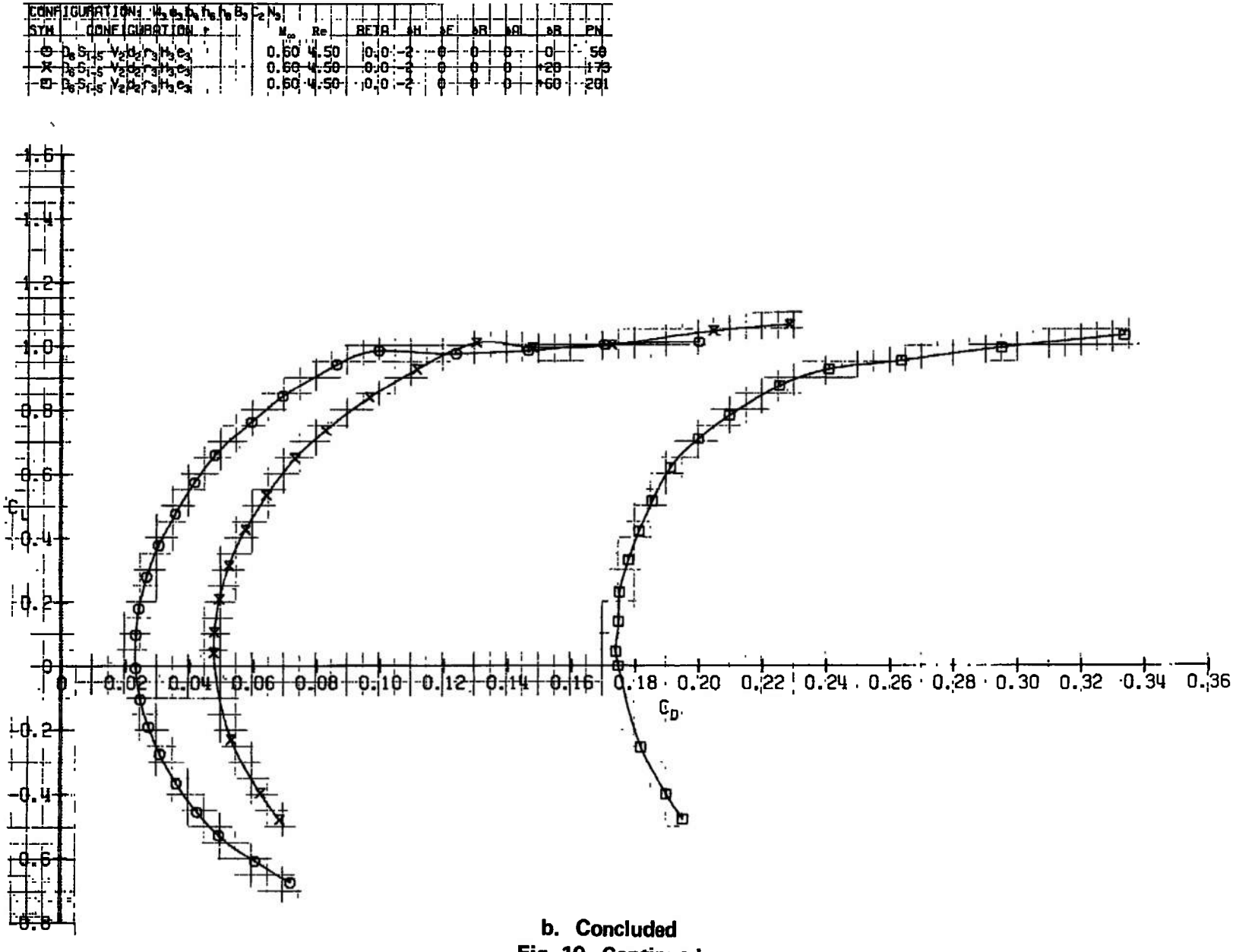

b. Concluded
Fig. 10 Continued

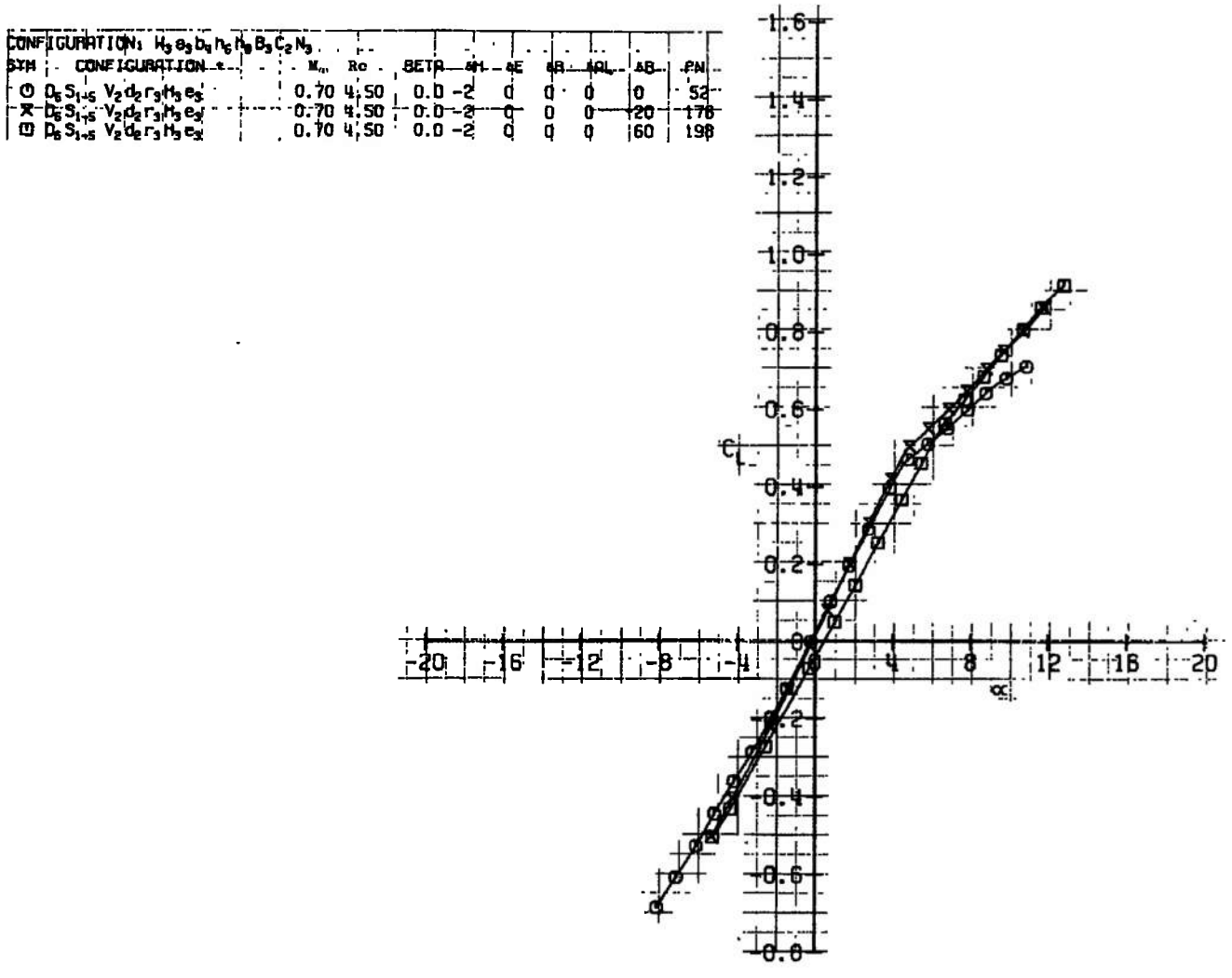

c. $M_\infty = 0.70$

Fig. 10 Continued

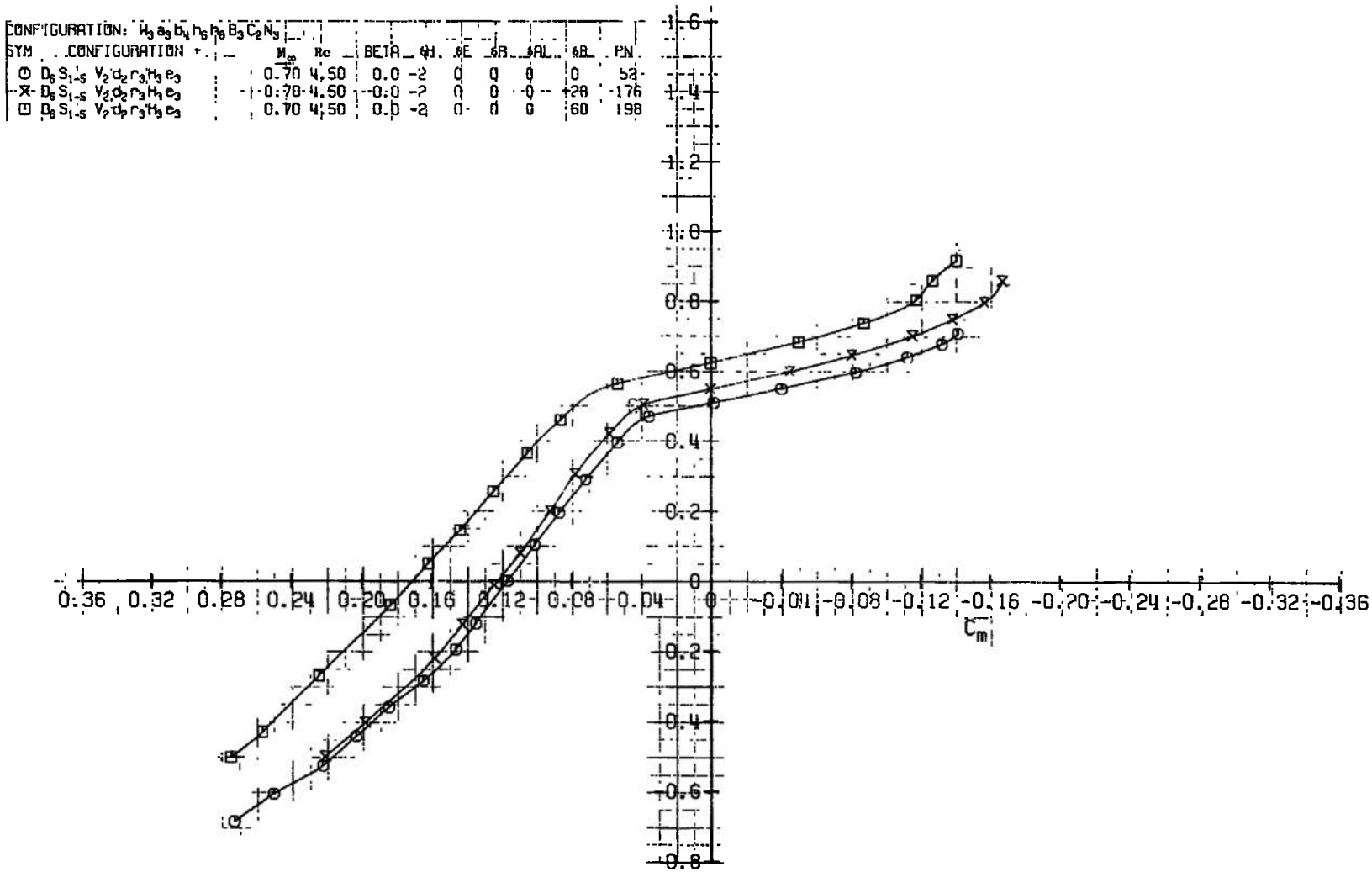

c. Continued

Fig. 10 Continued

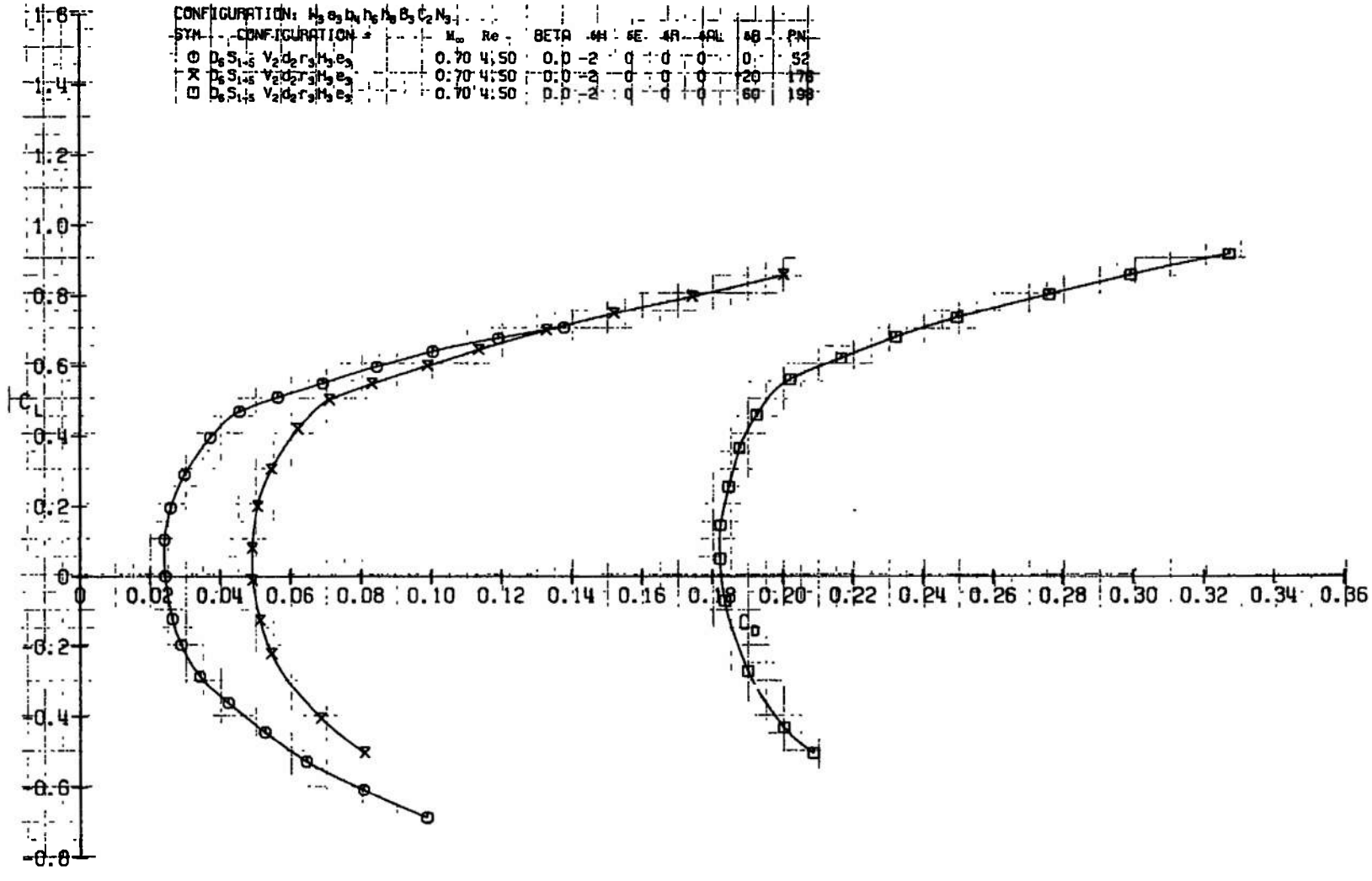

c. Concluded

Fig. 10 Continued

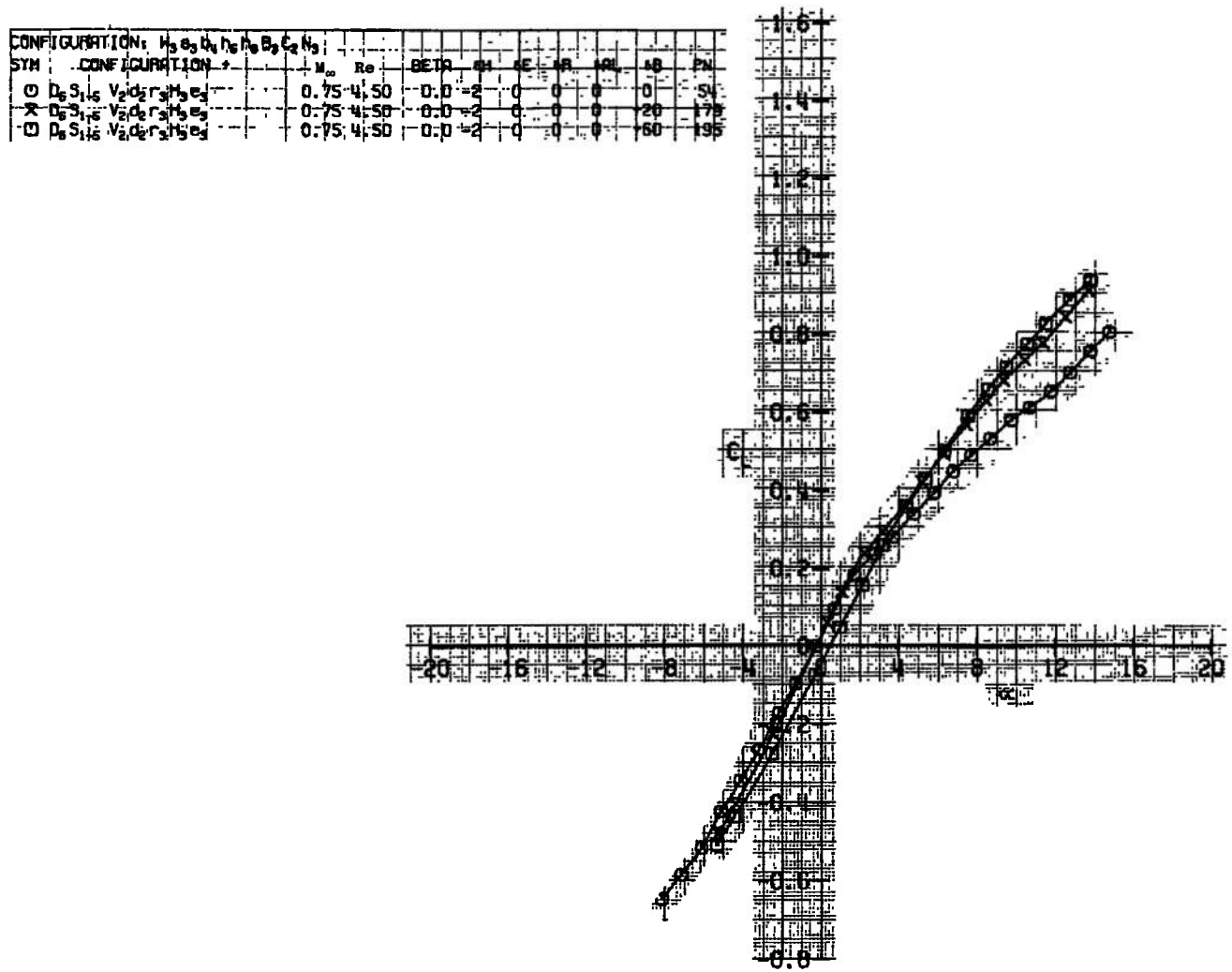

d. $M_\infty = 0.75$

Fig. 10 Continued

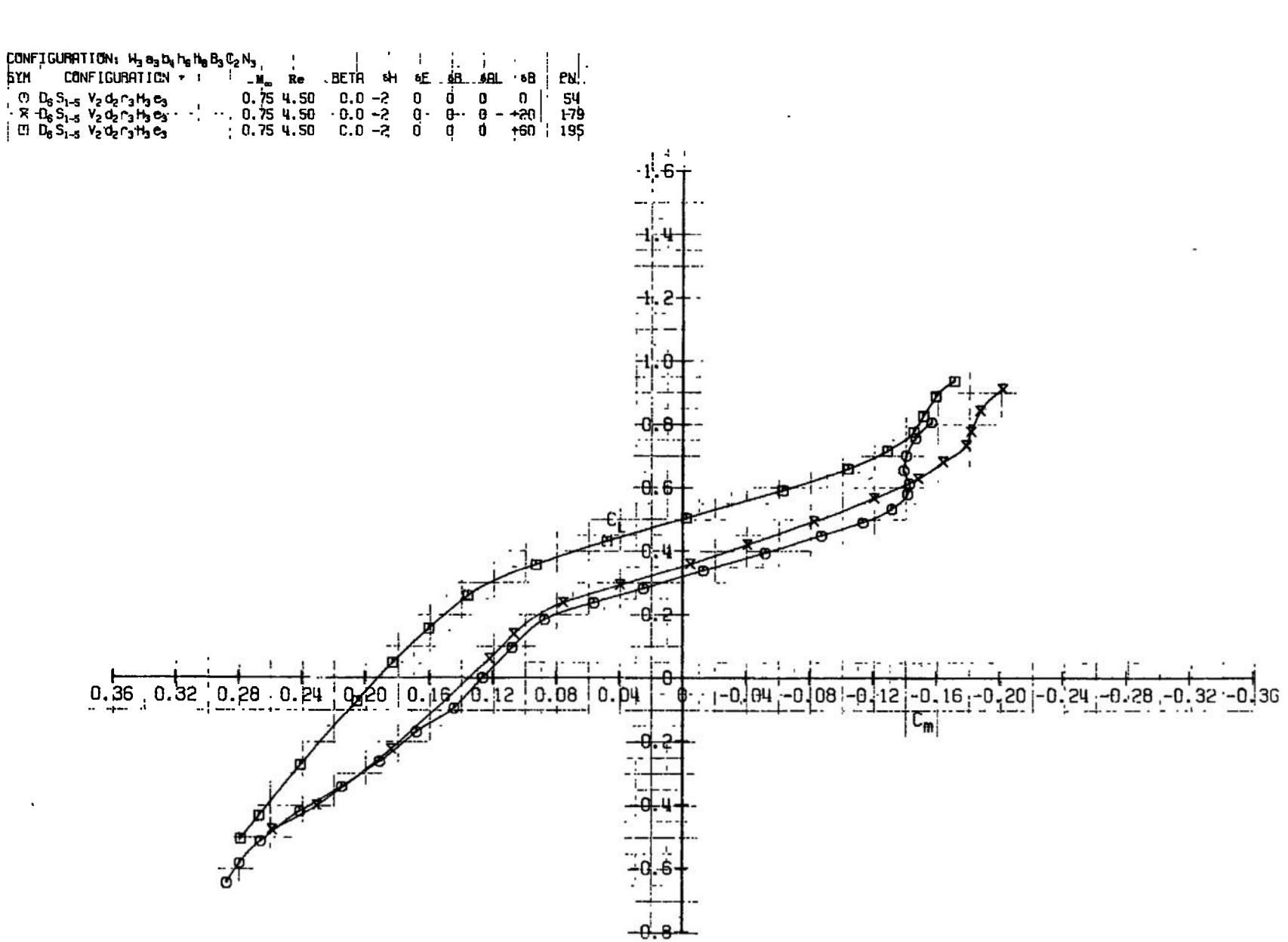

d. Continued

Fig. 10 Continued

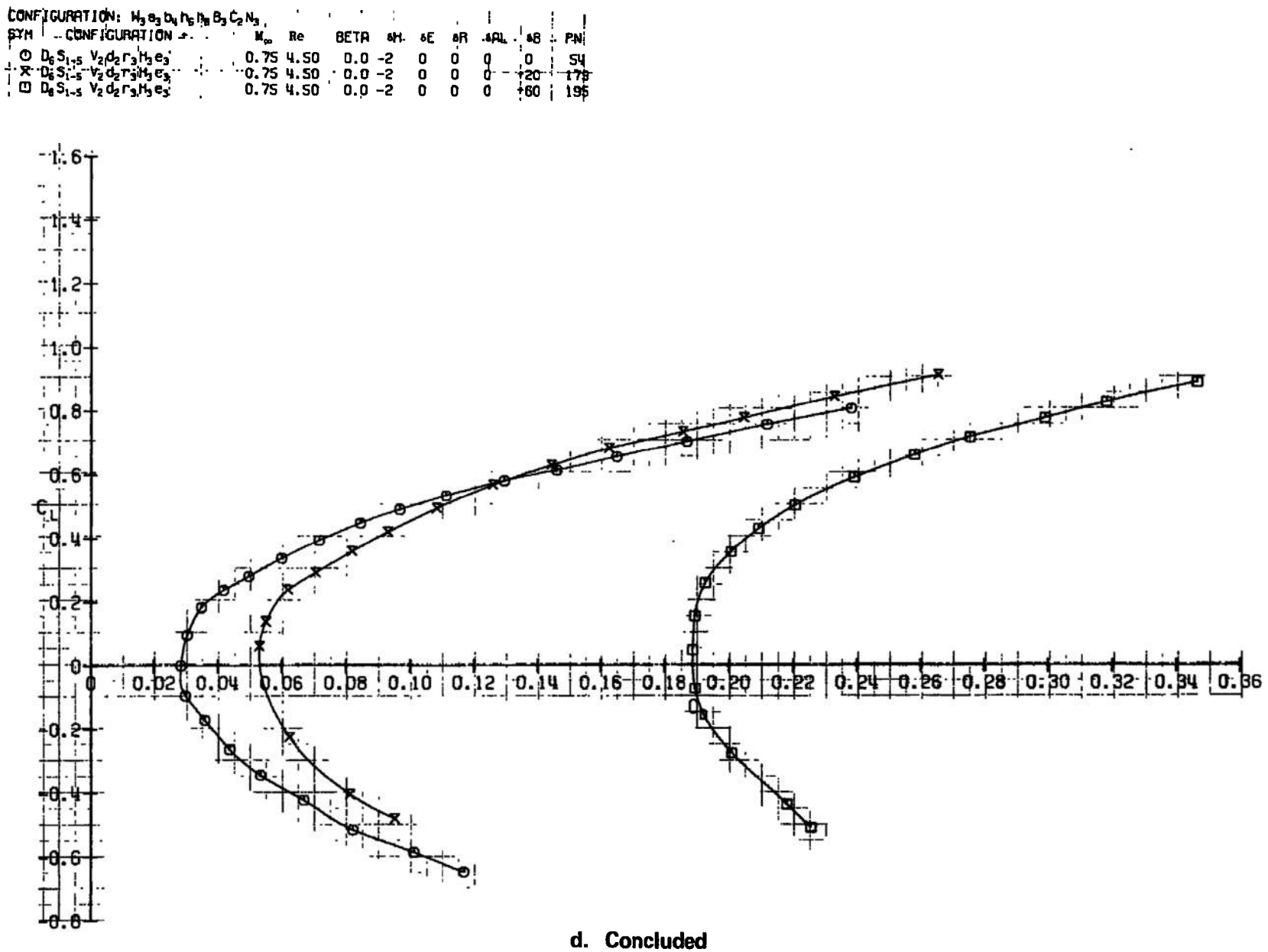

d. Concluded
Fig. 10 Continued

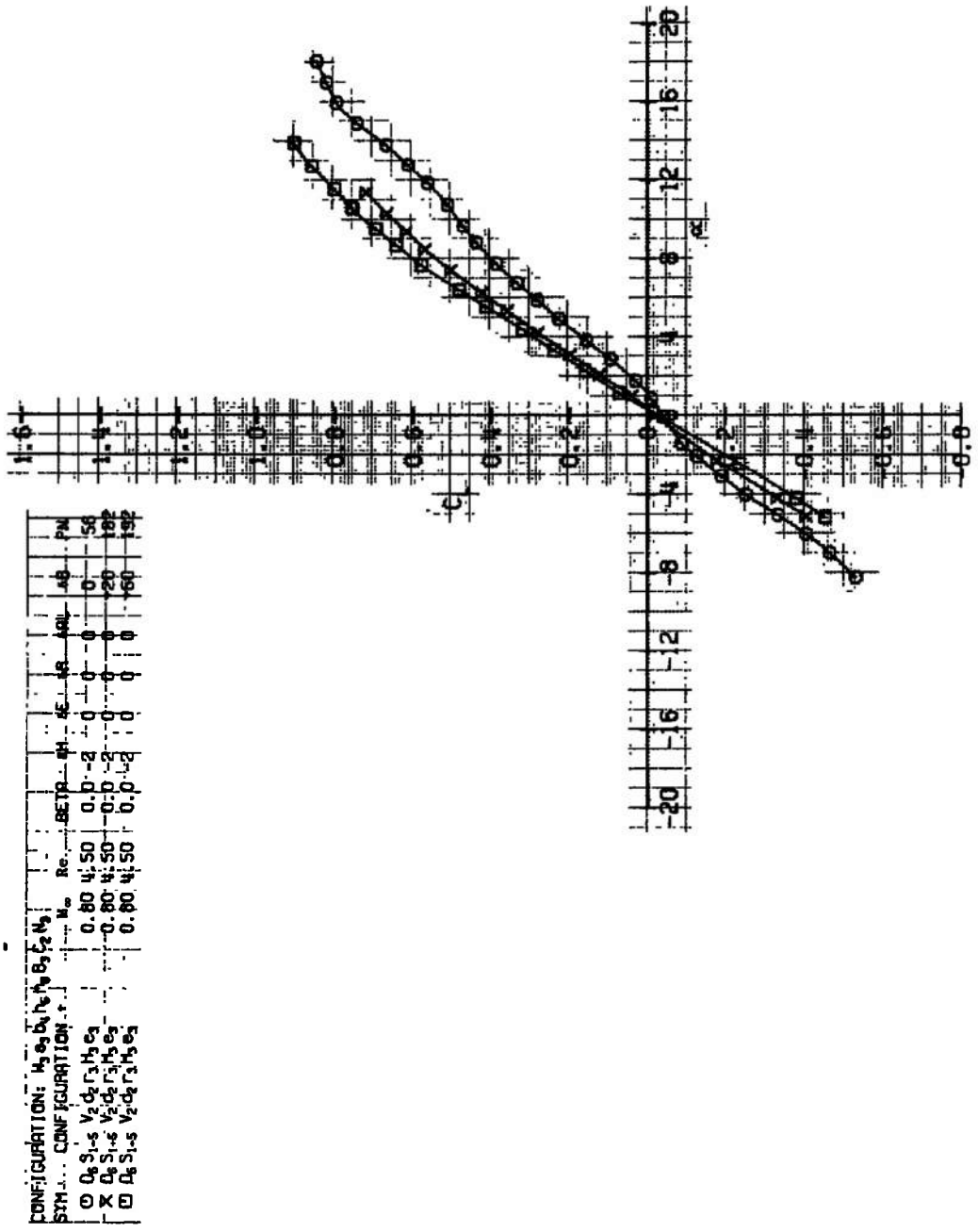

e. $M_\infty = 0.80$

Fig. 10 Continued

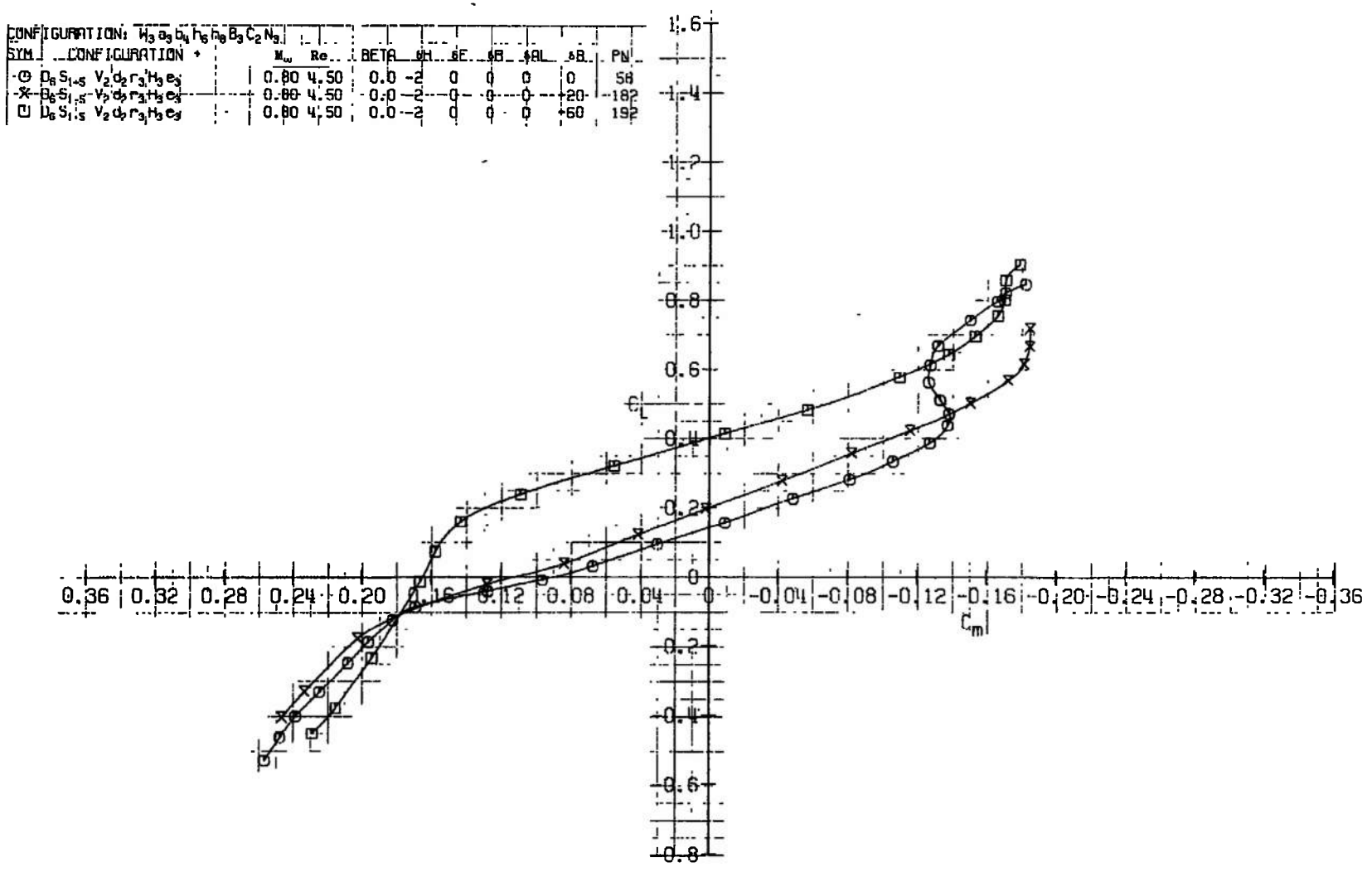

e. Continued

Fig. 10 Continued

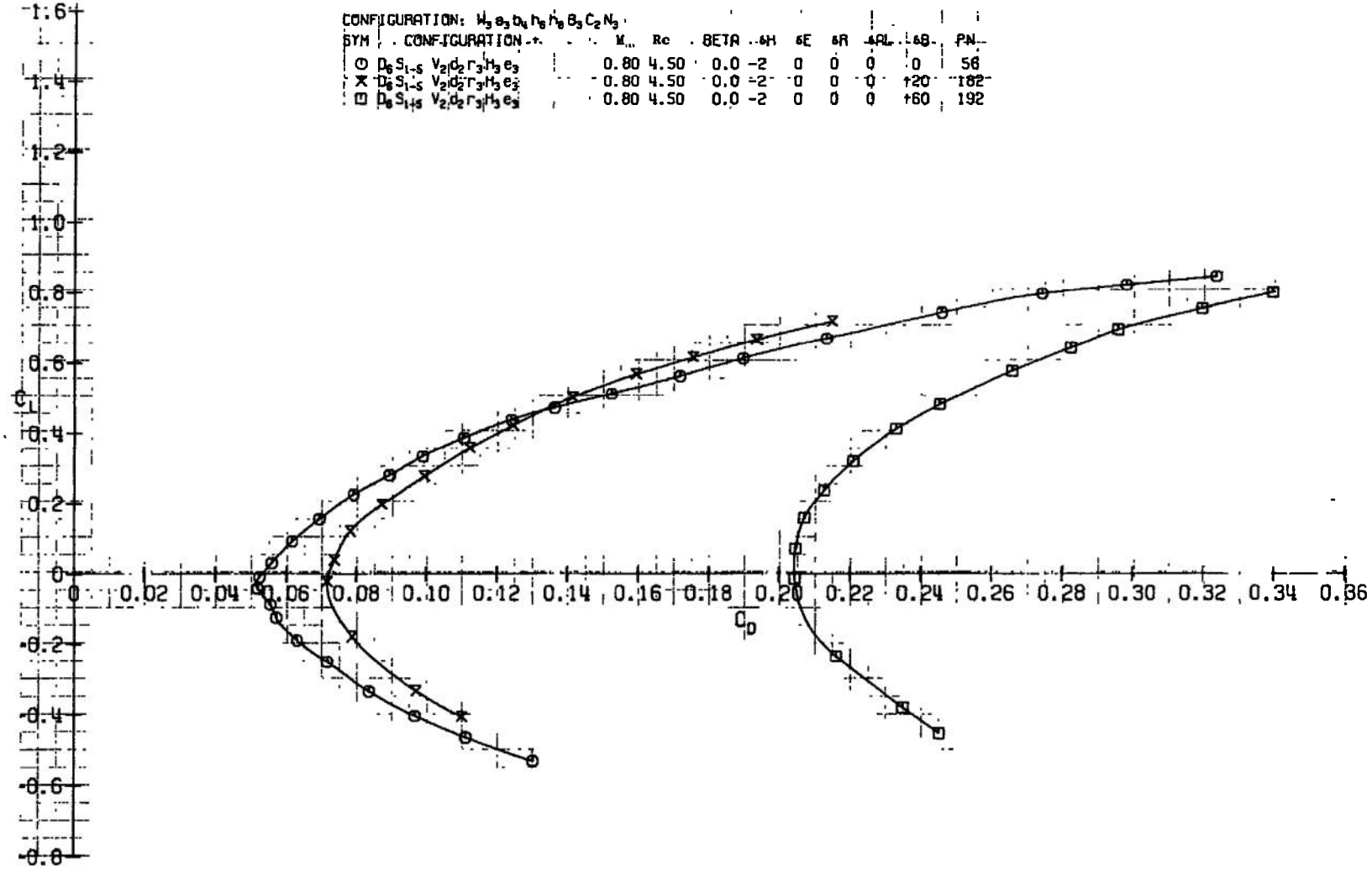

e. Concluded

Fig. 10 Concluded

TABLE I
INDEX TO MODEL COMPONENTS

Symbol	Components
a_3	Aileron
B_3	Body
b_4	Speed Brake
C_2	Canopy
d_2	Dorsal
D_6	Duct
D_7	Duct with Core Cowl
h_1	Dual Ejecton Rack
H_3e_3	Horizontal Tail with Elevator
$h_{6,\ 8}$	Flap Track
N_3	Nacelle
S_{1-5}	Pylons
V_2r_3	Vertical Tail with Rudder
$w_1{}^6$	500-lb Bomb, six, MK82
$w_1{}^{18}$	500-lb Bomb, eighteen, MK82
$w_2{}^{10}$	Napalm Bomb, ten, BLU-1/B
W_3	Wing

TABLE I (Concluded)

X	$W_3a_3h_6h_8B_3C_2N_3$ (Basic Configuration)
XD_6	
XD_6S_{1-5}	
$XD_6S_{1-5}V_2d_2r_3$	
$XD_6S_{1-5}V_2d_2r_3H_3e_3$	
$XD_7S_{1-5}V_2d_2r_3H_3e_3$	
$XD_6S_{1-5}V_2d_2r_3H_4e_3$	
$XD_6S_{1-5}w_1{}^6V_2d_2r_3H_3e_3$	
$XD_6S_{1-5}w_1{}^{18}V_2d_2r_3H_3e_3$	
$XD_6S_{1-5}w_2{}^{10}V_2d_2r_3H_3e_3$	

TABLE II
SUMMARY OF TEST DATA

Configuration X = $W_3a_3b_4h_6h_8B_3C_2N_3$	α, deg	β, deg	RN x 10^{-6}	Controls	Mach Number 0.30	0.60	0.70	0.75	0.80
					Part Number				
Effect of M_∞ and R_N									
XD_6	V	0	2.3		454	453	---	---	---
XD_6S_{1-5}					427	429	445	444	443
$XD_6S_{1-5}V_2r_3$					337	340	---	---	---
$XD_6S_{1-5}V_2r_3H_3e_3$					49/271	28/279	90	92	91
$XD_6S_{1-5}V_2r_3H_4e_3$					369	377	411	409	---
$XD_6S_{1-5}V_2r_3H_3e_3$			2.7		---	---	58	60	62
XD_6S_{1-5}			4.5		---	431	433	435	437
$XD_6S_{1-5}V_2r_3$					---	341	343	345	347
$XD_6S_{1-5}V_2r_3H_3e_3$					---	50/288	52/118	54/283	56/280
XD_6			7.0		---	449	450	451	452
XD_6S_{1-5}					---	439	440	441	442
$XD_6S_{1-5}V_2r_3$					---	350	351	352	353
$XD_6S_{1-5}V_2r_3H_3e_3$					---	56	68	70	72
Effect of Stores				δ_E, deg					
$XD_6S_{1-5}w1^{6}_{1-3}V_2d_2r_3H_3e_3$			2.3	10	260	261	263	266	267
$XD_6S_{1-5}h1_{1-4}w1^{18}_{1-5}V_2d_2r_3H_3e_3$			2.3		241	243	245	247	249
			4.5		---	---	253	25[illegible]	---
$XD_6S_{1-5}w2^{10}_{1-5}V_2d_2r_3H_3e_3$			2.3		215	217	235	233	231
			4.5		---	225	227	223	229
			7.0		---	219	221	---	---
Elevator Effectiveness				δ_E, deg					
$XD_6S_{1-5}V_2d_2r_3H_3e_3$			2.3	10	97	109	---	---	---
				5	99	104	---	---	---
				0	46*	48*	---	---	---
				-5	100	103	---	---	---
				-10	101	102	---	---	---

TABLE II (Continued)

Configuration X = $W_3a_3b_4h_6h_8B_3C_2N_3$	α, deg	β, deg	RN x 10^{-6}	Controls	Mach Number 0.30	0.50	0.70	0.75	0.80
					Part Number				
Elevator Effectiveness (continued)				δ_E, deg					
$XD_6S_{1-5}V_2d_2r_3H_3e_3$	V	0	4.6	10	---	111	120	122	130
				5	---	112	118	124	129
				0	---	50*	52*	54*	56*
				-5	---	113	117	123	128
				-10	---	114	116	125	127
			2.3	10	367	381	---	---	---
				5	368	380	---	---	---
				0	369	377	---	---	---
				-5	371	376	---	---	---
				-10	372	375	---	---	---
			4.5	10	---	383	395	397	---
				5	---	384	394	398	407
				0	---	385	392	399	406
				-5	---	387	391	401	405
				-10	---	388	390	402	404
Horizontal Stabilizer Effectiveness				δ_H, deg					
$XD_5S_{1-5}V_2d_2r_3H_3e_3$			2.3	2	318	319	---	---	---
				0	327	328	---	---	---
				-2	46*	48*	---	---	---
			4.5	2	---	320	321	322	323
				0	---	329	330	331	332
				-2	---	50*	52*	54*	56*
Aileron Effectiveness				δ_A, deg / δ_B, deg					
$XD_6S_{1-5}V_2d_2r_3H_3e_3$			2.3	20 / 0	134	146	---	---	---
				10	135	145	299	296	---
				5	136	144	---	---	---

TABLE II (Continued)

Configuration X = $W_3a_3b_4n_6h_8B_3C_2N_3$	α, deg	β, deg	RN x 10^{-5}	Controls δ_A, deg	Controls δ_B, deg	Mach Number 0.30	0.60	0.70	0.75	0.80
						Part Number				
Aileron Effectiveness (continued)										
$XD_6S_{1-5}V_2d_2r_3H_3e_3$	V	0	2.3	0	0	46*	48*	90*	92*	91*
				-5		137	143	---	---	---
				-10		138	142	298	297	---
				-20		139	141	---	---	---
			4.5	20		---	148	---	---	---
				10		---	149	156	162	158
				5		---	150	---	---	---
				0		50*	52*	52*	54*	56*
				-5		---	151	---	---	---
				-10		---	152	155	161	159
				-20		---	153	---	---	---
			2.3	30	20	167	---	---	---	---
				20		---	188	---	---	---
				10		168	187	---	---	---
				0		169	186	---	---	---
				-10		170	185	---	---	---
				-20		---	184	---	---	---
				-30		171	---	---	---	---
			4.5	10		---	174	175	180	181
				0		---	173	176	179	182
				-10		---	172	177	178	183
			2.3	30	60	209	---	---	---	---
				10		208	203	---	---	---
				0		207	204	---	---	---
				-10		206	---	---	---	---
				-30		205	---	---	---	---
			4.5	10		---	202	197	196	191

TABLE II (Continued)

Configuration X = $W_3a_3b_4h_6h_8B_3C_2N_3$	α, deg	β deg	RN $\times 10^{-6}$	Controls		Mach Number 0.30	0.60	0.70	0.75	0.80
						Part Number				
Aileron Effectiveness (continued)				δ_A, deg	δ_B, deg					
$XD_6S_{1-5}V_2d_2r_3H_3e_3$	V	0	4.5	0	60	---	201	198	195	192
↓			4.5	-10		---	200	199	194	193
Horizontal Tail Dihedral Effects				δ_H, deg	δ_B, deg					
$XD_6S_{1-5}V_2d_2r_3H_4e_3$			2.3	0	0	369*	---	---	---	---
↓			4.5	0	0	---	385*	392*	399	406*
			2.3	0	-60	414	---	---	---	---
			4.5	0	-60	---	418	420	421	422
$XD_6S_{1-5}V_2d_2r_3H_3e_3$			2.3	10	0	45*/271	---	---	---	---
↓			4.5	10	0	---	50*/288	52*	54*	56*/280
			2.3	10	-60	207*	---	---	---	---
			4.5	10	-60	---	201*	198*	195*	192*
Rudder Effectiveness				δ_R, deg						
$XD_6S_{1-5}V_2d_2r_3H_3e_3$			2.3	0		46*/271	48*/279	---	92*	---
↓				10		272	278	---	295	---
				20		273	277	---	---	---
			↓	30		274	275	---	---	---
			4.5	0		---	50/286	52*	54*/283	56*/280
			↓	10		---	290	286	284	282
				20		---	292	---	---	---
			↓	30		---	293	---	---	---
Lateral-Directional Characteristics										
XD_6S_{1-5}			2.3			427*	429*	---	---	---
$XD_6S_{1-5}V_2d_2r_3$			↓			337*	340*	---	---	---
$XD_6S_{1-5}V_2d_2r_3H_3e_3$	↓	↓	↓			46*/271	48*/279	---	---	---

TABLE II (Concluded)

Configuration X = $W_3a_3b_4r_6h_8B_3C_2N_3$	α, deg	β, deg	RN x 10^{-6}	Controls	Mach Number 0.30	0.60	0.70	0.75	0.80
					Part Number				
Lateral-Directional Characteristics (continued)									
$XD_6S_{1-5}V_2d_2r_3H_4e_3$	V	0	2.3		359*	377	---	---	---
XD_6S_{1-5}		5			428	430	---	---	---
$XD_6S_{1-5}V_2d_2r_3$					338	339	---	---	---
$XD_6S_{1-5}V_2d_2r_3H_3e_3$					270	294	---	---	---
$XD_6S_{1-5}V_2d_2r_3H_4e_3$					370	379	---	---	---
XD_6S_{1-5}		0	4.5		---	431*	433*	435*	437
$XD_6S_{1-5}V_2d_2r_3$					---	341*	343*	345*	247
$XD_6S_{1-5}V_2d_2r_3H_3e_3$					50*/288	52*	54*/283	54*/283	56*/280
$XD_6S_{1-5}V_2d_2r_3H_4e_3$					---	385	392*	399*	---
XD_6S_{1-5}		5			---	432	434	436	438
$XD_6S_{1-5}V_2d_2r_3$					---	342	344	346	348
$XD_6S_{1-5}V_2d_2r_3H_3e_3$					---	280	287	285	281
$XD_6S_{1-5}V_2d_2r_3H_4e_3$					---	380	393	400	---
Effect of Core Cowl									
$XD_6S_{1-5}V_2d_2r_3H_3e_3$		0	2.3		46*	48*	---	---	---
$XD_7S_{1-5}V_2d_2r_3H_3e_3$			2.3		304	305	---	---	---
$XD_6S_{1-5}V_2d_2r_3H_3e_3$			7.0		---	68*	68*	70*	72*
$XD_7S_{1-5}V_2d_2r_3H_3e_3$			7.0		---	309	307	312	313
Pressure Data									
$XD_{6R}D_{7L}S_{1-5}V_2d_2r_3H_3e_3$			2.3		22	7	---	---	---
↓			4.5		---	10	13	15	18
			7.0		---	9	---	---	20
Internal Drag Data									
$XD_6S_{1-5}V_2d_2r_3H_3e_3$			2.3		27	39	---	---	---
↓			4.5		---	38	36	---	---
			7.0		---	34	32	30	29

* Listed Elsewhere

UNCLASSIFIED

Security Classification

DOCUMENT CONTROL DATA - R & D

(Security classification of title, body of abstract and indexing annotation must be entered when the overall report is classified)

1 ORIGINATING ACTIVITY *(Corporate author)*
Arnold Engineering Development Center
Arnold Air Force Station, Tennessee 37389

2a. REPORT SECURITY CLASSIFICATION
UNCLASSIFIED

2b. GROUP
N/A

3 REPORT TITLE
AERODYNAMIC CHARACTERISTICS OF A 0.12-SCALE MODEL OF THE A-9A AIRCRAFT AT MACH NUMBERS FROM 0.30 TO 0.80

4 DESCRIPTIVE NOTES *(Type of report and inclusive dates)*
Final Report - August 17 to 24, 1971

5. AUTHOR(S) *(First name, middle initial, last name)*
Warren E. White, ARO, Inc.

6. REPORT DATE	7a. TOTAL NO OF PAGES	7b. NO OF REFS
December 1971	132	1

8a. CONTRACT OR GRANT NO

b. PROJECT NO.

c. Program Element 64211F

d. System 329A

9a. ORIGINATOR'S REPORT NUMBER(S)
AEDC-TR-71-271

9b. OTHER REPORT NO(S) *(Any other numbers that may be assigned this report)*
ARO-PWT-TR-71-207

10 DISTRIBUTION STATEMENT Distribution limited to U.S. Government agencies only; this report contains information on test and evaluation of military hardware; December 1971; other requests for this document must be referred to Aeronautical Systems Division (SDXT), Wright-Patterson AFB, OH 45433.

11. SUPPLEMENTARY NOTES
Available in DDC.

12. SPONSORING MILITARY ACTIVITY
Aeronautical Systems Division (SDXT), Wright-Patterson AFB, OH 45433

13. ABSTRACT

Wind tunnel tests were conducted at Mach numbers from 0.30 to 0.80 and Reynolds numbers from 2.3 to 7.0 million on a 0.12-scale model of the A-9A aircraft to determine the effects of control surface deflections on the aerodynamic characteristics of the airplane. The results showed that the horizontal stabilizer was 20 to 50 percent more effective in pitching moment per degree of deflection than the elevator, the rudder remained effective at all Mach numbers, and the aileron deflections produced significant effects on lift, drag, and pitching and rolling moment. Minimum drag was increased by approximately 100 and 600 percent for speed brake deflections of 20 and 60 deg, respectively, at Mach numbers from 0.70 to 0.80.

Distribution limited to U. S. Government agencies only; this report contains information on test and evaluation of military hardware; December 1971; other requests for this document must be referred to Aeronautical Systems Division (SDXT), Wright-Patterson AFB, OH 45433.

DD FORM 1 NOV 65 1473

UNCLASSIFIED

Security Classification

14. KEY WORDS	LINK A		LINK B		LINK C	
	ROLE	WT	ROLE	WT	ROLE	WT
A-9A						
jet aircraft						
control surfaces						
aerodynamic characteristics						
subsonic flow						
transonic wind tunnels						

AFSC
Arnold AFS Tenn.